

ENERGY LABORATORY

MASSACHUSETTS INSTITUTE  
OF TECHNOLOGY

MITNE-249, C.3

NUCLEAR ENGINEERING  
READING ROOM - M.I.T.

DELAYED NEUTRON ASSAY  
TO TEST SORBERS FOR  
URANIUM-FROM-SEAWATER APPLICATIONS  
by  
C.K. NITTA, F.R. BEST and M.J. DRISCOLL  
Energy Laboratory Report No. MIT-EL 82-008  
Nuclear Engineering Department  
Report No: MITNE-249  
February 1982



NUCLEAR ENGINEERING  
READING ROOM - M.I.T.

DELAYED NEUTRON ASSAY  
TO TEST SORBERS FOR  
URANIUM-FROM-SEAWATER APPLICATIONS

by

C.K. NITTA, F.R. BEST and M.J. DRISCOLL  
Energy Laboratory Report No. MIT-EL 82-008  
Nuclear Engineering Department  
Report No: MITNE-249

February 1982

DELAYED NEUTRON ASSAY  
TO TEST SORBERS FOR  
URANIUM-FROM-SEAWATER APPLICATIONS

by

C.K. Nitta, F.R. Best and M.J. Driscoll

Energy Laboratory  
and  
Department of Nuclear Engineering

Massachusetts Institute of Technology  
Cambridge, Massachusetts 02139

Final Report of the  
Uranium from Seawater Project  
for FY 1981

Funded by the  
U.S. Department of Energy  
Grand Junction Office  
Bendix Field Engineering Corporation

administered by the

MIT Energy Laboratory

Energy Laboratory Report No: MIT-EL 82-008

Nuclear Engineering Department Report No: MITNE-249

Under Contract No.

80-499-E

February 1982

Other reports of interest:

Prospects for the Recovery of Uranium from Seawater

F. Best, M. Driscoll  
MIT-EL-80-001  
January 1980

Proceedings of a Topical Meeting on the Recovery of  
Uranium from Seawater

F. Best, M. Driscoll (editors)  
MIT-EL-80-031  
December 1980

Systems Studies on the Extraction of Uranium from Seawater

M. Driscoll, F. Best  
MIT-EL-81-038  
November 1981

Delayed Neutron Assay to Test Sorbers for Uranium-  
from-Seawater Applications

C. Nitta, F. Best, M. Driscoll  
MIT-EL-82-008  
February 1982

These reports may be ordered from:

Massachusetts Institute of Technology  
Energy Laboratory Information Center  
Report Distribution E40-400  
77 Massachusetts Avenue  
Cambridge, MA 02139  
U. S. A.

DELAYED NEUTRON ASSAY  
TO TEST SORBERS FOR  
URANIUM-FROM-SEAWATER APPLICATIONS

by

C.K. NITTA, F.R. BEST and M.J. DRISCOLL

Abstract

Delayed Fission Neutron (DFN) assay has been applied to the measurement of uranium content in sorbers exposed to natural seawater for the purpose of evaluating advanced ion exchange resins. DFN assay was found to be particularly suitable for such testing because it is selective, non-destructive, yields quantitative results in the submicrogram range, and requires relatively simple sample preparation. Surplus components for a DFN system were obtained from the Lawrence Livermore National Laboratory, modified, re-assembled, and calibrated for use with M.I.T. irradiation facilities, following which procedures were developed, evaluated and applied to the experiments at hand.

Four experimental ion exchange resins developed by the Rohm and Haas (R&H) Company specifically for uranium-from-seawater applications were evaluated, together with hydrous titanium oxide (HTO), the leading inorganic sorber for this purpose. Two types of tests using natural seawater were employed: batch loading experiments (paralleling similar tests done by R&H), and fixed-bed column loading experiments using a test facility at the Woods Hole Oceanographic Institute (WHOI). While some qualitatively consistent trends were evident among the various experiments, important quantitative inconsistencies were noted. The WHOI tests most closely approximated true in-service conditions; hence, more importance is assigned to these results.

The MIT/WHOI tests confirmed 1.5 mm HTO particle bed uptake of approximately 300 ppm U for a 30 day exposure, in good agreement with the results reported by other laboratories, worldwide. An anion exchange resin employing an amidoxime functional group also achieved this level of performance, and, in addition, exhibited considerably superior mechanical properties. Moreover, the resin performance is expected to improve when its properties are optimized for the present application.

## ACKNOWLEDGEMENTS

This work was performed as part of the "Uranium-from-Seawater Project" carried out by the M.I.T. Energy Laboratory/Nuclear Engineering Department under contract to the U.S. Department of Energy, Grand Junction Office, Bendix Field Engineering Corporation. The work presented in this report has been performed by the Principal author, Cynthia K. Nitta, who has submitted substantially the same report in partial fulfillment of the requirements for the SM degree in Nuclear Engineering at MIT.

This report constitutes the final report for FY 1981 under the subject contract. Attention is also called to the companion topical report: "Systems Studies on the Extraction of Uranium from Seawater" by M.J. Driscoll and F.R. Best, MIT-EL81-038, MITNE-248, November 1981. We would like to thank the MIT Nuclear Reactor Laboratory personnel for their assistance, in particular Mr. Kwan Kwok, Mr. Emmett Robb and Mr. William Fecych. Laboratory work was greatly facilitated by advice from Mr. Anthony Mendoza at the Woods Hole Oceanographic Institute and Dr. Stephen G. Maroldo at the Rohm and Haas Company. Typing was ably handled by Ms. Linda Clapp.

## NOTICE

This report was prepared as an account of work sponsored by the United States Government. Neither the United States nor the United States Department of Energy, nor any of their employees, nor any of their contractors, subcontractor, or their employees, makes any warranty, express or implied, or assumes any legal liability or responsibility for the accuracy, completeness or usefulness of any information, apparatus, product or process disclosed, or represents that its use would not infringe privately owned rights.

## TABLE OF CONTENTS

Abstract.....	3
Acknowledgements.....	4
Table of Contents.....	5
List of Figures.....	9
List of Tables.....	11
Chapter 1	Introduction..... 12
1.1	Foreword..... 12
1.2	Background..... 14
1.2.1	Choice of Counting Method..... 14
1.2.2	Principles of Delayed Fission Neutron Counting..... 14
1.2.3	Application to Resin Performance Testing..... 19
1.2.4	Advantages of Sorber Capacity Loading Experiments in Natural Seawater..... 21
1.3	Outline of the Organization of the Present Work..... 22
Chapter 2	Delayed Fission Neutron Counting System... 24
2.1	Introduction..... 24
2.2	Irradiation and Counting Facilities..... 24
2.2.1	Description of the Irradiation Facility..... 24
2.2.2	Origins of the DFN Counting System. 28
2.3	Delayed Fission Neutron Counting System... 29
2.3.1	Description of Detector and Counter..... 29
2.3.2	Calibration of Electronics..... 32
2.3.2.1	Detector Plateau Curves... 32
2.3.2.2	Counter Threshold Setting. 34



	2.3.2.3	Calibration of Detectors with Neutron ( $^{252}\text{Cf}$ ) and Gamma Ray ( $^{60}\text{Co}$ ) Sources..	34
2.4		Delayed Neutron Irradiation and Counting..	35
	2.4.1	Background Count Determination -- Contribution from Cosmic Radiation and Laboratory Background.....	35
	2.4.2	Contribution from Polyethylene Contamination.....	36
	2.4.3	Neutron Absorption in Sorbers.....	38
		2.4.3.1 Unloaded Sorber Counting..	38
		2.4.3.2 Effect of Varying Sorber Weight with Constant Uranium Content.....	40
	2.4.4	Uranium Standards for Calibration..	44
		2.4.4.1 Introduction.....	44
		2.4.4.2 Uranium Dioxide ( $\text{UO}_2$ ) Preparation.....	46
		2.4.4.3 Uranyl Nitrate ( $\text{UO}_2(\text{NO}_3)_2 \cdot$ $6\text{H}_2\text{O}$ ) Preparation.....	47
		2.4.4.4 NBS Uranium Standard.....	52
	2.4.5	Normalization to a Common Flux Level.....	53
	2.4.6	Reproducibility.....	55
		2.4.6.1 Geometric Considerations..	55
		2.4.6.2 Electronic Stability.....	56
2.5		Summary.....	58
Chapter 3		Sorber Loading Experiments.....	59
	3.1	Introduction.....	59
	3.2	Seawater Sampling and Uranium Content Determination.....	60
		3.2.1 Massachusetts Baywater.....	60
		3.2.2 Woods Hole Seawater.....	60
		3.2.3 Seawater Uranium Content Determination.....	61
	3.3	Equilibrium Experiments.....	63
		3.3.1 Purpose.....	63
		3.3.2 Seawater Filtration.....	63
		3.3.3 Sorber Preparation and Processing..	64
	3.4	Column Experiments.....	65
		3.4.1 Design Objectives and Problems.....	65
		3.4.2 Description of Fixed-Bed Columns...	66
		3.4.3 Maintenance.....	70

	3.4.3.1	System Fouling due to Algae.....	70
	3.4.3.2	Oxidation of Metal Components.....	71
	3.4.3.3	Loading Operation.....	72
	3.4.3.4	Seawater Temperature Variations.....	73
	3.4.4	Preparation of Column Sorber Samples for Irradiation.....	73
	3.5	Summary.....	74
Chapter 4		Results and Discussion.....	76
	4.1	Introduction.....	76
	4.2	Seawater Uranium Content.....	76
	4.3	Sorber Performance.....	78
	4.3.1	Equilibrium Experiments.....	78
	4.3.2	Column Experiments.....	85
	4.4	Summary.....	91
Chapter 5		Conclusions and Recommendations.....	93
	5.1	Introduction.....	93
	5.2	Delayed Fission Neutron (DFN) Counting System.....	94
	5.3	Column Loading Experiment.....	98
	5.4	Sorber Performance and Development.....	100
	5.5	Conclusion.....	105
References			106
Appendices			108
	A.1	Data: Contributions to Background.....	109
	A.1.1	Polyethylene Uranium Contamination.....	109
	A.1.2	Neutron Absorption in Sorbers: Unloaded Sorber Counting.....	110
	A.1.3	Neutron Absorption in Sorbers: Effect of Varying Sorber Weight with Constant Uranium Content.....	111

A.2	Uranium Calibration Data.....	112
A.2.1	Average Neutron Flux Normalization Factors.....	112
A.2.2	Uranium Dioxide and Uranyl Nitrate Data.....	113
A.2.3	Uranium Dioxide Error Calculation..	117
A.2.4	Uranyl Nitrate Error Calculation...	118
A.3	Sorber Loading Data.....	121
A.3.1	Sample Normalization and Uranium Content Calculation, and Discussion of the Propagation of Uncertainties.....	121
A.3.2	Equilibrium Experiment Loading Data.....	124
A.3.3	Column Experiment Loading Data.....	125
A.3.4	Properties of Sorbers after 16 Hours in Seawater from Experiments Performed by the Rohm and Haas Company.....	126
A.3.5	Equilibrium Experiment: Rohm and Haas Company Laser-Induced Fluorescence Measurement.....	127
B.	Minimum Level of Detection.....	128
C.	User's Guide to the Delayed Fission Neutron (DFN) Counting Facility.....	133
D.	Rohm and Haas Company Report: Extraction of Uranium from Seawater with Synthetic Ion Exchange Resins.....	141

## LIST OF FIGURES

<u>Figure No.</u>	<u>Title</u>	<u>Page</u>
2.1	Schematic of Irradiation and Counting Facilities	26
2.2	Schematic of Reuter-Stokes $^3\text{He}$ Detectors	30
2.3	Schematic of $^3\text{He}$ Tube Array	31
2.4	Delayed Neutron Detector Circuit Diagram	33
2.5	Polyethylene Rabbit and Vials	37
2.6	Polyethylene Contamination: Plot of Net Counts/Minute versus Polyethylene Weight	39
2.7	Blank Resin Neutron Absorption: Plot of Net Counts versus Resin Weight	41
2.8	Resin Neutron Absorption: Plot of Net Counts/Minute versus Resin Weight for Constant Uranium Content	43
2.9	Uranium Dioxide as a Calibration Standard: Plot of Net Counts/Minute/gmU versus gmU	48
2.10	Uranyl Nitrate as a Calibration Standard: Plot of Net Counts/Minute/gmU versus gmU	51
3.1	Schematic of an Ion-Exchange Column Installed at the Woods Hole Oceanographic Institute	65
3.2	Schematic of Plexiglass Ion-Exchange Column Section	69
4.1	Equilibrium Experiment: Plot of Net Counts/Minute/gm sorber versus Sorber Weight per Liter of Natural Seawater (2.9 ppb) for HTO and XE318	79
4.2	Equilibrium Experiment: Plot of Net Counts/Minute/gm sorber versus Sorber Weight per Liter of Natural Seawater (2.9 ppb) for AID, SGM245 and SGM251	80
4.3	Column Experiment: Plot of Uranium Content versus Natural Seawater Exposure Time	87

4.4

Column Experiment: Plot of Uranium Content  
versus Natural Seawater Volume Exposure

89

## LIST OF TABLES

<u>Table No.</u>	<u>Title</u>	<u>Page</u>
1.1	Delayed Neutron Precursor Groups: Abundances and Half-lives for Thermal Fission of $^{235}\text{U}$	17
2.1	Normalization Factors used to Correct for Variability in Neutron Flux	54
5.1	Comparison of M.I.T. and Rohm and Haas Company Data on Sorber Performance	104

## CHAPTER I

## INTRODUCTION

1.1 Foreword

The development of an economically viable process for the recovery of uranium from seawater has become of increasing interest in recent years because of uncertainties in the future supply of moderate cost conventionally-mined uranium ores, the slow pace toward deployment of fuel recycle and breeder reactors, and a slackening of enthusiasm for advanced fossil fuel alternatives. It is estimated that there are 4 billion short tons of yellow cake uranium equivalent in the oceans, enough to sustain thousands of light water reactors of current design for thousands of years. Through extensive research into the recovery of this resource, primarily in Europe and in Japan, it has become clear that present mass transfer technologies of the fixed and fluidized-bed types must be substantially improved and carefully optimized if they are to be utilized in an economic uranium-from-seawater extraction process (B2). As suggested by Best and Driscoll (B3), the recovery cost is highly dependent upon the uranium loading capacity and kinetics of the sorber used in the recovery bed: high sorber capacity reduces the frequency and increases the yield of the elution process, and faster

kinetics permit high rates of loading and product recovery.

Motivated by these considerations, a joint effort between the Nuclear Engineering Department/Energy Laboratory of the Massachusetts Institute of Technology and the Rohm and Haas Company, was started under U.S. Department of Energy sponsorship with the primary objective of developing a sorber material for uranium-from-seawater applications which is superior to the hydrous titanium oxide (HTO) currently regarded as the material of choice. Four ion exchange resins having two different chemical functional groups on two different polymer supports were chosen from several candidate sorbers manufactured and screened at the Rohm and Haas Company. These resins were evaluated at M.I.T. (in comparison with alkali-stabilized HTO obtained from Uranerzbergbau-GmbH), for mechanical, loading and kinetic performance in natural seawater experiments. The present work describes the design, fabrication and execution of sorber loading experiments performed at M.I.T. and at the Woods Hole Oceanographic Institute, and the development of a delayed fission neutron counting facility and procedure to measure the uranium content and other performance characteristics of the loaded sorbers.



## 1.2 Background

### 1.2.1 Choice of Counting Method

Analysis of trace quantities of fissionable materials in chemical complexes found in nature has been a subject of extensive research and development. Such analyses can be carried out by various methods, including spectrophotometry, colorimetry, polarography, fluorimetry, and fission track-etch methods (A2). However, these methods can be time-consuming and can require elaborate chemical processing of samples prior to measurement. Although generally limited to fissionable nuclides, the delayed fission neutron technique offers several advantages over these methods, including the capability of rapid, nondestructive, and repeatable analyses, low sensitivity to gamma radiation interference, minimum levels of detection in the nanogram range (B4), and minimal activation of samples.

### 1.2.2 Principles of Delayed Fission Neutron Counting

When a heavy nuclide absorbs a neutron and undergoes fission, a small fraction of the fission products decay by neutron emission. These delayed neutron emitters or precursors can be categorized into six groups with half-lives ranging from fractions of a second to just under a minute. For thermal fission of  $^{235}\text{U}$ , the delayed neutron yields and

half-lives are shown in Table 1.1. These neutrons can be used to measure the amount of fissile material in a sample which is irradiated in a neutron flux and rapidly transferred to a neutron detector system for counting.

The total number of counts for a given detector system and specified irradiation, decay and counting times is given by (B1):

$$C_T = (\epsilon v m N_A \sigma_f \phi / A) \sum_{i=1}^6 [(\beta_i / \lambda_i) (1 - e^{-\lambda_i t_0}) (e^{-\lambda_i t_i}) (1 - e^{-\lambda_i \Delta t})] + B \quad (1.1)$$

- where
- $\epsilon$  = intrinsic plus geometric efficiency of the counting system (counts per delayed neutron emitted during the counting period)
  - $v$  = average number of neutrons emitted per fission
  - $m$  = mass of fissionable nuclide (grams)
  - $N_A$  = Avogadro's number
  - $\sigma_f$  = microscopic fission cross section of the fissionable nuclide ( $\text{cm}^2$ )
  - $\phi$  = neutron flux at sample exposure site ( $\frac{\text{neutrons}}{\text{cm}^2 \cdot \text{sec}}$ )
  - $A$  = atomic mass number of the fissionable nuclide
  - $\beta_i$  = fraction of delayed neutrons emitted in group  $i$
  - $\lambda_i$  = decay constant of delayed neutron precursor group  $i$  ( $\text{sec}^{-1}$ )
  - $t_0$  = irradiation time (seconds)

$t_i$  = decay time (seconds)

$\Delta t$  = counting time (seconds)

B = total background

It can be seen that the counts vary linearly with the mass of the fissionable nuclide.

If the neutron flux and the fissionable mass are known, then the efficiency can be calculated from the measured counts. Alternatively, as is more often the case, the counting system can be calibrated using a standard of known composition. Equation 1.1 holds for a single irradiation, decay, and counting cycle. Samples can be put through any number of cycles to improve counting statistics. In the present work, single cycles were employed because of limitations in sample transfer and timing capabilities.

To maximize the count, the parameters  $\phi$ ,  $\nu$ ,  $t_0$ ,  $t_1$ , and  $\Delta t$  can be varied. The neutron flux,  $\phi$ , depends on the available irradiation facility and should be as high as possible. The intrinsic and geometric efficiency,  $\epsilon$ , depends on the design of the detectors, the moderating material in which they are imbedded, and their electronics; it also depends on the positioning of the sample within the detector assembly (as will be discussed in detail later). The irradiation time should be about three half-lives of the most abundant delayed neutron group of interest so that the production of that

Table 1.1  
Delayed Neutron Properties for Thermal Fission of  $U^{235}$

---

<u>Group</u>	<u>Half-Life (Seconds)</u>	<u>Fractional Yield (<math>\beta</math>)</u>
1	55.72 $\pm$ 1.28	0.000215 $\pm$ 0.000020
2	22.72 $\pm$ 0.71	0.001424 $\pm$ 0.000059
3	6.22 $\pm$ 0.23	0.001274 $\pm$ 0.000143
4	2.30 $\pm$ 0.09	0.002568 $\pm$ 0.000072
5	0.610 $\pm$ 0.083	0.000748 $\pm$ 0.000059
6	0.230 $\pm$ 0.025	0.000273 $\pm$ 0.000052

---

precursor group will approach saturation. For  $^{235}\text{U}$ , this is group number two, with a half-life of  $22.72 \pm 0.71$  seconds.

(Although group four has a higher yield, its 2.30 second half-life is too short to allow for handling time and decay of short-lived gamma interference.) As the irradiation time is increased, the net count reaches an asymptotic maximum. The minimum decay time is controlled by interference from  $^{17}\text{N}$  neutron and gamma ray emission with a 4.16 second half-life ( $^{17}\text{N}$  is produced by the  $^{17}\text{O}$  (n,p) reaction), and from  $^{16}\text{N}$  gamma ray emission with a 7.11 second half-life ( $^{16}\text{N}$  is produced by the  $^{16}\text{O}$  (n,p) reaction); this rules out decay times less than about 20 seconds. This limitation arises in part because the detector, in the present work, was calibrated to discriminate against  $^{60}\text{Co}$  gamma rays which have energies of 1.17 and 1.33 MeV, much lower than that of the  $^{16}\text{N}$  gammas which have energies of 6.13 and 7.11 MeV. For a decay time on the order of 60 seconds, these interferences from  $^{17}\text{N}$  and  $^{16}\text{N}$  have decayed enough to be considered negligible. However, the 2.75 MeV and 1.37 MeV gamma rays from  $^{24}\text{Na}$  are still a problem, and are discussed elsewhere (see Section 3.2, Sea-water Sampling and Uranium Content). Another constraint on the minimum decay time involves the sample transfer and handling time. After irradiation, the sample is held for 15 seconds to determine if its activity is low enough to be transferred to the Nuclear Chemistry Lab (NW13-207) via a pneumatic tube. By the time it reaches the experimenter in NW 13-207, the sample has already decayed for 18 to 20 seconds. Manual transfer

of the sample from the receive station to the detector takes another five seconds if the sample is left in the rabbit for counting. Therefore, a standard total decay time of about 60 seconds ensures an adequate interval allowing for transfer and handling procedures. On the high side, the decay time is limited by the decrease in the ratio of net to background counts due to the decay of the delayed neutron precursors. The same ratio decreases with increasing counting time for the same reason.

Hence, the selection of an optimum set of operating parameters involves a complicated compromise among several competing parameters. The values employed in the present work represent a typical compromise, namely: irradiation time = 60 seconds, delay time = 60 seconds, counting time = 60 seconds.

### 1.2.3 Application to Resin Performance Testing

The delayed fission neutron (DFN) counting method is a convenient technique for measuring the uranium content in solids when the  $U^{235}$  content (or that of another fissionable species of interest) is greater than about 0.01 ppm. Samples merely have to be weighed and encapsulated in measuring vials for counting. Some samples might additionally require concentration prior to analysis.

Sorbers loaded with uranium from seawater can thus be analyzed for uranium content very easily with this technique, if there are appropriate irradiation and counting facilities available. The technique does not require large amounts of sorber sample for measurement, and irradiated samples can be retained for additional evaluation since the activation of the samples is minimal and the samples do not have to be physically or chemically altered during the measurement process. A further advantage of this technique in sorber loading measurements is its nondestructive nature. Some equilibrium experiments in the present work produced as little as 0.1 gram of loaded sorber for evaluation. Thus, the samples could not only be measured by the DFN technique, but could also be measured using alternative methods for comparison. This is possible because a negligible amount of the fissionable nuclide of interest is actually consumed during a single irradiation and counting procedure when the irradiation is on the order of a few minutes or less.

Application of this approach to the measurement of uranium in seawater samples is not as convenient as for sorber samples because of sodium activation and high energy gamma ray interference during handling and counting, and the generally lower uranium concentration involved. These problems are discussed elsewhere (see Sections 1.2.2, Principles of Delayed Fission Neutron Counting, and 3.2, Seawater Sampling and Uranium Content).

#### 1.2.4 Advantages of Sorber Capacity Loading

##### Experiments in Natural Seawater

Uranium in seawater is found primarily in the dissolved state in the form of a uranyl tricarbonate ion,  $\text{UO}_2(\text{CO}_3)_3^{-4}$ . The rate of mass transfer is generally related to the difference in concentration of the chemical species involved between the solution and sorber phases. If the concentration of the uranium-bearing ion in loading experiments is greater than that found in natural seawater, then the rate of mass transfer will be increased and the kinetic characteristics observed under experimental conditions will be different from those observed under natural, and therefore practical operating conditions. Furthermore, the maximum value of the uranium capacity will be affected by the magnitude of the driving force for mass transfer; sorbers loaded in solutions of higher concentration will generally demonstrate a higher capacity than those loaded in a solution of lower concentration. Many of the experiments conducted to date to quantify the performance of sorber candidates for potentially economic uranium extraction processes have used spiked concentrations of uranium in their seawater solutions (M2, S1, Y1). Coprecipitation of uranium with hydrous titanium oxide has been demonstrated to be as much as 30% higher in spiked 50 ppm seawater solutions than in natural



seawater (01). Thus, the concentration of the seawater in which sorbers are tested greatly affects their measured loading properties. If sorbers are to be used in natural seawater extraction processes, then experimental testing in seawater of natural uranium concentration is essential.

### 1.3 Outline of the Organization of the Present Work

The present work is organized into chapters, sections, and subsections detailing the development of a Delayed Fission Neutron (DFN) counting system and the sorber loading experiments conducted at M.I.T. to test candidate sorbers for uranium-from-seawater applications. Chapter 2 presents a description of the irradiation and counting facilities, along with the procedures required for calibration of the counting system. The development of background and uranium standards for counting calculations are then discussed, and the processes by which the data are normalized to a common neutron flux condition and evaluated for reproducibility are presented. Chapter 3 details the equilibrium and ion-exchange column experiments which provide the uranium-loaded sorber samples to be counted by the DFN system. Chapter 4 summarizes the results of the loading experiments and explains how the uranium concentration of the natural seawater used in those experiments was determined. In Chapter 5, the

implications of the results presented in the previous chapter are discussed, together with an evaluation of the column loading and DFN counting system, and conclusions and recommendations. The Appendices document detailed numerical data from all of the experimental procedures described above. A report summarizing the work done by the Rohm and Haas Company is included in the present work in Appendix D. Appendix C is the user's manual for the DFN counting system.

## CHAPTER II

## DELAYED FISSION NEUTRON COUNTING SYSTEM

2.1 Introduction

In the previous chapter, the objectives of the present work were stated and a general discussion of the theory of the delayed fission neutron (DFN) technique was presented. In this chapter, the details of the DFN counting system and its calibration will be discussed. The development of a reliable uranium calibration standard will then be described. Finally, considerations important to the calculation of sorber uranium content and the reliability of such measurements are described.

2.2 Irradiation and Counting Facilities2.2.1 Description of the Irradiation Facility

The MITR-II Research Reactor is a 5MW thermal H<sub>2</sub>O moderated, D<sub>2</sub>O and graphite reflected unit fueled by highly enriched plate-type aluminum fuel; the LPH1 irradiation facility is a pneumatic tube system which extends into the graphite reflector region. Samples are placed in a small rabbit (4.4 cm O.D. x 8.9 cm long) and inserted or ejected from the reactor irradiation site with differential air pressure applied through the pneumatic tubes. This insertion can be performed from the

Nuclear Chemistry Laboratory (NW 13-207) or at the send station in the Secondary Chemistry Area within the reactor containment building. The components of the irradiation and counting facilities are shown schematically in Fig. 2.1.

The rabbits are inserted tangentially to the reactor core to help insure that the longitudinal flux gradient is small. The radial flux gradient would be expected to be greater than the longitudinal gradient, but because the vials inside the rabbits typically have small diameters (in the present work, 1.1 cm and 1.3 cm, O.D. for resin, uranyl nitrate and  $\text{UO}_2$  samples and 1.6 cm for large polyethylene samples), the absolute difference in the flux should be as small radially as it is longitudinally. Measurement of the flux gradient by Almasoumi (A1) showed a maximum decrease of 5% in the thermal flux between the positions 2 cm and 6 cm from the near reactor end of the pneumatic tube. The radial flux, measured in the epithermal energy region only, was found to vary as much as 25% over a radial distance of 0.5 cm. Hence, it is clear that the geometry of the sample under irradiation is crucial to the accuracy and reproducibility of measurement. Geometric considerations are discussed in greater depth elsewhere (see Section 2.4, Reproducibility: Geometric Considerations).

After insertion into the pneumatic tube at the send station, the rabbit containing the sample is exposed to a

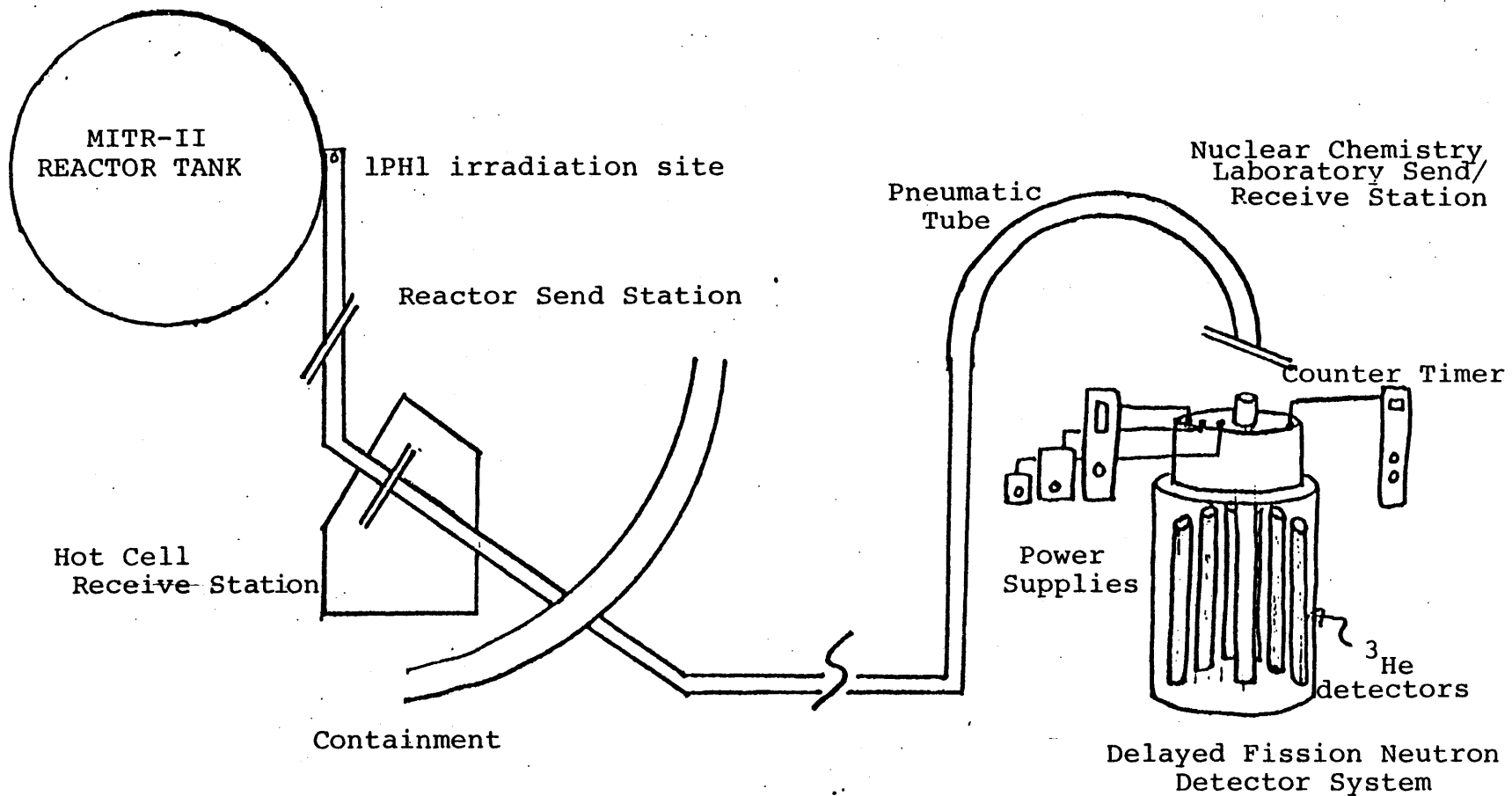


Fig. 2.1 Schematic of Irradiation and Counting facilities.

neutron flux of approximately  $8 \times 10^{12}$  neutrons/cm<sup>2</sup> . sec for a time period set either by the operator at the send station or by the experimenter in NW 13-207(R1). Air is continuously flowing in the LPH1 tube, to cool the rabbit and to keep it positioned at the end of the tube closest to the reactor core. After the set irradiation time has passed, the rabbit is automatically ejected from the reactor into the hot cell (a lead brick enclosed area) next to the reactor send station. (The ejection can also be performed manually. Manual ejection overrides automatic ejection.) Inside the hot cell, a Geiger-Müller area monitor measures the activity level at the end of a period of time specified by a timer inside the reactor control room. In the present work, the timer was set to fifteen seconds, although it can be set to any time interval between zero and sixty seconds. If, after fifteen seconds, the exposure dose rate was greater than  $10 \text{ mR/hr}$  at a meter, then the 'send' to NW 13-207 was to be aborted and the sample would remain inside the hot cell. Otherwise, with the blower turned on, the sample would arrive in NW 13-207 in 17 to 20 seconds after ejection from the reactor. In NW 13-207, an automatic decay timer is triggered by a photo-sensitive switch as the rabbit leaves the reactor. Upon arrival in NW 13-207, another switch closes a valve to stop the flow of air in the pneumatic tube, and the rabbit drops into a lead-brick enclosed send/receive station under the force of gravity.

From the preceding, it is clear that the decay time is limited to greater than about twenty seconds by the physical transfer time from the reactor to NW 13-207, primarily because of the fifteen second holding time in the hot cell. This holding time could be reduced as long as the samples gave an acceptably low dose to the experimenter upon arrival in NW 13-207.

#### 2.2.2 Origins of the DFN Counting System

The detector assembly whose description follows was obtained on loan from the Grand Junction, Colorado, office of the Department of Energy (DOE). It was designed and used previously by the Lawrence Livermore National Laboratory (LLNL) from 1977 to 1979 when they participated in the National Uranium Resource Evaluation (NURE) Program established by the Atomic Energy Commission (later the Energy Research and Development Administration, now the DOE), to evaluate domestic uranium resources. At LLNL, approximately 30,000 solid and liquid samples were analyzed using this detector system (along with a gamma coincidence counting system) to measure uranium content down to a lower limit of 0.01 and 0.0001 ppm uranium for solids and liquids, respectively. LLNL reduced background interference by lowering the entire detector assembly into a deep hole in the ground far from the reactor and surrounding the detector with concrete shielding.

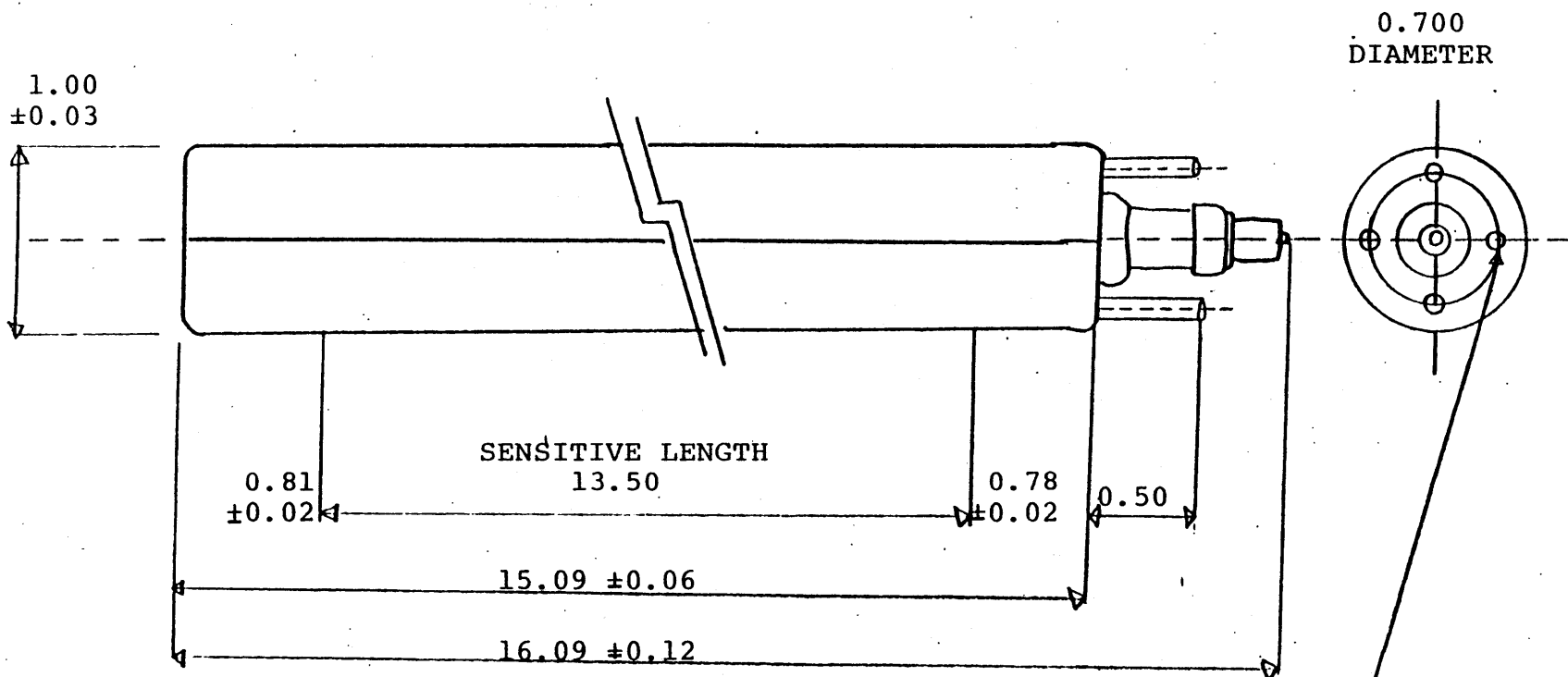
## 2.3 Delayed Fission Neutron Counting System

### 2.3.1 Description of Detector and Counter

The delayed fission neutron detector consists of twenty Reuter-Stokes  $^3\text{He}$  'proportional counters' (see Fig. 2.2) arranged in a radial array around the central rabbit-holding tube (see Fig. 2.3). A removable rabbit holder sits within the central tube which, along with the  $^3\text{He}$  tubes, is embedded in a polyethylene neutron moderator. The central rabbit-holding tube is surrounded by approximately 4.45 cm of lead. On top of the polyethylene detector assembly sits the electronic circuitry which processes the signals leaving the detectors. The  $^3\text{He}$  tubes are powered by a variable high-voltage power supply (ORTEC model 459). The  $\pm 15$  volt and + 5 volt logic power supplies are connected through BNC leads to the top of the detector assembly. The output signals from the tubes are summed and leave the detector assembly through a BNC cable to a counter-scaler (Tennelec model TC 545A) which must be set for the desired counting time and input signal threshold magnitude.

The electronics and detector were mounted on a movable cart for transport between experimental, diagnostic and storage sites. The irradiated samples were received from the 1PH1 tube and counted in the Nuclear Chemistry Laboratory (room NW 13-207). No additional shielding was placed around the assembly to shield against atmospheric neutrons or high-energy gamma rays, because the minimum level of detection was found to be approximately  $9 \times 10^{-9}$  grams of  $^{235}\text{U}$  (see Appendix B),





FILL GAS PRESSURE: 4 ATM  
 NEUTRON SENSITIVITY: 32 CPS/nV  
 PLATEAU: LENGTH = > 300 V  
           SLOPE = < 2%/100 V  
 RANGE: 1100 - 1300 V  
 MATERIAL: 304 STAINLESS STEEL

0.06 DIAMETER  
 EXHAUST TUBE  
 0.50 LONG ON  
 0.349 RADIUS

Fig.2.2 Schematic of the Reuter-Stokes <sup>3</sup>He Proportional Counter  
 (All dimensions in inches).

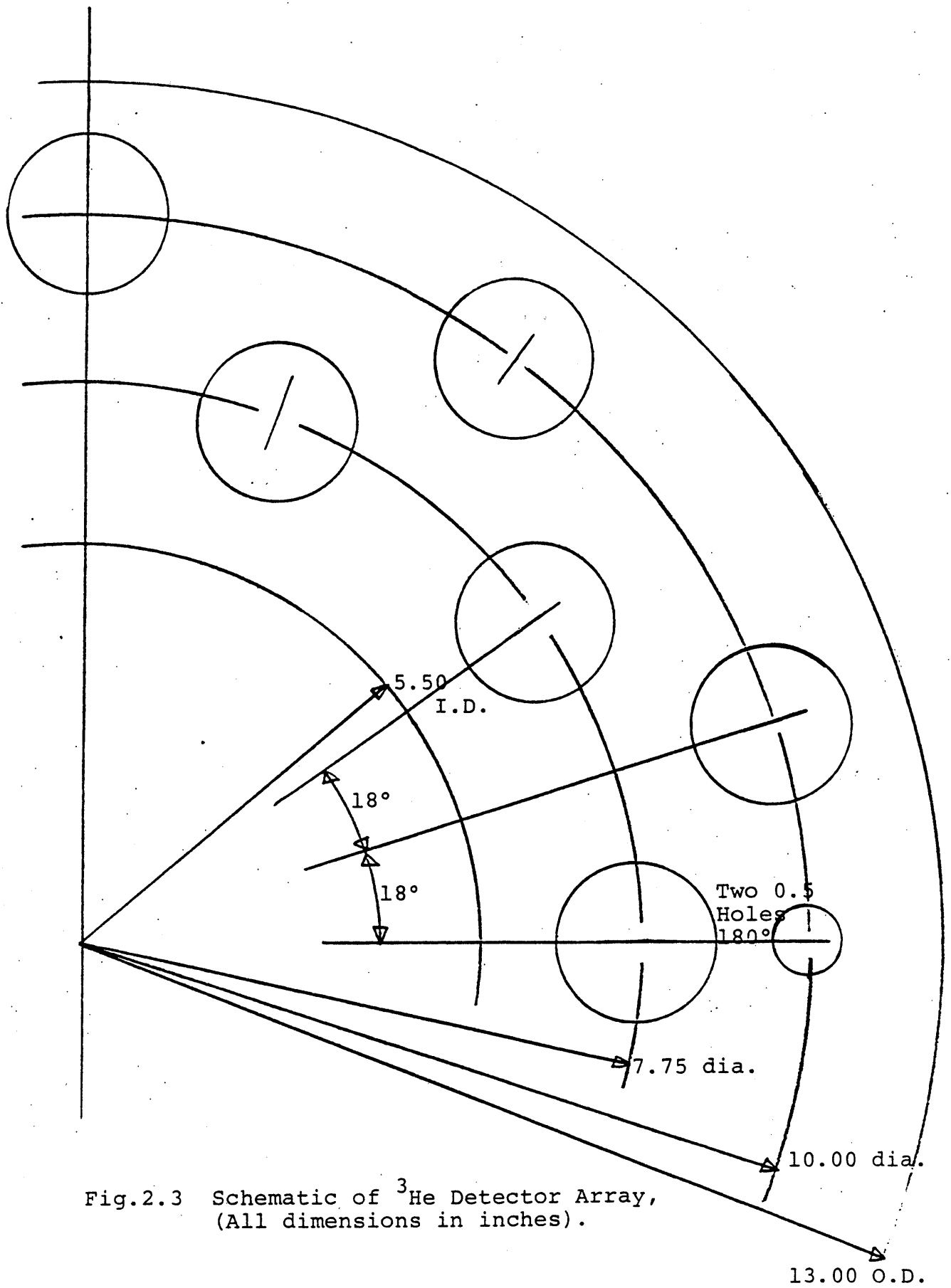


Fig.2.3 Schematic of  $^3\text{He}$  Detector Array,  
(All dimensions in inches).

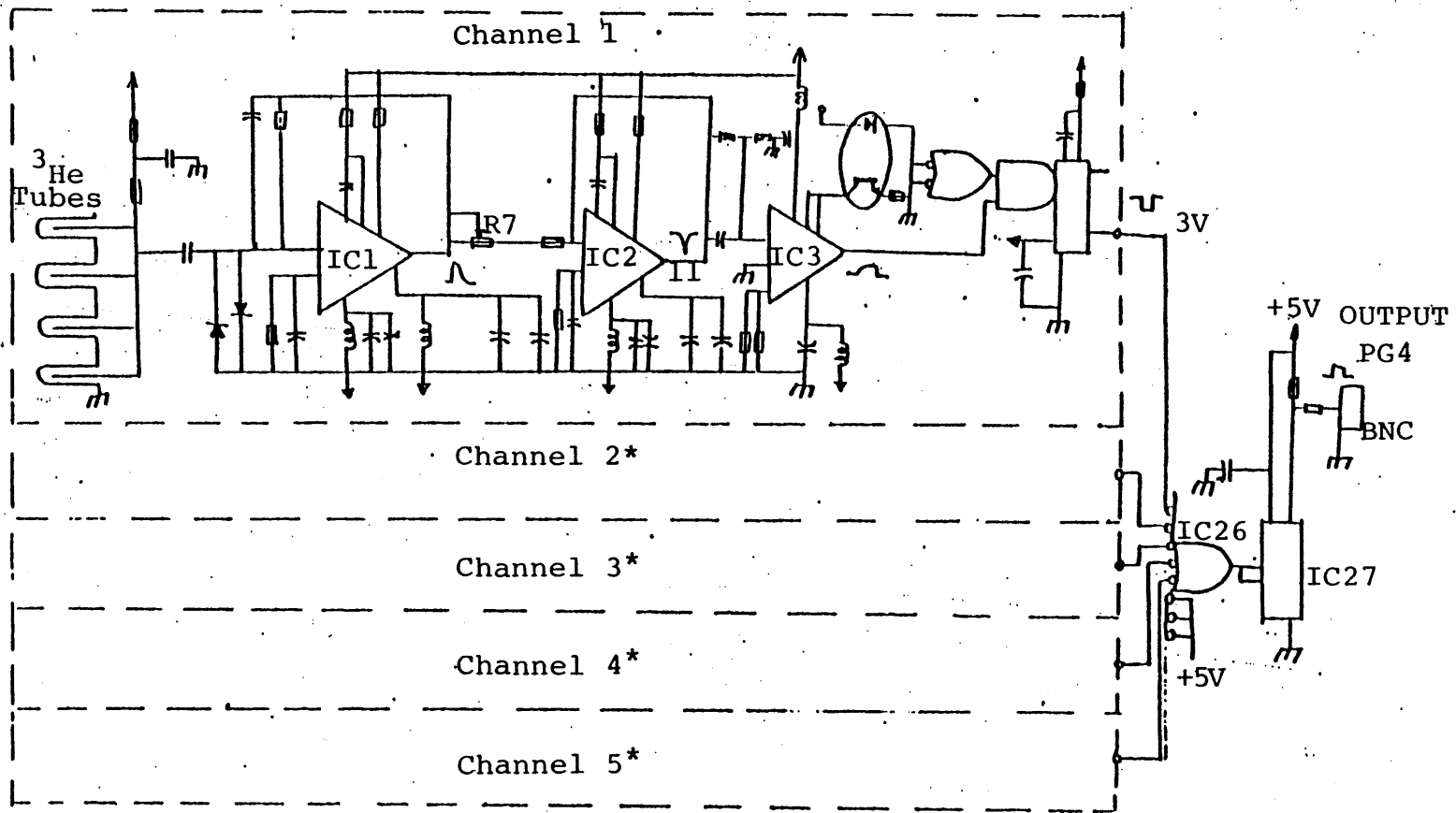
a sufficient sensitivity for the current application. Moreover, the "total background" was dominated by activity contributed by the polyethylene rabbit used to hold the sample - a component not ameliorated by external shielding. Also, shielding would have resulted in only a slightly improved sensitivity, since the minimum level of detection is proportional to the square root of the background. These considerations plus the additional weight of the shielding led to a decision to forego its use, at least in the near term.

### 2.3.2 Calibration of Electronics

#### 2.3.2.1 Detector Plateau Curves

The twenty  $^3\text{He}$  tubes are organized electronically into five groups of four on circuit cards extending radially round the central rabbit tube. Output signals from each card are summed at integrated circuit (IC) number 26 (see circuit diagram, Fig. 2.4).

Plateau curves of counts per set counting time were made for each set of four tubes to determine the high voltage operating range which would provide the greatest counting stability with respect to small fluctuations in voltage. To accomplish this, all cards except the card of interest were disconnected at the inputs of the summing gate (IC26), and a plateau curve was determined for a single card. Since the



\*(Channels 2 through 5 are identical to Channel 1).

Fig. 2.4 Delayed Neutron Detector System  
Circuit Diagram

high voltage is applied to all of the tubes simultaneously, the set voltage should lie on the plateau of counts versus voltage for all of the cards. The high voltage value was chosen to be 1260 volts. The manufacturer, Reuter-Stokes, specifies an operating range of 1100 to 1300 volts for these tubes. (Specifications for the tubes are given in Fig. 2.2.) For the physical mechanisms involved in the detection of neutrons using  $^3\text{He}$  tubes, see Knoll (K1).

#### 2.3.2.2 Counter Threshold Setting

With the high voltage power supply setting at 1260 volts, the output signals from the detector assembly (PG 4, see Fig. 2.4) are positive square waves of 3.5 volts and 1.5 microseconds in magnitude and duration, respectively. The threshold setting on the Tennelec TC 545A counter-scaler must be set such that it will count pulses of this magnitude and polarity.

#### 2.3.2.3 Calibration of the Detectors with Neutron ( $^{252}\text{Cf}$ ) and Gamma-ray ( $^{60}\text{Co}$ ) Sources

A schematic circuit diagram of the electronics which make up the delayed neutron detector system (not including the counter/timer) is shown in Fig. 2.4. The magnitude of the signal at the output of IC2 for each set of four  $^3\text{He}$  tubes is regulated by a variable resistor (numbered R7). This resistance must be adjusted to maximize the signal to noise ratio

of neutron versus gamma-induced pulses. Generally, the gamma pulses are of lower energy than the neutron pulses. These signals were simulated by using a  $^{252}\text{Cf}$  neutron source (activity  $\approx 5\mu\text{Ci}$ ) and a  $^{60}\text{Co}$  gamma-ray source (activity  $\approx 16\mu\text{Ci}$ ).  $^{60}\text{Co}$  produces gamma rays of energies 1.17 and 1.33 MeV.

An oscilloscope was used to monitor the signal along the circuit and the signal at IC2, pin 11, was adjusted to a magnitude of -0.3 volts for the  $^{60}\text{Co}$  1.33 MeV gamma-rays compared to -4.5 volts for the  $^{252}\text{Cf}$  neutron pulses. This resulted in acceptance of the output pulse for the neutrons, and rejection of that due to gamma rays.

## 2.4 Delayed Neutron Irradiation and Counting

### 2.4.1 Background Count Determination - Contribution from Cosmic Radiation and Laboratory Background

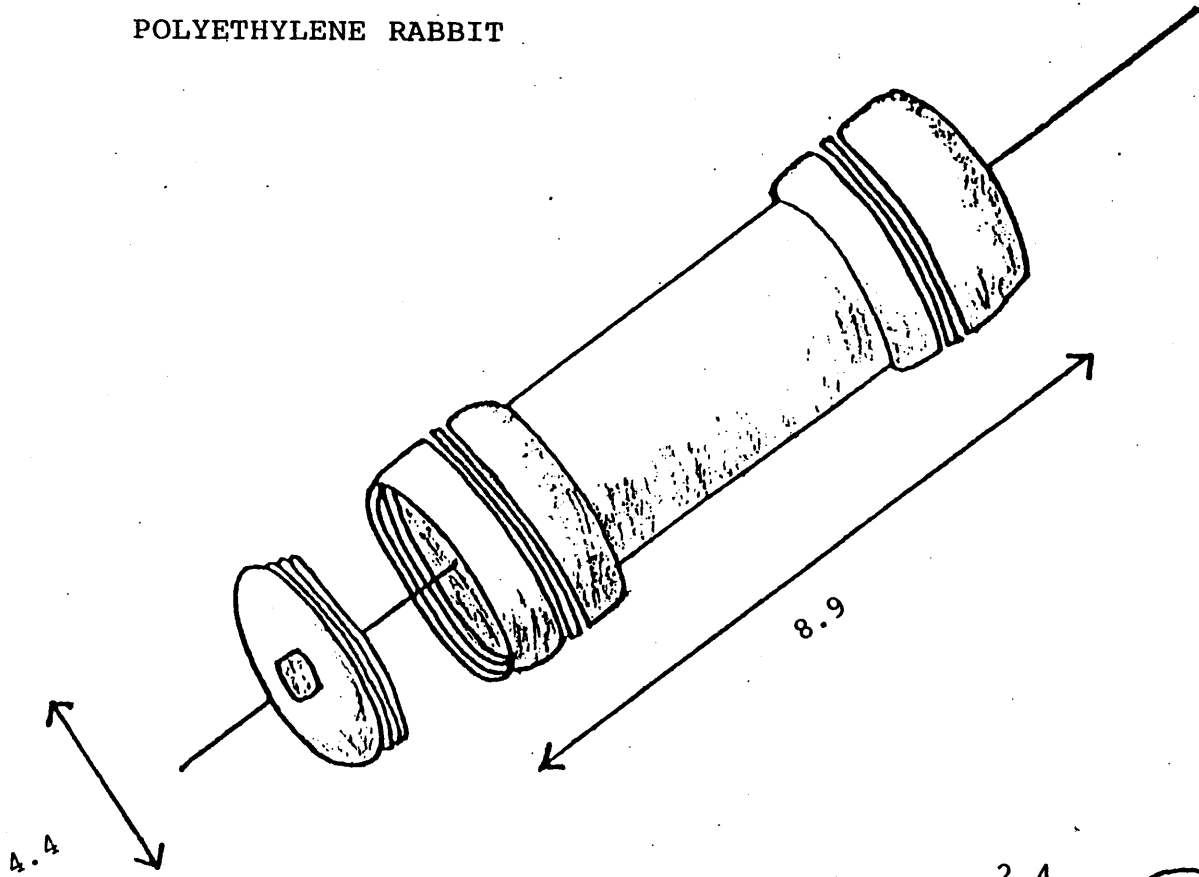
When the detector was made to count for one minute without a rabbit sample or radioactive source in the detector's central rabbit tube, the number of counts per minute ranged from 85 to 180, depending upon the detector system's location. In the Nuclear Chemistry Laboratory, NW 13-207, where all of the delayed fission neutron counting was done, the background ranged from 140 to 180 counts per minute and was primarily dependent upon the level of high energy  $\gamma$  activity inside the room at counting time from radiochemical operations performed

by others using the facility. Thus, the variability in background counts implies that the detector may have been counting some high energy gamma photons emitted by other activation analysis experiments. The background level was monitored during counting experiments by periodic counting of an empty central rabbit tube. This component of the background was included in the "total background" which was subtracted from the gross counts to obtain the net counts per minute for each sample.

#### 2.4.2 Contribution from Polyethylene Contamination

Although it was known that fissionable material could have been left on the surface of the reusable polyethylene rabbits, it was felt that washing with detergents and rinsing with distilled water was an adequate cleaning procedure. Thus, after this cleaning, surface contamination should not be sufficient to account for the observed increase in counts per minute of the irradiated but empty polyethylene rabbits over air background. In order to check for intrinsic uranium content, various weights of polyethylene rabbits were prepared by combining polyethylene components of different weights (see Fig. 2.5). These samples were irradiated in the LPH1 pneumatic tube and counted in the delayed fission neutron detector. The polyethylene samples weighing under 10 grams were weighed on the Mettler microbalance to  $\pm 5 \times 10^{-5}$  grams. Those over

POLYETHYLENE RABBIT



POLYETHYLENE VIALS

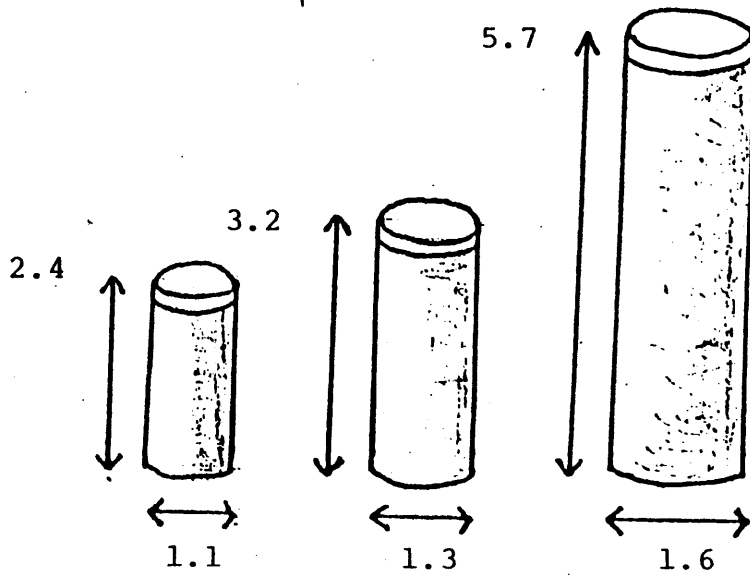


Fig. 2.5 Rabbit and Vial Dimensions (cm)



10 grams were weighed using a pan balance with sliding weights to  $\pm 0.05$  grams. The average air background counts were subtracted from the gross counts for each polyethylene sample to determine the net counts.

The net counts versus polyethylene weight are plotted in Fig. 2.6. The data are recorded in Appendix A1. There is a clear linearity which corresponds to a polyethylene uranium content of approximately 71 parts per billion. This is a non-negligible uranium content which must be taken into consideration, especially when the polyethylene weight of the uranium standard samples varies significantly from that of the sorber samples. Otherwise, measurement of the standard would produce counts which are not directly proportional in number to the uranium in the standard alone.

#### 2.4.3 Neutron Absorption in Sorbers

##### 2.4.3.1 Contamination

Unloaded sorbers (sorbers not yet exposed to uranium in solution) were irradiated and counted to determine whether a trend with increasing sorber weight could be observed. If present, this could indicate flux depression, activation of signal-inducing radionuclides, trace uranium contamination of sorber material, or some combination of these circumstances. Sorbers were rinsed with distilled water, dried in a drying

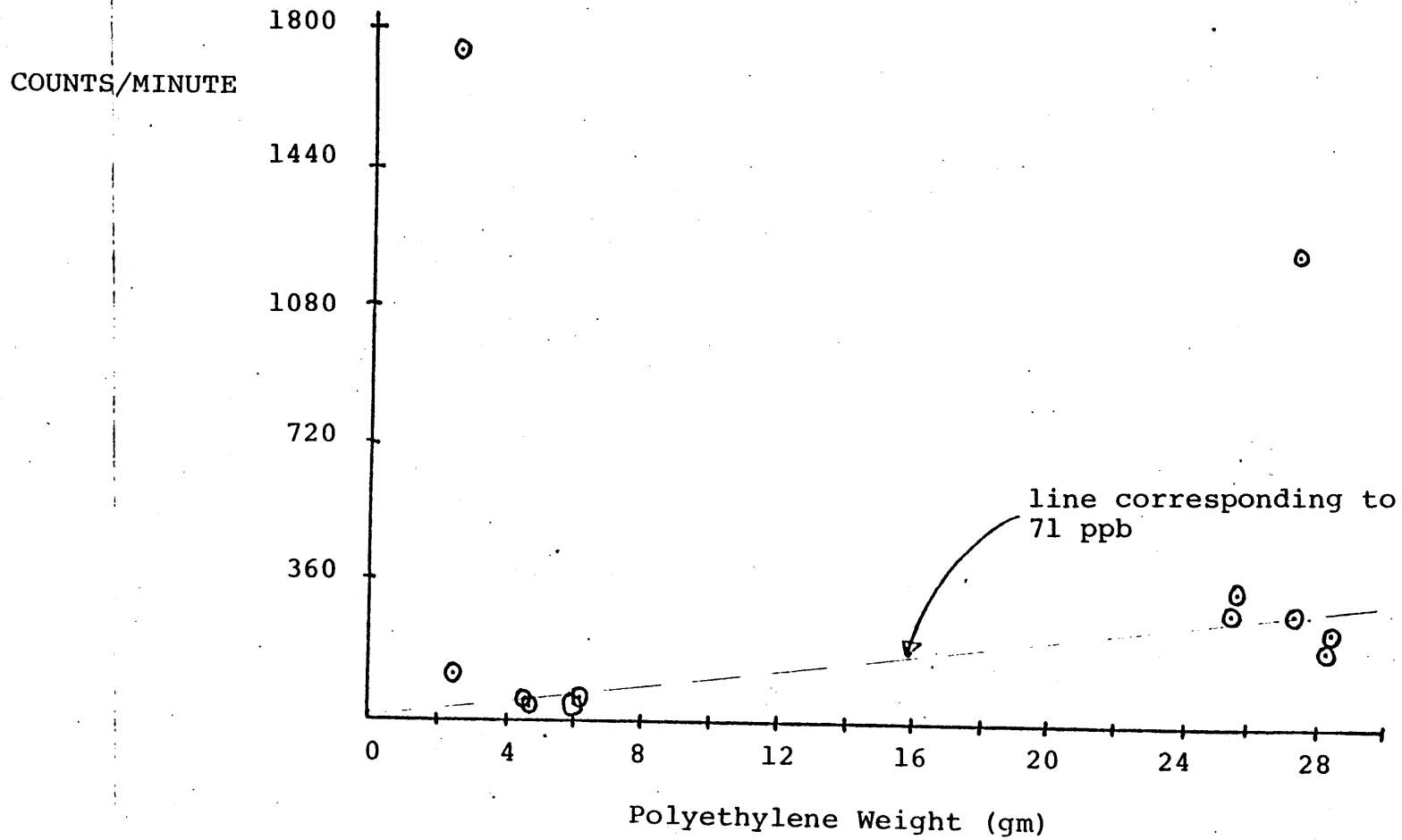


Fig. 2.6 Results of Experiments to Determine the Uranium Content in Polyethylene

oven at 50° C, stored in a dessicator until weighing, crushed to ensure uniform uranium distribution, and weighed immediately upon removal from the dessicator. This procedure was identical to that used to prepare uranium-loaded sorbers for counting, except for the absence of uranium.

The background counts included air and polyethylene counts which were determined by counting irradiated blanks comprised of two empty vials held in place with styrofoam inside the rabbit. The only difference between the blanks and the sorber samples was the absence of sorber. The background counts from these blanks were subtracted from the gross counts for the sorber samples to obtain the net counts due to the sorber itself.

Results are shown in Fig. 2.7. For numerical data, see Appendix A1. There is no consistent trend of increasing count rate per unit mass with increasing sorber weight for any of the sorbers. Hence, it can be concluded that the delayed neutron count due to uranium would not be affected by its presence in varying weights of sorber.

#### 2.4.3.2 Effect of Varying Sorber Weight with Constant Uranium Content

As a further investigation into the effect of neutron absorption by the sorber materials, a series of irradiation measurements were done on varying weights of sorbers to which

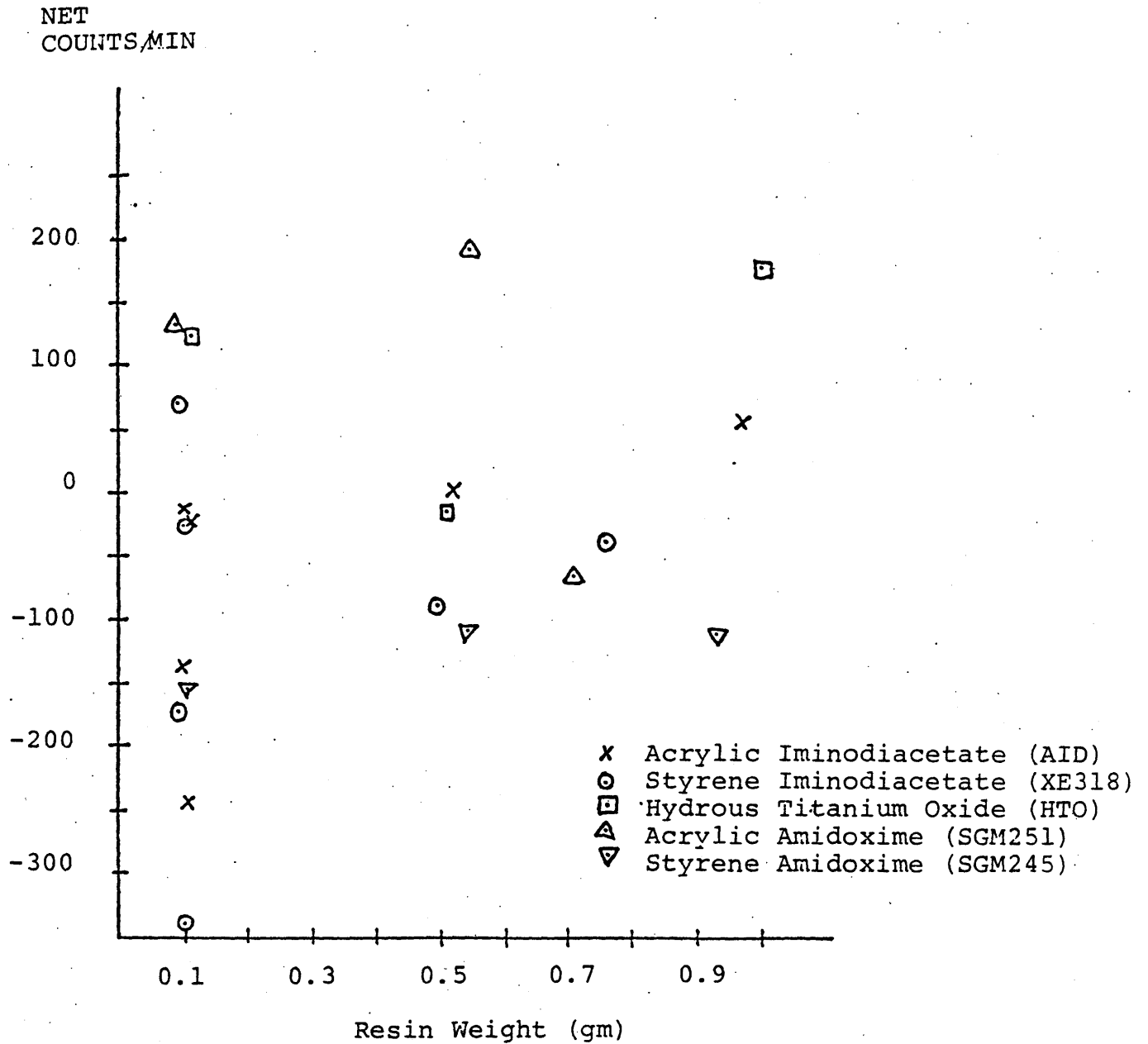


Fig. 2.7 Delayed Fission Neutron Counts per Minute  
Versus Blank Resin Weight

a constant amount of uranyl nitrate solution had been added.  $1.00 \pm .01$  ml of a  $1.4993 \times 10^{-3}$  gm/cm<sup>3</sup> ( $2.986 \times 10^{-3}$  Molar) uranyl nitrate solution was evaporated with sorbers whose weight varied from 0.1 to 1.0 gram, at 50° C for approximately three days. The uranyl nitrate did not appear to be well mixed in the resin and was clearly adsorbed onto the first layer of resin with which it came into contact at the top of the vial. However, subsequent stirring with a small metal spatula resulted in a fairly homogeneous mixture.

Background counts were determined by irradiating unloaded sorbers in the same configuration as the sorbers loaded with uranyl nitrate. Net counts per minute were determined by subtracting the background from the gross counts; for the background determination, samples containing approximately the same weight of sorber as in the uranium-loaded samples were used.

The results are shown in Fig. 2.8. For numerical data, see Appendix A1. Overall, the counts appear to be fairly constant over the range of sorber weights investigated. It was felt that the two low data points at high sorber weight are anomalous (see Recommendations, Section 5.5), and that the resin does not, in fact, depress the neutron flux to any appreciable degree.

Based on results from this experiment, it was considered acceptable to determine the background counts for each

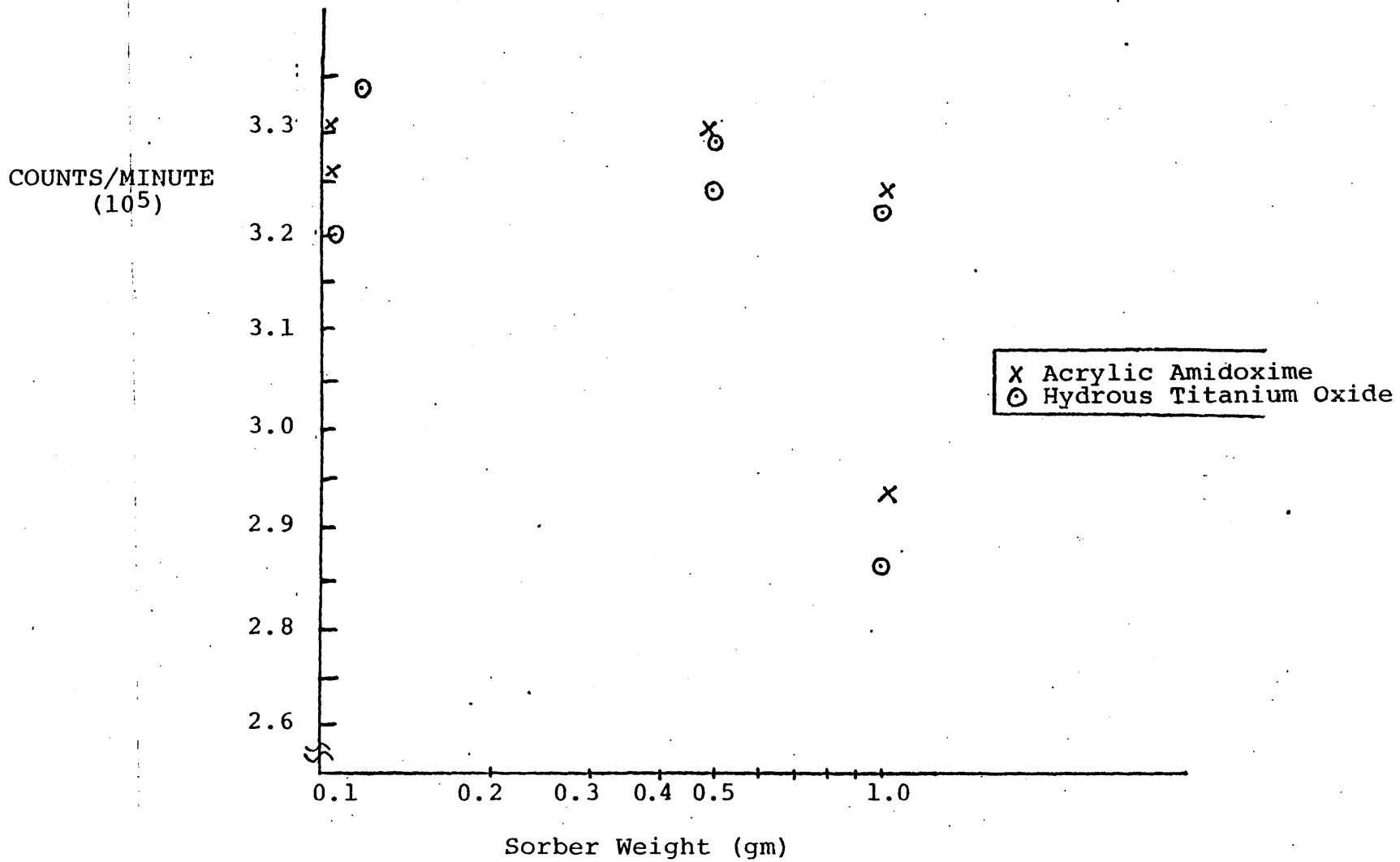


Fig. 2.8 The Effect of Varying Sorber Weight on Delayed Fission Neutron cts/min for a Constant Uranium Content

sorber as the average of counts for blank sorbers having different weights since it was shown that the neutron count was independent of the weight of sorber present. The effect of uranium contaminated polyethylene was considered unimportant here because the difference in polyethylene weight (less than 0.2 grams) between samples would produce a difference in counts (less than 2 counts/minute) which was insignificant compared to the number of counts due to the uranyl nitrate (on the order of 300,000 counts/minute).

#### 2.4.4 Uranium Standards for Calibration

##### 2.4.4.1 Introduction

The basis for the delayed fission neutron counting is the assumption that any sample containing a fissionable isotope will release delayed neutrons in a regular manner in numbers directly proportional to the mass of fissionable isotope present. If two samples are irradiated, allowed to decay and counted in the same way, then it is assumed that any difference in the counts per unit time is due to differences in the mass of fissionable material present. Although the absolute count to mass ratio depends on the fissionable isotope involved, sample geometry, and counting system efficiency, linearity between delayed fission neutron counts and fissionable mass has been demonstrated for over five orders of magnitude (B1). It is therefore essential for system calibration to

measure the counts for a known amount of fissionable material which has been handled in precisely the same manner as samples of unknown fissionable material content so that a given number of counts can be correlated to a given mass.

Uranium depletion due to irradiation in a calibration sample can be shown to be negligible so that the standard can be run several times and its uranium content assumed to be constant.

For all of these uranium calibration measurements, the background counts, which were subtracted from the gross counts to produce the net counts, were determined by preparing, irradiating and counting blank air rabbits containing polyethylene vials and styrofoam in geometries identical to those rabbits containing uranium samples. In this way, background due to atmospheric radiations was also accounted for. The uranium samples were positioned in the vials and rabbits such that the uranium was closest to the end of the LPH1 tube during irradiation and closest to the bottom of the detector during counting. The rabbits were always counted along with the samples.



#### 2.4.4.2 Uranium Dioxide (UO<sub>2</sub>) Preparation

Uranium dioxide, in the form of a dense brown powder of molecular weight 270.03 and melting point of 2500°C, was used to prepare irradiation standards. Uranium samples ranging from  $10^{-7}$  grams to  $10^{-4}$  grams were required to establish the linearity of counts versus uranium weight in a range useful for assaying part per million loadings of gram weights of resin, and, at the upper limit, consistent with radiation safety considerations. It became clear that samples less than approximately  $5 \times 10^{-5}$  grams were impractical because of the high density (and small size) of the powder particles and also, because this weight approaches the dependable lower limit of the Mettler microbalance.

The uranium dioxide was dried overnight in a drying oven at 50°C. It was then placed in a dessicator and brought to room temperature for storage until weighing. The UO<sub>2</sub>

prepared for the 7/24/81 irradiation (rerun on 8/28/81) was taken from the dessicator and samples were weighed while the rest of the  $\text{UO}_2$  was exposed to air. It can be seen from Fig. 2.9 that the counts per minute per gram of uranium for samples irradiated on 7/24/81 and 8/28/81 decrease with increasing uranium or uranium dioxide weight. This is consistent with the absorption of atmospheric water which would cause a decrease in the apparent uranium dioxide content of a sample, since the preparation order was from low to higher weights.

The  $\text{UO}_2$  prepared for the 10/1/81 and 10/23/81 irradiations was returned to the dessicator while each sample was being weighed to minimize water absorption. These results are also shown in Figure 2.9. The average number of counts per minute per gram of natural uranium for all of these normalized data is  $3.478 \times 10^8$  which is 5% higher than the value for the National Bureau of Standards (NBS) uranium sample,  $3.3044 \times 10^8$ . The average value for subsets of measurements taken on a single irradiation date vary from the NBS average significantly more than 5%. (For numerical data, see Appendix A2.) Factors responsible for variation among measurements on the same sample are discussed later (see Section 2.4.5, Normalization to a Common Flux Level.)

#### 2.4.4.3 Uranyl Nitrate ( $\text{UO}_2(\text{NO}_3)_2 \cdot 6\text{H}_2\text{O}$ ) Preparation

Uranyl nitrate is a bright yellow crystalline material of hydrated molecular weight 502.13 and melting point of

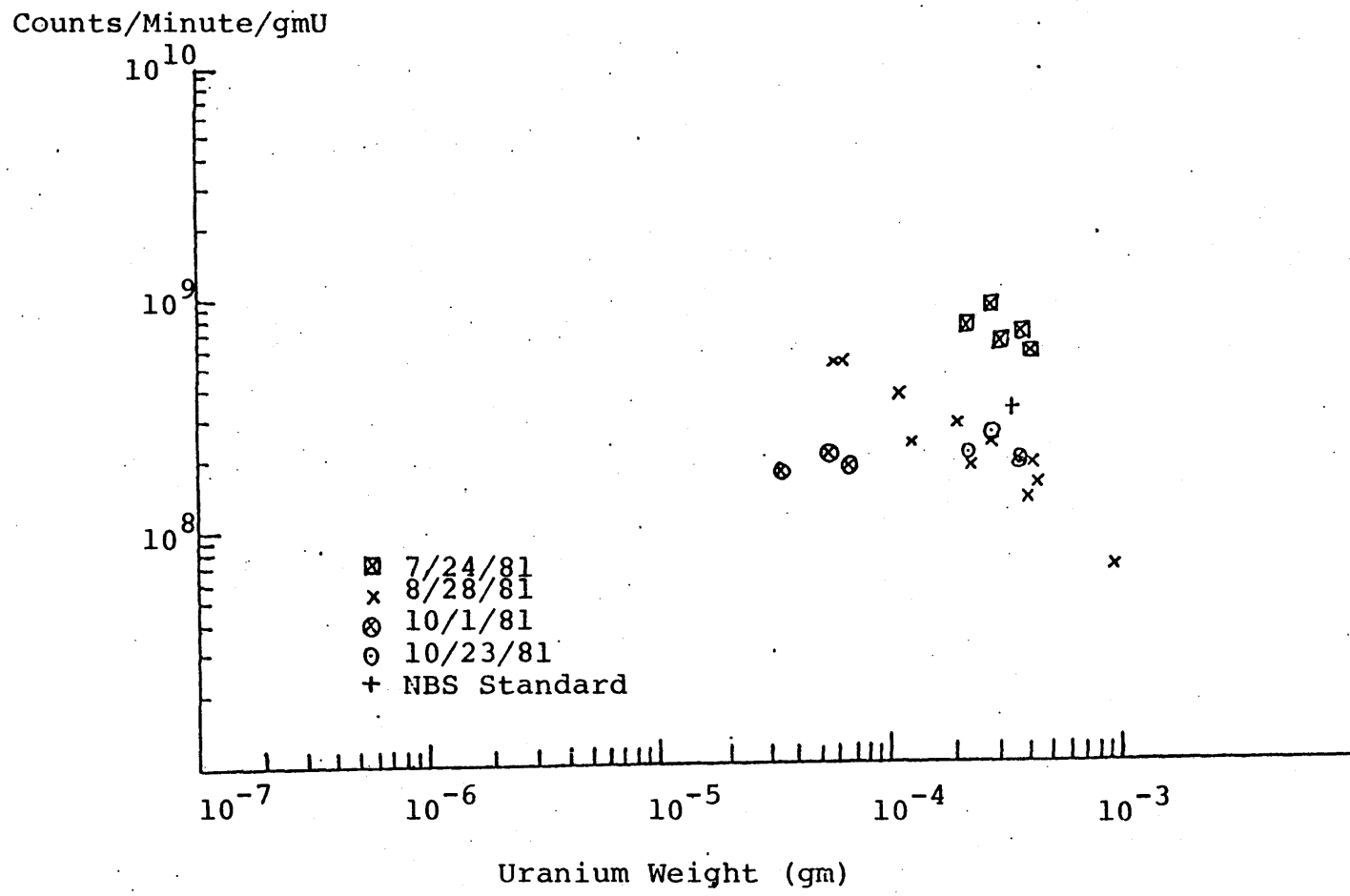


Fig. 2.9 Uranium Dioxide as a Calibration Standard: Cts/min/gmU versus Uranium Weight

100°C in air. Because of hydration, the true weight of a sample is difficult to determine. However, the advantage of this compound over uranium dioxide as a uranium standard is that it can be dissolved in water and then diluted to any desired low concentration. A disadvantage, namely greater probability of sample leaks, can be overcome by evaporating the solution in each sample prior to irradiation. Uncertainties in uranium content arise from variation in water of hydration content, powder weighing, solution volume determination, sorption by container walls and losses during evaporation.

Uranyl nitrate was dried in an oven at 50°C for two days and stored in a desiccator until weighing. Three samples of varying weight, less than a gram, were each dissolved in 100 ml of water in calibrated glass flasks and mixed by shaking. One ml of these stock solutions was diluted to 10 ml in another set of 10 ml calibrated glass flasks. Subsequent dilutions were performed in the same manner, by diluting one ml of a stronger solution with water to form 10 ml of less concentrated solution. By this procedure, concentrations as low as  $2.9 \times 10^{-7}$  gram uranyl nitrate per ml containing  $1.4 \times 10^{-7}$  grams of  $U^{nat}$  were obtained.

One ml of a solution was then pipetted into a 2.4 x 1.1 cm polyethylene vial and evaporated at 50°C in a drying oven. These vials were heat-sealed and placed upside-down in 3.2 x 1.3 cm vials which were themselves sealed and inserted upside-down into a rabbit, held in place by styrofoam. Two samples were prepared for each solution concentration.

Measurements of representative samples from this set of uranyl nitrate solutions were performed during each irradiation run after 7/24/81. The results are shown in Fig. 2.10. Any two samples containing the same amount of uranyl nitrate which were counted on any one irradiation date or on different irradiation dates showed very good reproducibility. The degree of reproducibility for these duplicate samples declined for later irradiations probably due to contamination of the vials during storage in a radioactive materials preparation room between irradiations, even though sample vials were rinsed in acetone before they were placed into rabbits. The six points at  $7 \times 10^{-6}$  grams represent measurements of two different samples on three irradiation dates. The fact that these six points are significantly lower than the rest of the data points suggests that they contain less uranium than indicated by their calculated weights. Although the reproducibility for duplicate samples seemed very good, and could thus be used to normalize data from one date to another, there was not enough uniformity in the data to warrant much confidence in any one of these measurements, or even in an average value for determination of a 'counts-to-uranium-ratio' (nevertheless, the average value for all of the uranyl nitrate data is  $3.187 \times 10^8$ , within 4% of the NBS uranium standard average value of  $3.304 \times 10^8$  counts per minute per gram of  $U^{nat}$ ). Therefore, a calibration standard of more precisely known uranium content was sought.

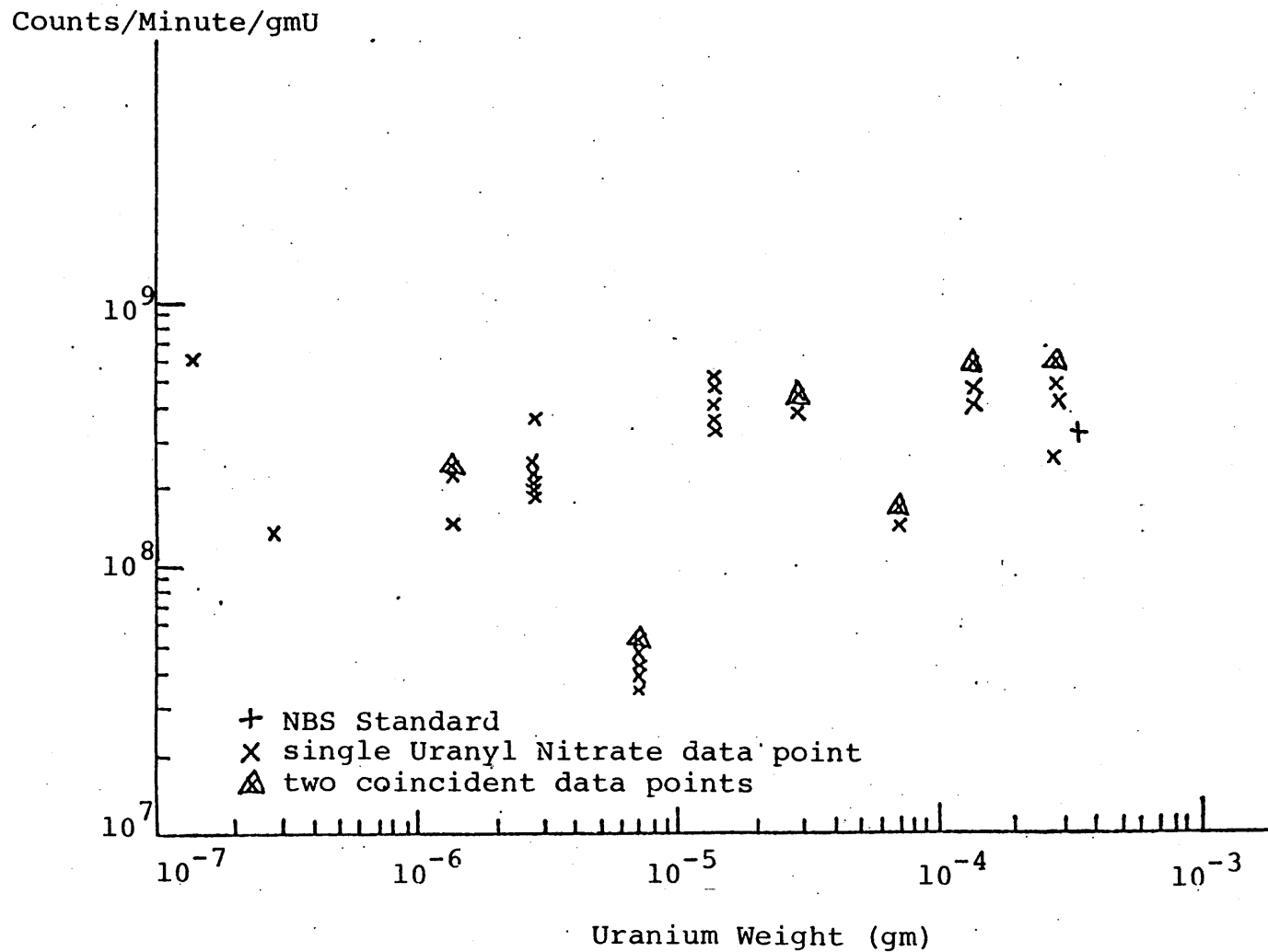


Fig. 2.10 Uranyl Nitrate as a Calibration Standard:  
 cts/min/gmU versus Uranium Weight

#### 2.4.4.4 NBS Uranium Standard

A glass disk manufactured by the National Bureau of Standards containing  $461.5 \pm 1.1$  ppm uranium was obtained from the Earth and Planetary Sciences Department of M.I.T. Because this material was originally to be used for a fission track etch standard, it was highly homogeneous. The disk was machined down to a diameter which would fit into a vial of outer diameter 1.3 cm while contained in its own sealed polyethylene bag. This bag was approximately the same weight (about 2 grams) as the 1.1 x 2.4 cm vial used for primary containment of the Uranium Dioxide and Uranyl Nitrate powders and so the same blank air rabbit configuration was used for determination of background counts per minute. The numerical data for the NBS standard is given in Appendix A1. The cts/min/gmU value for the measurement taken on 10/1/81 was 58% lower than those taken on 10/23/81. The 10% lower average neutron flux in the pneumatic tube on the earlier date cannot fully explain this discrepancy; one would expect only a 10% lower count value since counts are directly proportional to flux (see Eq. 1.1). Another factor which could have decreased the count was the geometry of the sample during irradiation. On 10/1/81, the NBS Standard was about 2 cm farther away from the end of the pneumatic tube than it was on 10/23/81.

The two measurements of the NBS Standard taken on 10/23/81 produced values for the cts/min/gmU that were within 0.1% of one another. The calculated (one sigma) uncertainties for each of those values was 0.5%. Hence, the reproducibility

of the measurement was excellent. For this reason, the average value of  $3.3044 \times 10^8$  cts/min/gmU obtained in these runs was used to convert all normalized cts/min values into uranium content for all of the sorber measurements in the present work. The normalization of cts/min to equivalent neutron flux conditions on 10/23/81 is described below.

#### 2.4.5 Normalization to a Common Flux Level

Variations in the neutron flux between irradiations were minimized by irradiating samples long after the MITR-II reactor had reached equilibrium following start-up, and by normalizing all counts to those for the 10/23/81 irradiation. For a sample counted on a given date and also counted on 10/23/81, a ratio of net counts per minute for 10/23/81 to net counts for the given date was calculated and an average value for this ratio was determined. Subsequently, all net counts were multiplied by this average normalization factor for their respective irradiation date.

The conversion factor found with the NBS uranium standard was then used to determine the uranium content of the sample from the normalized net counts per minute. These average normalization factors together with their calculated uncertainties are tabulated in Appendix A.2.1. A sample normalization and uranium content calculation is shown in Appendix A.3.1.

In general, the effective flux was found to vary by roughly  $\pm 15\%$  from run to run, when calculated by the procedure discussed above.



TABLE 2.1

Normalization factors used to  
correct for variability in  
neutron flux

Run Index i	Date	$\phi_5/\phi_i$ (fission product current)	$\phi_5/\phi_i$ (uranium samples)
1	7/24/81	0.931086	1.071285
2	8/6/81	1.011236	1.274246
3	8/28/81	1.010674	0.892772
4	10/1/81	0.920224	1.170632
5	10/23/81	1.0 (by definition)	1.0 (by definition)

Another approximate method used to determine the variability in neutron flux was provided by MITR instrumentation, specifically, the "Channel 7" fission chamber which is installed near the 1PH1 irradiation site. The ratio of this value on 10/23/81 to that measured at any other time is theoretically equivalent to the ratio of the neutron flux available at the irradiation site. Variations in neutron flux were estimated using this current ratio and were compared to analogous values obtained from uranium sample counts as discussed above. Normalization factors for sets of runs calculated with both techniques are presented in Table 2.1; it is clear that the ratios do not correspond on any given irradiation date, and neither do they follow a trend with respect to different dates. Because the uranium sample ratios were more likely to reflect neutron flux conditions at the sample irradiation site, these ratios were used to correct for variations in the flux rather than the channel 7 current ratios.

#### 2.4.6 Reproducibility

##### 2.4.6.1 Geometric Considerations

It was essential when comparing the counts per minute for two different samples that all handling operations and physical characteristics exclusive of uranium content be made as nearly identical as possible. This was made clear during the first irradiation on 7/24/81 when differences of almost 50% in the net counts per minute per gram U between

uranium dioxide samples was observed for the first five samples. These particular samples had been inserted into the reactor in a random geometry (that is, the top or bottom of the rabbit was not indicated). Consequently, the sample position during irradiation might have varied as much as 8.3 cm from sample to sample. When the rabbit insertion direction was controlled to place the uranium (in the bottom of the smallest vial) closest to the end of the pneumatic tube, the maximum difference in the counts per minute per gram decreased to less than 35%. Another notable discrepancy (58%) due to a similar geometric factor in the irradiation of the NBS uranium standard has already been discussed.

The differences in geometry of the samples during counting were not considered as important as those during irradiation since the active length of the equal-sensitivity zone in the detector's central tube is much longer than differences in axial position; and there was not much variability in radial position (less than 0.6 cm) since samples were always counted inside their rabbits which fit into the detector's central rabbit tube snugly.

#### 2.4.6.2 Electronic Stability

To ensure the electronic stability of the delayed fission neutron detector circuitry, several precautions were taken for each set of irradiations.

When producing the plateau curves prior to setting the level of the high voltage power supply an increase in the counts

per minute was observed for several hours after setting the high voltage to a certain value. The circuit did not reach a stable equilibrium as reflected by constant counts per unit time until it had been set at the same voltage level overnight. For each set of irradiations then, the circuit was allowed to warm-up overnight at the counting site, with an applied voltage of 1260 volts.

Fluctuations in 60 Hz line frequency were observed occasionally and were monitored by measuring the counts per minute with an empty central rabbit tube between every two or three sample counts and comparing these background air values to those taken prior to and during the irradiation sequence. These counts per minute "air values" varied from an average of 160 to 180 on any given day, depending on the level of activity present in the Nuclear Chemistry Laboratory, and could vary randomly from 135 to 185 during the irradiation.

The stability of the circuit was checked immediately before and after the irradiation run by noting the average counts per minute induced by a  $^{252}\text{Cf}$  neutron-emitting source. At least five measurements, each of minute-long duration, were made to determine the average value before and after uranium sample counting: differences of less than three percent were found for  $^{252}\text{Cf}$  counts.

After all of the uranium and resin samples had been irradiated and counted, plateau curves of counts per six minutes versus high voltage were made. These runs showed

that the plateau region had shifted up to well over 1300 volts, higher than the manufacturer's suggested maximum operating voltage for these  $^3\text{He}$  tubes. It is not known at this time why this shift occurred.

## 2.5 Summary

In this chapter, irradiation and counting facilities were described together with calibration procedures for the counting electronics. Irradiation and counting procedures were discussed, taking into consideration laboratory background, polyethylene uranium contamination and neutron absorption by sorber material. The laboratory background and polyethylene contamination were included in a total background measurement; the total background count rate was subtracted from the gross count rate, to give the net count rate. The effect of neutron flux depression in varying weights of sorber was shown to be negligible.

The use of Uranium Dioxide and Uranyl Nitrate for uranium calibration standards was investigated; the use of these standards were found to be less reliable than that of a uranium standard obtained from the National Bureau of Standards. Procedures for normalization of all delayed fission neutron (DFN) counting data to a common basis were presented.

Finally, steps to insure reproducibility were discussed.

CHAPTER III  
SORBER LOADING EXPERIMENTS

3.1 Introduction

In Chapter 2, the development of a Delayed Fission Neutron (DFN) counting system was described. Two types of sorber loading experiments were conducted which provided uranium-bearing samples for counting on the DFN system. In this Chapter the design and execution of these sorber loading experiments are described. First, the techniques for seawater sampling and uranium content determination are discussed. Next, the equilibrium experiments conducted at M.I.T. are described and compared with similar experiments performed at the Rohm and Haas Company. Then, the design and fabrication of sorber test columns installed at the Woods Hole Oceanographic Institute, and their operation are described. Finally, procedures for preparing sorber samples for irradiation and counting are discussed.

### 3.2 Seawater Sampling and Uranium Content Determination

Natural seawater was taken from both Massachusetts Bay in Winthrop, Mass., and Woods Hole Bay in Woods Hole, Mass. All of the seawater samples for laboratory equilibrium experiments were taken with six Nalgene brand polyethylene liter bottles which had been cured in natural seawater for at least seven days to allow the polyethylene and seawater to come to equilibrium with respect to their uranium content, since uranium has been known to diffuse from solutions into their containers.

#### 3.2.1 Massachusetts Baywater

The Massachusetts Bay water was used only for the equilibrium experiment to test the Acrylic Iminodiacetate ion-exchange resin. The water samples were taken where the seawater depth was approximately six feet, about 100 feet out at high tide.

#### 3.2.2 Woods Hole Seawater

The Woods Hole water was taken from a seawater inlet installed by the Redfield Laboratory of the Woods Hole Oceanographic Institute. The seawater inlet is located at the end of a long pier where the water is 60 feet deep; it is collected

at a depth of 15 feet. The water is pumped into 4 wax-lined cement tanks each having a capacity of 5,000 gallons. The water then moves by gravity from the Bigelow Building to the Wet Lab of the Redfield Laboratory. The water is known to be of slightly lower uranium concentration than the 3.34 ppb average for open sea water due to mixing with fresh water from streams which empty into the Woods Hole Bay. (see Section 4.2, Seawater Uranium Content).

Although it is known that the average uranium concentration of seawater does not generally vary significantly with location (K2), it was also known that the concentration varies in proportion to salinity. Since Woods Hole seawater was known to be of lower salinity than the average for ocean water (D1), it was important to measure the uranium concentration directly, because this affects the mass transfer kinetics more than any other factor.

### 3.2.3 Seawater Uranium Content Determination

The mass transfer kinetics of any system is controlled by many factors, one of the most important of which is the concentration of the species of interest in different regions of the system. The uranium content of the sorbers after contact with seawater is readily detectable by the delayed fission neutron system described in this work, for uranium content greater than 2 micrograms. Although there are 3.4 micrograms of uranium in a liter of 3.34 ppb seawater, this



volume is difficult to irradiate unless it is reduced by evaporation, which requires a long sample preparation time for such a volume. (It is noted in passing that depleted seawater from equilibrium experiments contains even less uranium and therefore aggravates this problem).

Another problem with neutron irradiation of seawater is that all of the other elements in seawater, especially Na and Cl, are activated along with the uranium. This makes the irradiated samples extremely radioactive and therefore difficult to handle. Since the half-life of the most abundant gamma-ray emitter ( $\text{Na}^{24}$  with  $T_{1/2} = 15$  hours) is much longer than that of the delayed neutron precursor of interest (Group 2 at 22.7 seconds), the delayed neutron counting technique is not convenient for seawater uranium content determination, unless the sample transfer and handling can be done remotely.

Activation analysis for  $\text{Np}^{239}$  peaks was an alternative method for measuring uranium in seawater. It was not known whether the  $\text{Np}^{239}$  would be distinguishable above the Compton scattering background from larger peaks of other isotopes, but the concentration of  $\text{U}^{238}$  could be calculated from cross sections and concentration of  $\text{Np}^{239}$ . Four seawater samples from both Massachusetts Bay and Woods Hole (Mass.) Bay were irradiated for five minutes in a flux of approximately  $8 \times 10^{12}$  neutrons/cm<sup>2</sup>/second, allowed to decay for approximately one week and then gamma-peak spectra were taken.

### 3.3 Equilibrium Experiments

#### 3.3.1 Purpose

The purpose of this set of experiments was to reproduce similar experiments performed as a screening procedure for ion-exchange resin performance by the resin manufacturer, the Rohm and Haas (R&H) Company. Filtered natural seawater was poured into one liter polyethylene wide-mouth jars. A known weight of sorber was added to each liter and the contents inside the sealed jars were mixed on a shaker table for sixteen hours. The sorber was then separated from the seawater by filtration. After rinsing with distilled water and drying, the sorber's uranium content was determined by delayed fission neutron counting. It was expected that reducing the weight of sorber exposed to a constant volume of uranium would result in greater uranium loading per gram of sorber. Uranium content was plotted versus sorber weight per liter. These results were then compared to R&H data.

#### 3.3.2 Seawater Filtration

Seawater for each set of sorber equilibrium experiments was taken from water collected at the same time at one location. Except for the Acrylic Iminodiacetate equilibrium experiments in which Massachusetts Baywater was used, seawater was taken from the seawater main of the Redfield wet lab at the Woods Hole Oceanographic Institute. It was filtered by vacuum filtration using filter paper (Schleider and Schuell, #595) to remove gross particulate matter.

After loading, the separation of sorber from depleted seawater was also performed by vacuum filtration. The presence of fine algae along with sorber on the filter paper demonstrated that all of the particulates had not been removed from the water by the pre-loading filtration.

### 3.3.3 Sorber Preparation and Processing

Dry sorber weights of 0.1, 0.5, 1.0 and 1.5 grams were measured on a Mettler microbalance to an accuracy of approximately  $5 \times 10^{-6}$  grams. (For subsequent error calculations, a more conservative value of  $5 \times 10^{-5}$  grams was used). Four of the sorbers, (all except the styrene iminodiacetate), had to be weighed in the wet state prior to uranium loading to preserve their uranium loading ability. For these wet sorbers, empirically determined factors were used to calculate wet sorber weights corresponding to 0.1, 0.5, 1.0 and 1.5 grams. In addition, the Hydrous Titanium Oxide sorber sample required chemical activation of its uranium loading capability by soaking in dilute (pH 6-7) hydrochloric acid for eight hours prior to contacting it with seawater. The weighed sorber samples were then added to the prefiltered liter containers of seawater (at ten minute intervals to allow for the handling time required to separate the sorber from the seawater at the end of the 16 hour exposure).

After separation by filtration, sorber samples were rinsed in a 10 ml beaker with two 5 ml volumes of distilled water. To minimize the absorption of water from air, and thus

achieve a more accurate measurement of the true sorber weight, the samples were dried at 50°C in an oven for two days and allowed to come to room temperature in a dessicator until weighing. The weighing was done immediately after removing the sorbers from the dessicator, to determine irradiation sample weight.

### 3.4 Column Experiments

#### 3.4.1 Design Objectives and Problems

The testing of sorber performance in natural seawater requires access to clean, uranium-undepleted seawater and its contact with a fixed amount of sorber for specified amounts of time, seawater volume or flowrate. Several problems were encountered in achieving the test objectives.

The Redfield Laboratory of the Woods Hole Oceanographic Institute provided natural seawater taken from the Woods Hole Bay, which is biologically active relative to mid-ocean water and therefore rich in particulate matter which readily clogs any system having restricted flow passages. This can be alleviated by prefiltering the seawater. However, filtration of seawater prior to contact with the sorber also produced a large pressure drop which decreases the flow rate. Fortunately, filtration does not affect the uranium content of the seawater since less than 0.3% of uranium in seawater is found in particulate matter (M1), the remainder being in the dissolved state.

Negligible recycling of depleted seawater occurs in the Redfield Lab system.

### 3.4.2 Description of Fixed-Bed Columns

Three fixed-bed ion-exchange columns were designed to load sorbers with uranium by intimate contact with natural seawater for various times and seawater volumes. A diagram of the basic components of each column system is shown in Fig. 3.1. Each system was supported by galvanized steel supports nailed to a wooden frame, which was then stacked against a wall of the "Wet Lab" of the Redfield Laboratory at the Woods Hole Oceanographic Institute (Woods Hole, Mass). Seawater flows from a central collecting site at the end of a long pier into a pipe main which feeds into the "Wet Lab". Each column takes its feedwater from this main. Upon leaving the main, the water was filtered [using polypropylene string-type cartridges (FACET model CF10MCE)] (in a polyvinyl chloride (PVC) double filter housing (FACET model P2)). Water then flows through the column (with the bypass valve closed, see Fig. 3.1). At start-up, this direct flow would not fill the column completely, so that the bypass valve was opened periodically, diverting flow around the column, and causing a reversal in flow direction through the adsorber bed, which resulted in displacement of trapped air by water. Normal downward flow was restored by closing the bypass valve. The volume of water flowing through the column over a period of time was measured with a water meter (Hersey model 1" 550) at the outlet of the column. All meter data have been corrected using calibration curves measured at M.I.T.

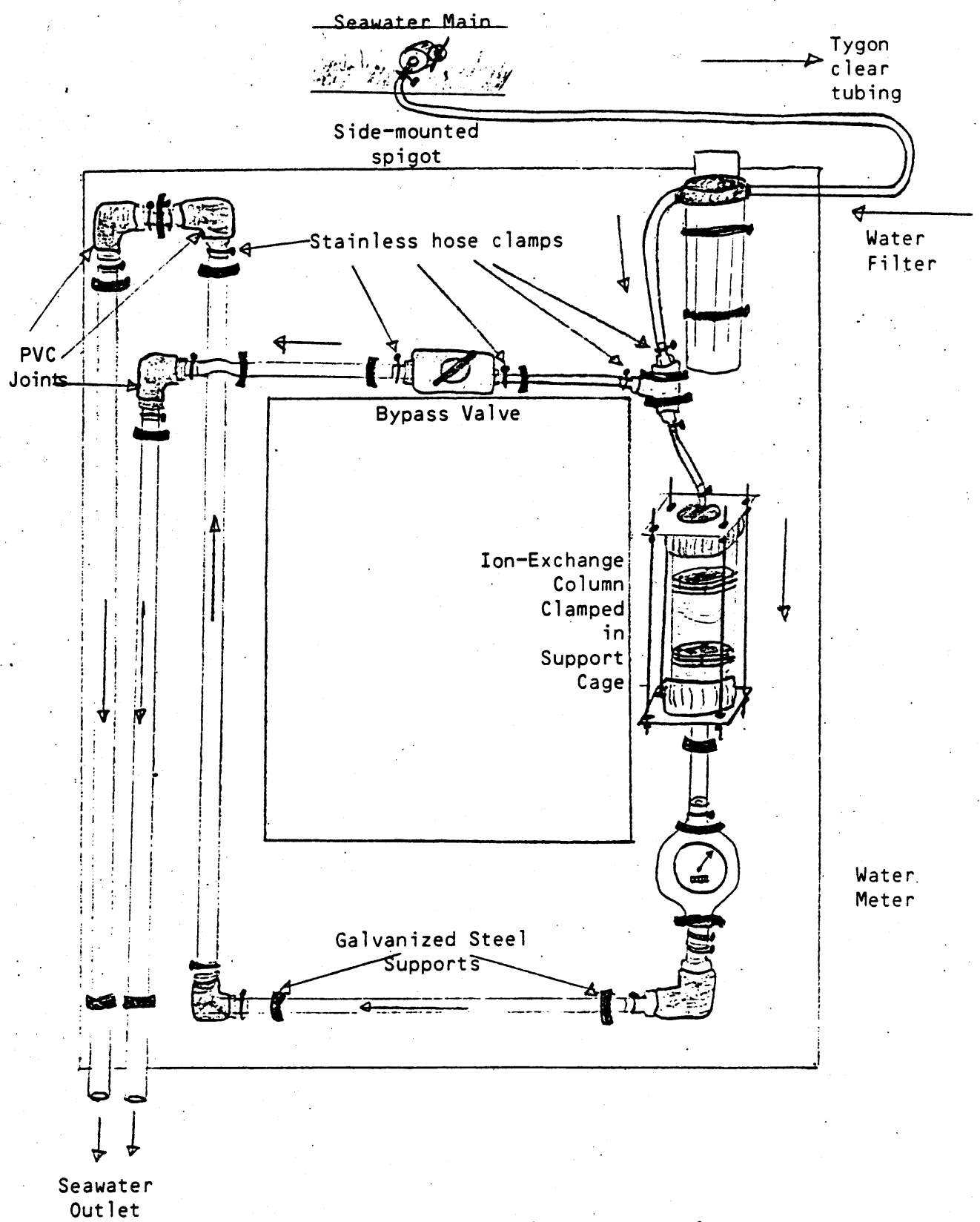


Fig.3.1 Schematic of an Ion-Exchange System Installed at the Woods Hole Oceanographic Institute

The "depleted" seawater flows out of the column and into a cement drainage ditch which leads out into the harbor, far from the inlet at the end of the pier, thereby assuring negligible recycle. Actually, flow loadings were designed to be so high that virtually none of the uranium was removed from any unit volume of seawater. Hence, all sorber in a given sample was at all times exposed to essentially fresh seawater.

Each sorber loading system contained a Plexiglass column section which was machined to hold sorber materials in a fixed-bed configuration. A schematic of the Plexiglass column is shown in Fig. 3.2. The outer Plexiglass cylinder holds the three-sectioned inner column in place. The middle inner section is closed-off on each end by a fine-mesh stainless steel screen held together between two Plexiglass rings. The lower screen has an o-ring surrounding the outer perimeter of the Plexiglass rings to insure a tight fit between the inner and outer cylinders which guarantees that water flows only through the sorber bed.

The columns are snap-fitted into PVC fittings (except for the bottom of column #2, which is screw-fitted), and these fittings are clamped to the ends of the column by the pressure from two aluminum plates and four stainless steel tie rods. Connections between fittings and the clear Tygon tubing are made with Teflon tape-sealed polyethylene connectors.

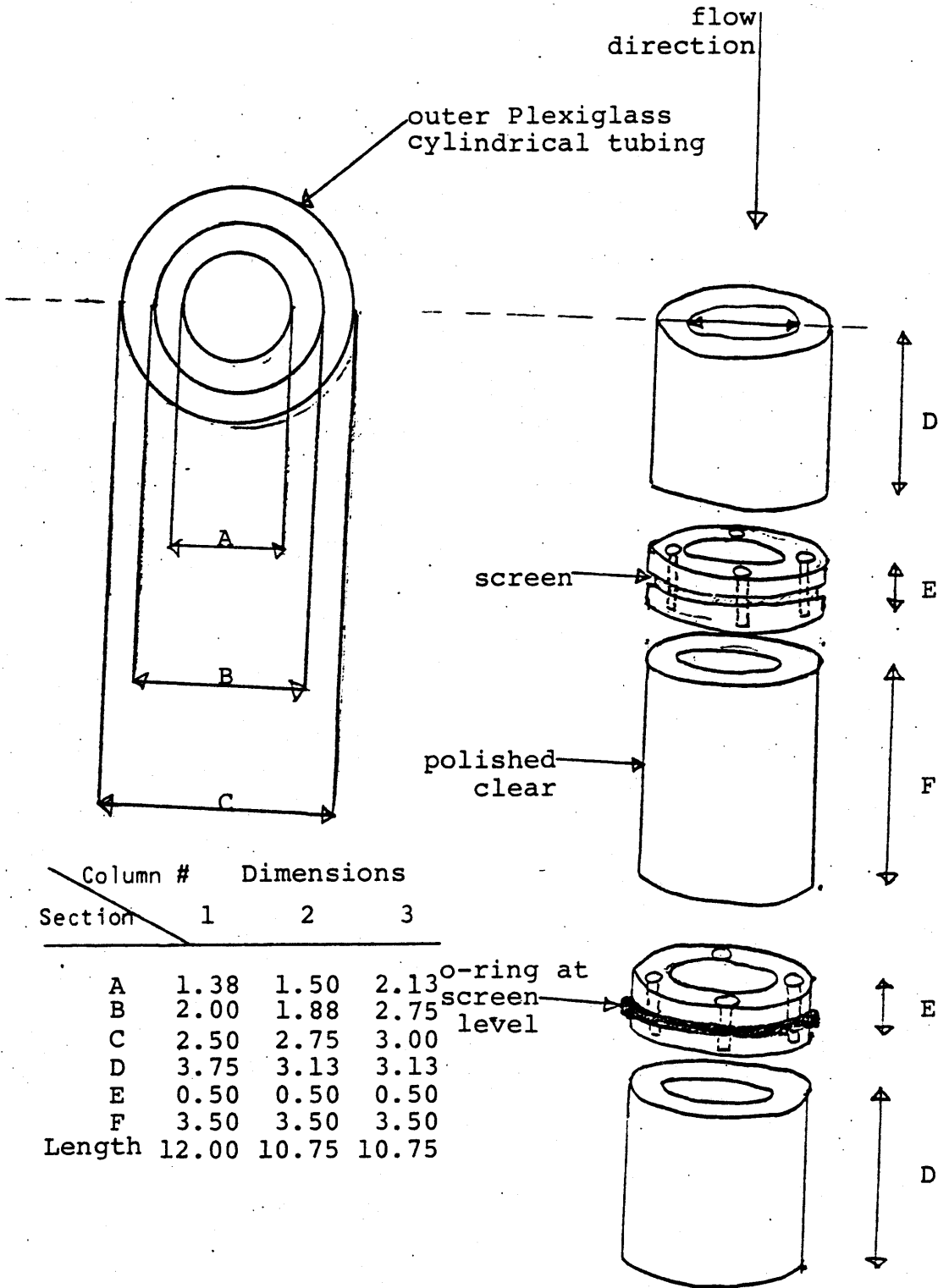


Fig. 3.2 Schematic of Plexiglass Ion-Exchange Column Section (All dimensions in inches)



### 3.4.3 Maintenance

#### 3.4.3.1 System Fouling due to Algae

Periodically during the operation of the loading cycles the seawater flow is inhibited by a buildup of algae and other biological growth, especially at locations where the area through which particulate matter must flow is restricted. The tendency to clog at the outlet from the seawater main for each column was reduced by mounting spigots at the side rather than at the bottom of the pipe main, since particulates in the water tended to settle near the bottom due to gravity, even though the flow out of each spigot could be as high as four gallons per minute. Occasionally, the spigots did clog when water conditions (high temperature, change in pH, etc.) promoted heavy biological growth, but were easily unclogged by inserting a flexible wire into the spigot outlets.

By noting the decrease in the flow rate through each column as a function of time, which typically ranged from an initial flow rate of over four gallons per minute down to less than one, it was determined that the filter cartridges had to be changed every three to four days of operation. It was convenient to dismantle the Plexiglass column structure at the same time, with flow stopped, to rinse off biological growth from both the top and bottom stainless steel screens. Also at this time, it was convenient to uncake the sorber particles, which typically became bound together into a solid disk due to accumulation of fine algae, even when the

seawater contacting the sorber had already been filtered. The geometry of the sorber particles determined, to a great extent, whether the particles would eventually cake. The hydrous titanium oxide (HTO) particles had a solid cylindrical shape which was large and irregular enough to allow fine algae to flow through the bed without causing caking. In contrast, the spherical macroporous ion-exchange resin particles were smaller than the HTO particles (on the order of 0.6 to 0.9 mm in diameter) and tended to trap the algae more readily. The sorbers were uncaked using a metal spatula, and then rinsed with a small volume of fresh seawater.

#### 3.4.3.2 Oxidation of Metal Components

Some stainless steel hose clamps had to be replaced because of oxidation in their worm drives, which prevented their adjustment. The stainless steel screens and screws inside the Plexiglass column oxidized where the metal surfaces contacted and were replaced when "rust" streaks became visible on the column walls.

A serious problem of oxidation at the bolt-rod interface of the aluminum plates which held the column together was overcome by coating the rod threads with an oil-based oxidation preventive treatment. This facilitated rapid dismantling and assembly of the column structure, which was necessary when flow was stopped for maintenance in the shorter loading runs.

After all of the column loading experiments had been completed, the entire system was completely flushed-out with

fresh water to prevent further biological growth until sorber loading is resumed.

#### 3.4.3.3 Loading Operation

Column experiments of one day, 3 day, 7 day and 30 day exposure times were performed for each sorber tested. Fixed beds of less than one-half inch thickness and up to 2 1/2" diameter were exposed to seawater flows ranging from over four to less than one gallon per minute at any time during the run. Note that this corresponds to extremely high flow loadings (up to 183 gallons/min ft<sup>2</sup>) -- much higher than in normal ion-exchange service. This insured both a low fluid-side resistance to mass transfer and negligible fluid-side uranium depletion. All three column systems were fed from the same seawater main at any given time. During start-up, the reversed flow maneuver discussed above would push some sorber up against the top screen (see Fig. 3.1) immediately after the flow direction was changed, but none of the sorber material was seen to escape past this top screen, and it eventually dropped back onto the packed bed which remained on the bottom screen. The containment of material at the top screen was achieved without the presence of an o-ring sealing the column (as used with the bottom screen) to prevent flow around the outer perimeter of the screen; the backflow pressure was not high enough to push sorber material around and past the top screen. After the column was full of seawater, the bed was made as uniform in thickness as possible: by opening the bypass valve and reversing the normal flow direction, the bed was expanded and then

allowed to settle uniformly by closing the bypass valve.

Loading times of 1, 3, 7 and 30 days were chosen to characterize sorber uptake versus time in natural seawater. It was projected that 30 days' exposure would provide sufficient time to saturate the sorber and thus determine its maximum capacity.

#### 3.4.3.4 Seawater Temperature Variations

Although it is known that increasing the temperature of a system generally improves the mass transfer kinetics and uranium uptake (Y2), it was impractical to attempt to control the temperature of the Woods Hole seawater, which varied between 64.8 and 74.5°F due to seasonal changes. The average water temperature during the loading cycle is listed with the measured resin uranium capacity for each column experiment in Appendix A.3.3.

#### 3.4.4 Preparation of Column Sorber Samples for Irradiation

Loaded samples were retrieved from the columns at the "Wet Lab" in the Redfield Laboratory of the WHOI and brought back to M.I.T. where they were prepared for irradiation to determine their uranium content. The sorbers were removed from the columns with a metal spatula along with the fine algae which had accumulated during the loading process. The samples were rinsed on site in fresh water in a Pyrex petrie dish to remove gross particulate matter and taken back to Cambridge in a damp state. The same day at M.I.T., they were rinsed with approximately 100 ml of distilled water, allowed

to dry at 50°C for at least two days, and stored in a dessicator at room temperature until weighing.

The weighing procedure involved crushing the sorbers to form a homogeneous powder and storing the crushed material in the dessicator while individual sorber samples were being weighed. This insured low moisture pickup by the samples. The greatest contribution to error in the sorber weight was the presence of low density biological contamination which was not removed during rinsing; this tended to reduce the measured uranium capacity of the sorber samples. This contamination tended to be greatest for the Styrene Amidoxime (SGM245), which was the ion-exchange resin of smallest particle diameter. Separation of the algae and ion-exchange resins was difficult because of the similar densities of the two materials.

Blank, unloaded sorbers were dried, crushed, and weighed in a manner similar to that for loaded sorbers; these were used to determine background counts for the uranium content measurements of the loaded sorbers.

### 3.5 Summary

The sampling and preparation of natural seawater from Massachusetts Bay and Woods Hole, Massachusetts was described in this chapter. Different methods for the determination of seawater uranium concentration were examined for their suitability to the present problem -- delayed fission neutron counting, activation analysis and salinity measurement.

The two types of sorber loading experiments, equilibrium

and fixed-bed column experiments, were described in detail. Operation and maintenance problems and their resolution, for the column experiments were discussed. Procedures for loading and preparing samples for irradiation and counting were also detailed.

CHAPTER IV  
RESULTS AND DISCUSSION

4.1 Introduction

Thus far, the irradiation and counting systems and procedures have been described, together with the two types of sorber loading experiments which provided the samples for irradiation and counting. In this chapter the seawater uranium content is first discussed, then the measurements of the uranium loading in the two experiments are presented. The results of the equilibrium experiments are compared to those of the Rohm & Haas (R&H) Company, possible explanations for differences are introduced, and the acceptability of laboratory (as opposed to field) procedures as a screening test for superior ion-exchange characteristics in resins is discussed. Lastly, the ion-exchange column experimental results are presented, along with a discussion of the mechanical durability of the sorbers. Sorber properties provided by the Rohm and Haas Company are given in Appendix A.3.4.

4.2 Seawater Uranium Content

The uranium concentration in seawater samples was not measured by delayed fission neutron counting because of the high gamma dose involved during the manual transfer of sea salt samples between the NW13-207 receive station and the

detector system. However, it is known that the uranium concentration in seawater varies directly with its salinity. In the salinity range from 30.3 to 36.2‰ (gm salt/kg seawater), the uranium/salinity ratio is constant and equal to  $9.34 \pm 0.56 \times 10^{-8}$  gram/gram, (K2). Thus, a salinity measurement of  $31 \pm 2$ ‰ taken at the Woods Hole Oceanographic Institute of the seawater in Woods Hole Bay (D1), corresponds to a uranium concentration of  $2.90 \pm 0.25$  gm salt/kg seawater, which is 13% lower than the 3.34 ppb average concentration of uranium in seawater worldwide. Therefore the uranium loading performance of the sorbers in the present work would generally be expected to be poorer than if the loading experiments had been performed with mid-ocean seawater.

There was no salinity measurement available for the Massachusetts Bay water.

An activation analysis performed on both Woods Hole and Massachusetts Bay seawater (see Section 3.2, Seawater Sampling and Uranium Content) was not successfully completed because the Compton scattering background from Br, present as an activation product obscured each of the  $^{239}\text{Np}$  gamma peaks of interest in the range from zero to four MeV, even after one week of decay time. In this experiment 100 ml seawater samples evaporated to dryness (which produced approximately 4.5 grams of salts) were irradiated for five minutes in a flux of  $8 \times 10^{12}$  neutrons/cm<sup>2</sup>/second.

Therefore, the salinity measurement was employed as the basis for selection of  $2.9 \pm 0.25$  ppb by weight as the seawater



uranium concentration for the equilibrium and column loading experiments.

### 4.3 Sorber Performance

#### 4.3.1 Equilibrium Experiments

As described in Section 3.3, varying weights of sorber were contacted with one liter of natural seawater for sixteen hours to reproduce, if possible, the results of similar experiments performed by the Rohm and Haas Company as a screening procedure for ion-exchange resin development, although their seawater experiments were performed with seawater having uranium concentrations as high as 5.9 ppb. Whereas the Rohm and Haas experiments measured uranium loss from the solution (by laser-induced fluorescence, LIF), in the present study the uranium uptake in the sorber was measured directly (by delayed fission neutron counting, DFN).

The uranium uptake versus sorber weight per liter of solution is plotted in Figs. 4.1 and 4.2 for Hydrous Titanium Oxide (HTO) and Styrene Iminodiacetate (XE318), and for Acrylic Iminodiacetate (AID) and Styrene Amidoxime (SGM245), respectively. The data for SGM251 showed no uranium uptake for any of the sorber weights for the DFN measurements; Rohm and Haas experiments at low concentration were not performed on SGM251. Each data point represents an average value for multiple measurements from the same equilibrium experiment. Detailed numerical data is documented in Appendix A.3.2.

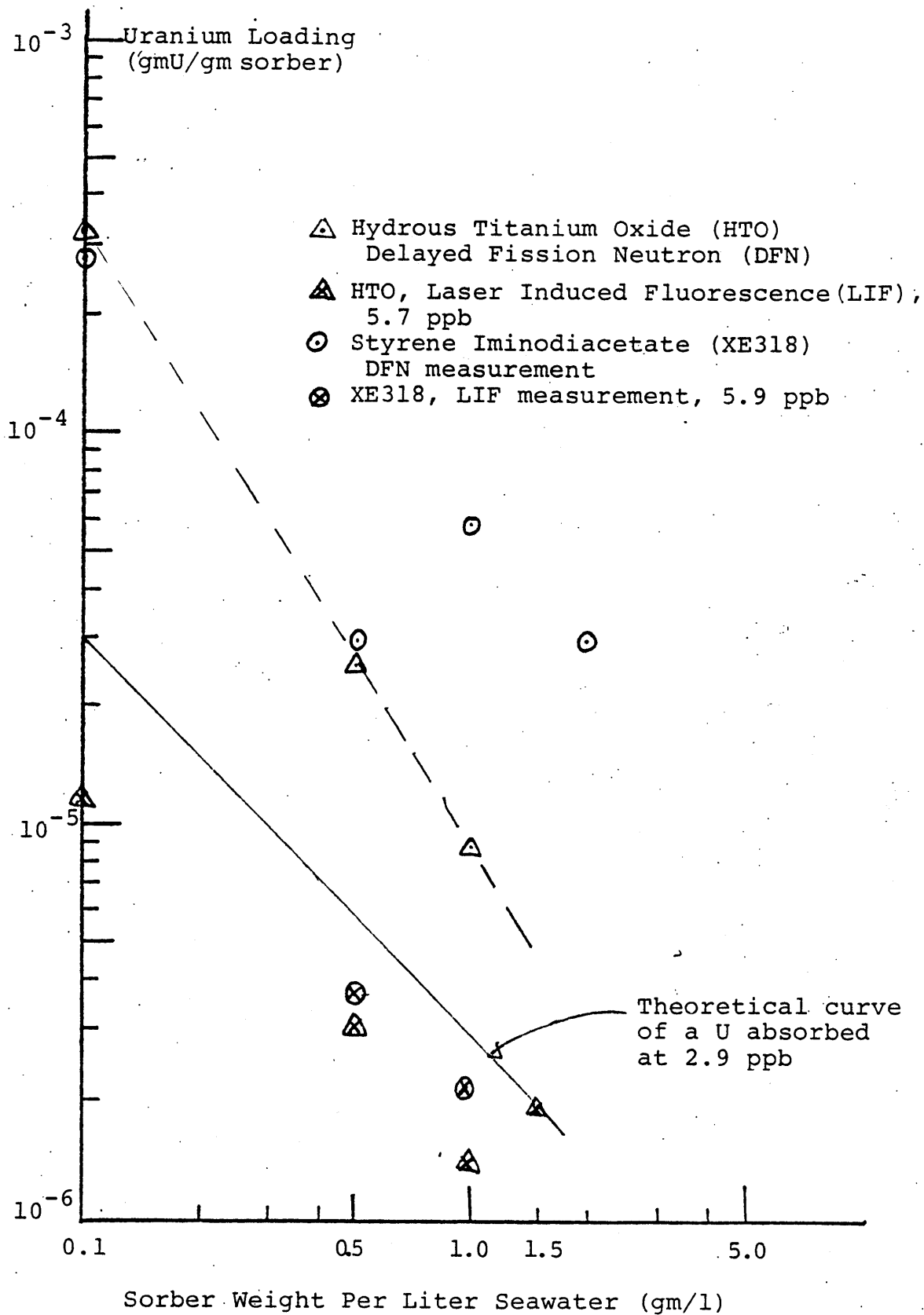


Fig. 4.1 Equilibrium Experiment:  
 Uranium Loading versus Sorber Weight  
 per Liter Seawater (2.9 ppb) for HTO  
 and XE318.

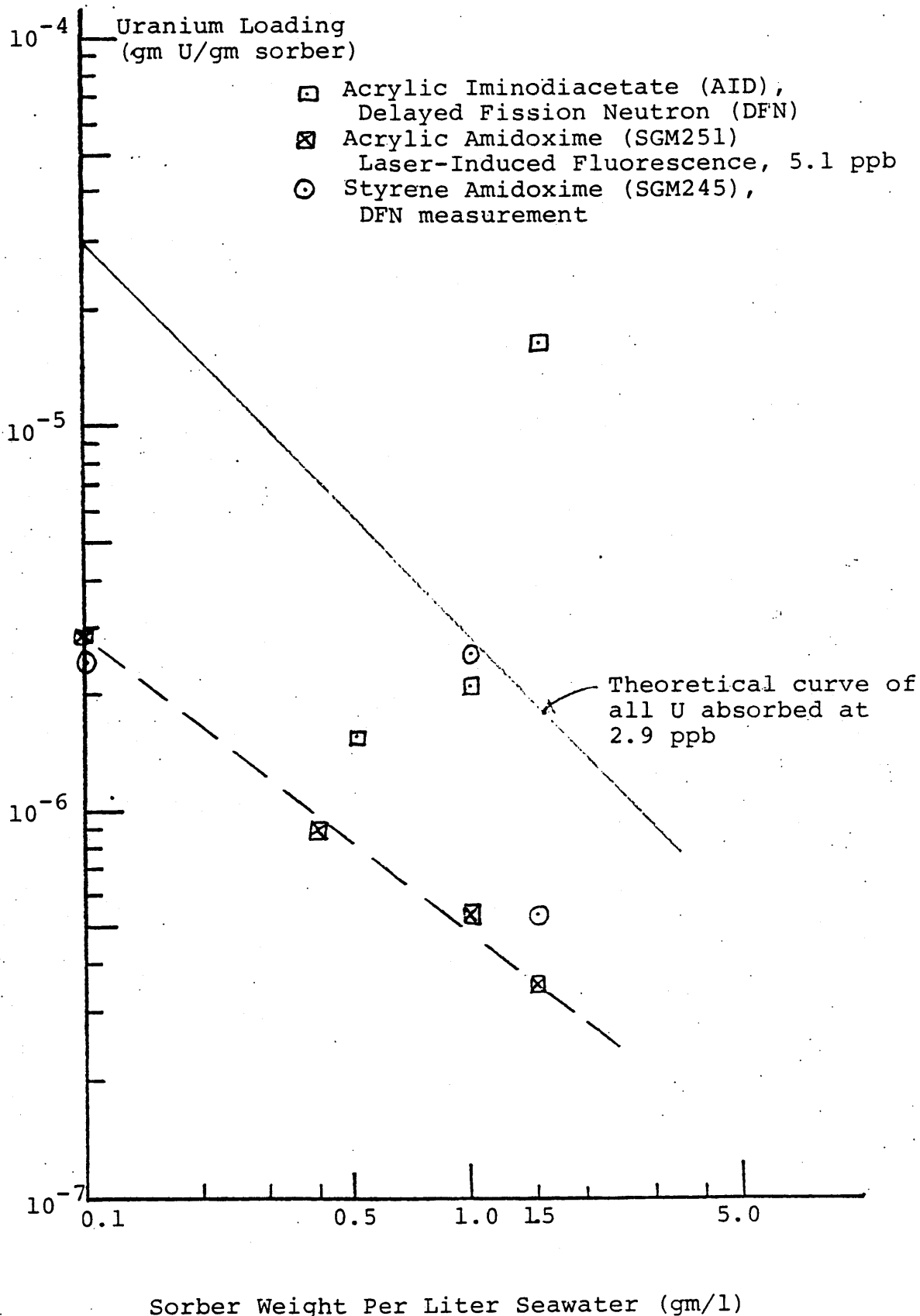


Fig. 4.2 Equilibrium Experiment:  
 Uranium Loading versus Sorber Weight  
 per Liter Seawater (2.9 ppb) for AID,  
 SGM251 and SGM245.

Both the HTO and the XE318 tended to have higher uranium loading per unit weight than the other sorbers. This would imply either that these sorbers had a greater capacity than the others if the conditions were truly those of an equilibrium system or that the mass transfer kinetics of these sorbers were superior to those of the other sorbers. According to a Rohm and Haas report (M3), there was no difference in resin performance after 16 hours or 6 days of exposure to near-natural (6 to 7 ppb U) seawater. Thus, superior loading for the XE318 compared to the other ion-exchange resins might be expected. (However, see Sections 4.3.2, Column Experiments Results and Discussion, and 5.5, Recommendations). In the M.I.T. equilibrium experiments, the XE318 exhibited loading superior to all sorbers, even HTO. In the Rohm and Haas experiment, XE318 was second to Acrylic Amidoxime (SGM251).

The liter of seawater used in each equilibrium loading experiment contained approximately 3 micrograms of uranium. Hence, the data points above  $3 \times 10^{-5}$  gm U/gm sorber are presumably in error. These points could indicate sample contamination or the counting of high energy gamma-rays from Na and Cl in the detectors. The latter possibility is not likely since the laboratory background count rate did not increase for the duration of any irradiation run. In any event, these results imply that the subject sorbers were highly effective in removing most of the uranium from solution.

The loading values for HTO and XE318 obtained by Rohm and Haas in the 6 and 25 ppb seawater experiments are given along with data for the other resins tested in Appendix A.3.5; (Equilibrium Experiment: Rohm and Haas Company Laser-Induced Fluorescence Measurements). Both HTO and XE318 showed one order of magnitude poorer loading than did the same sorbers loaded in the equilibrium experiments performed at M.I.T. Several explanations are possible. Since the laser-induced fluorescence (LIF) technique measures the uranium left in solution, some of the XE318 and HTO might have remained in the solution in the form of fine powder. These two sorbers are more likely to have experienced this kind of attrition than the other ion-exchange resins, since they were particularly easy to crush and have a chalky consistency relative to the hard-plastic consistency of the other resins. Thus the uranium remaining in solution may have included some which had sorbed onto these materials. Another possibility is that mass-transfer was suppressed due to the relatively high uranium concentration in the 'natural seawater,' since there exists (presumably reliable) data showing that in some cases, high uranium concentration actually decreased uranium loading in gel particles containing  $Ti(OH)_4(S1)$ . Furthermore, the 6 ppb "natural" seawater concentration compared to the 3 ppb world average suggests the possibility of either contamination or inaccurate measurement.

Generally, the Acrylic Iminodiacetate (AID) showed poorer performance than the HTO and XE318 under similar experimental

conditions in the present work. The DFN measurements consistently showed a significantly poorer performance by AID compared to XE318. AID was not exposed to natural seawater in the Rohm and Haas experiments, but AID exposed to 21.2 ppb seawater showed performance superior to both HTO and XE318 at the same seawater concentration (see Appendix A.3.5). This contradicts the results found in the M.I.T. phases of the present work.

However, in the sense that the measured capacity of AID increased rather than decreased with increasing sorber weight per liter of seawater, the DFN measurements of AID loading were contrary to expected behavior. A fixed amount of uranium distributed over greater sorber weight would be expected to produce a decreasing trend, which is observed for the other sorbers.

DFN measurements for the Styrene Amidoxime (SGM245) showed that it had better loading characteristics than the AID and the Acrylic Amidoxime but poorer than those for the XE318 and HTO. The peaking of the loading at 1.0 gm/l for the SGM245 is attributed to experimental error, (as is that for the XE318 data point at 1.0 gm/l). SGM245 was not exposed to natural seawater in the Rohm and Haas experiments. However, at 21.2 ppb, the SGM245 exhibited the poorest loading of all sorbers exposed to 21.2 ppb or greater seawater. Clearly, these results contradict those found in the present work.

DFN measurements for the Acrylic Amidoxime (SGM251) did not show any uranium pick-up by the resin. If this experiment had been the only screening procedure performed, then the SGM251 would be immediately disqualified as a suitable candidate for further ion-exchange development in uranium-from-seawater applications. However, Rohm and Haas has reported capacities of  $1.5 \times 10^{-5}$  and  $4.4 \times 10^{-5}$  gm U/gm resin for SGM245 and SGM251, respectively. In fact, in the 5.1 ppb seawater equilibrium experiments, the SGM251 showed loading performance superior to both the XE318 and HTO for both capacity and kinetics.

At this time, it is not possible to isolate the cause of these discrepancies; they could have been caused by a number of factors. The time of exposure may not have been adequate for the sorbers to reach equilibrium with the natural seawater or spiked solutions, but since all sorbers were loaded for the same amount of time, differences in uranium uptake may merely reflect superior mass transfer kinetics in a nonequilibrium state. In fact, nonequilibrium conditions are more likely to simulate the actual operating conditions of a practical extraction system than do equilibrium conditions. The initial concentration of the seawater used in these equilibrium experiments is probably the dominant factor affecting the loading performance of the sorbers. A higher initial concentration of uranium in seawater would theoretically increase the driving force for mass transfer from the solution to the sorber,

[although it has been demonstrated that the opposite can be true (S1)]. The Rohm and Haas data (see Appendix A.3.5) show this to be the case overall.

Generally, the DFN measurements of the present work showed sorber performance different from that shown in the Rohm and Haas experiments. Temperature effects on sorber loading are not a consideration since both sets of experiments were performed at room temperatures of approximately 22°C. Neither can this be explained by the loss or addition of uranium between the solution and the containers; loss of uranium from solution as measured by LIF would have been interpreted as a higher, not lower, sorber loading. On the other hand, addition of uranium from containers into the solution is not likely since the concentration of uranium in the solution is much higher than it could be in the container material and therefore there should be no driving force for diffusion in this direction. (Surface contamination is ruled out by the use of good laboratory procedure).

Because the DFN and LIF measurements produced such disparate and inconsistent results, it is recommended that, for the near term at least, all of the sorbers be tested in fixed-bed ion-exchange column experiments with natural seawater before any conclusions concerning their performance characteristics can be made.

#### 4.3.2 Column Experiments

As described in section 3.4, sorbers were exposed to varying volumes of natural seawater for 1, 3, 7 and 30 days



in fixed-bed columns at the Redfield Laboratory of the Woods Hole Oceanographic Institute. The uranium loading versus exposure time is plotted in Fig. 4.3. The supporting numerical data are given in Appendix A.3.3. A different view of the same experiment is shown in Fig. 4.4, where the uranium loading is plotted versus seawater volume exposure, (and the numerical data are given in Appendix A.3.3). Each data point represents an average value for multiple measurements made on sorber sampled from the same loading experiment. Information on the average temperature of the seawater during the loading run is not shown on the graphs but is given in Appendix A.3.3.

In Fig. 4.3, uranium uptake is seen to increase rapidly with exposure time; for one day exposures, all of the resins exhibit similar loading. After a few days, resin performance begins to differ, and the loading rate is not as great as it is initially. The Acrylic Amidoxime (SGM251) 30 day capacity is comparable to that of Hydrous Titanium Oxide (HTO) within experimental accuracy, but the consistently higher loading of the HTO over time tends to support the assertion that the HTO showed superior uranium-uptake throughout, although the SGM251 came very close to matching this performance. The average loadings at 30 days for HTO and SGM251 are 391 and 324 ppm, respectively. It is also noted that the SGM251 ion-exchange resin has not been optimized with respect to performance, whereas the HTO has been. The Styrene Admidoxime (SGM245) showed the next best performance with an average 30

Uranium Loading  
(gm U/gm sorber)

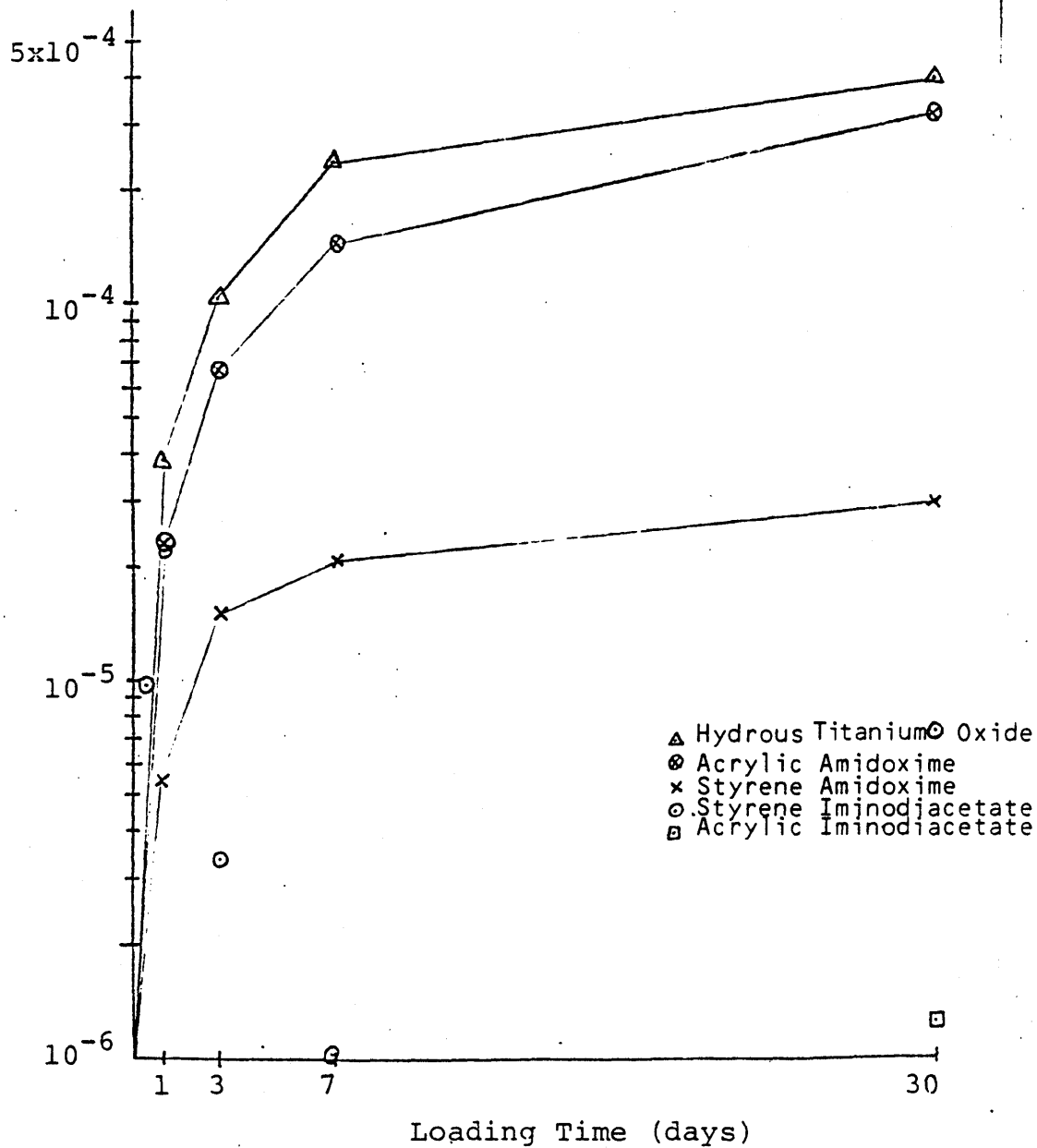


Fig. 4.3 Ion-Exchange Experiments:  
Uranium Loading versus  
Loading Time

day loading of 30 ppm. The Styrene Iminodiacetate (XE318) and Acrylic Iminodiacetate (AID) had average 30 day loadings of 23 and 1 ppm, respectively. This trend in performance is different from the trend predicted by the results of the M.I.T. equilibrium loading experiments. From those results, the XE318 would be expected to perform better than any of the other sorbers tested, even the HTO. In these column experiments, however, the XE318 out-performed only the AID.

Sorber performance similar to that for the loading versus time data can be observed in the loading versus seawater volume data shown in Fig. 4.4. However, between 3,000 and 4,000 ft<sup>3</sup>, the average SGM251 loading becomes greater than that for HTO. Also, the slope of the loading versus seawater volume plot is greater for the SGM251 than the HTO in this region, indicating that the resin capacity has not yet reached saturation. It is important to note that the average seawater temperature during the 30 day HTO loading was higher than that for the SGM251 loading, 72.7 versus 68.4°F, respectively, which would tend to improve the loading kinetics for the HTO compared to those for the SGM251.

Generally, the Amidoxime functional group was more effective in loading uranium than was the Iminodiacetate functional group. The polymer to which these functional groups are attached gives these ion-exchange resins their physical and structural properties. The acrylic-based resins (SGM251 and AID) showed the greatest structural integrity

Uranium Loading  
(gm U/gm sorber)

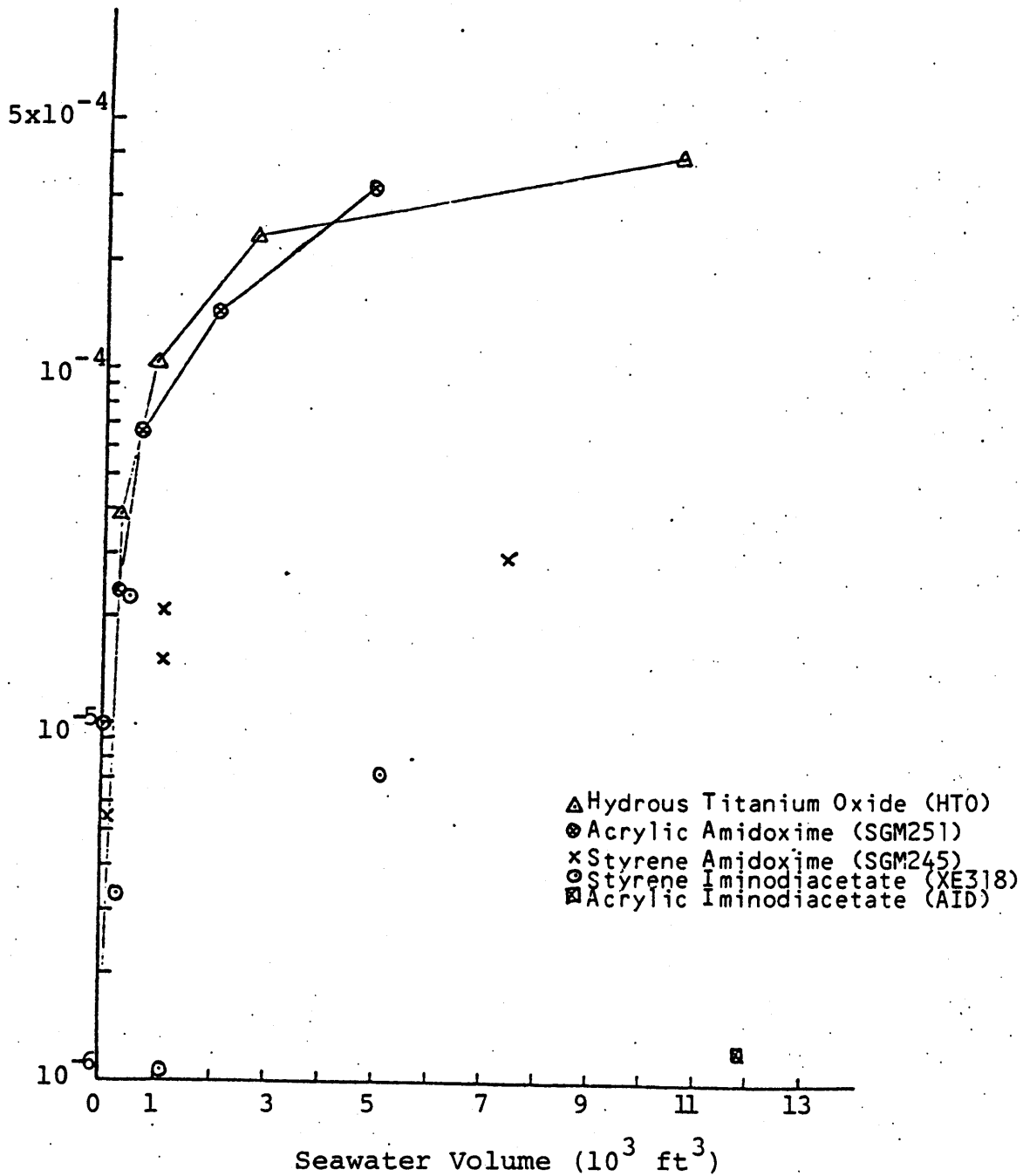


Fig. 4.4 Ion-Exchange Column Experiments:  
Uranium Loading versus Seawater  
Volume

during handling; these resins could not be crushed with a ceramic mortar and pestle before being weighed, (see Section 3.4.4, Preparation of Samples for Irradiation). The styrene-based SGM245 was equally strong and could not be crushed during sample preparation. These resins could easily withstand the structural demands of the highest flow loadings employed in this study. The styrene-based XE318, was easily crushed with a mortar but could withstand the pressure of being squeezed between one's fingers without any visible damage to the integrity of the spherical resin bead. The chalky HTO pellets were the most susceptible to handling damage; even when pressed between two fingers, there was visible loss of material from the pellet. Therefore, it is hypothesized that some attrition may have occurred during the HTO flow loading experiments.

Overall, the Acrylic Amidoxime exhibited the greatest uranium capacity, combined with superior mechanical durability among all of the ion-exchange resins tested.

The possibility that the DFN system counted high energy gamma rays has been mentioned previously (see section 4.3.1) but was dismissed as unlikely because of lead shielding surrounding the central rabbit tube during counting, and the absence of an increase in the laboratory background count rate over the duration of an irradiation run when activated samples were accumulating. Gamma-interference from  $^{24}\text{Na}$  can be further discounted by noting the loading behavior of the column resins in Fig. 4.3. Presumably, Na loading in the

sorbers would be saturated very quickly due to the high Na concentration in seawater. Any Na sorbed onto the material would be picked up in less than one day. If this were indeed the case, then from Fig. 4.3, the contribution by  $^{24}\text{Na}$  gamma-interference to the maximum loading capacity for HTO and SGM251 would be less than 10%, that is, on the order of the calculated experimental accuracy for the subject measurements.

#### 4.4 Summary

Seawater uranium content determination by activation analysis or delayed fission neutron counting proved to be impractical because of high energy gamma emission from  $^{24}\text{Na}$  and  $^{80}\text{Br}$ . Major obstacles included masked  $^{239}\text{Np}$  peaks due to Compton background in activation analysis, and intolerably high exposure dose for both techniques. Salinity measurements taken at the Woods Hole Oceanographic Institute (WHOI) provided a salinity measurement for WHOI seawater which was converted to a uranium concentration. This value (2.9 ppb U) was used throughout the present work.

Sorber loading in M.I.T. equilibrium experiments did not generally correspond to results of the Rohm and Haas (R&H) Company. Differences in experimental conditions could not explain the order of magnitude discrepancies encountered. Column loading results in flowing seawater at WHOI yielded a performance ranking different from that found in equilibrium experiments at either MIT or R&H. The highest WHOI loadings were for Acrylic Amidoxime (SGM251) and Hydrous Titanium

Oxide (HTO) with 324 and 391 ppm U respectively, for 30 day exposure to natural seawater. Effects of seawater exposure volume and temperature variations on the relative ranking of SGM251 and HTO were discussed.

CHAPTER V  
CONCLUSIONS AND RECOMMENDATIONS

5.1 Introduction

In the present work, delayed fission neutron (DFN) counting was used to measure the uranium content of sorbers loaded during equilibrium and ion-exchange column experiments.

Sorber uranium loading performance in the column experiments was found to be different from that predicted by the equilibrium screening experiments. In this chapter, conclusions which can be drawn from the execution of the experiments and from their results are discussed. First, the DFN counting system and procedure are assessed with respect to their applicability to the present problem and their accuracy. Next, the sorber loading in the fixed-bed column system is evaluated. Then sorber performance is discussed with respect to improved mechanical properties and uranium capacity. Recommendations for future research in uranium-from-seawater sorber testing and for improving the DFN counting technique are presented. Finally, a few remarks summarizing the findings of the present work are offered.



## 5.2 Delayed Fission Neutron (DFN) Counting System

In Chapter 2 of this work, "Delayed Fission Neutron Counting System", the irradiation facilities, transfer system and counting apparatus were described, together with irradiation and counting procedures which were developed within the theoretical and practical constraints of these systems. In general, the DFN system was very reliable in determining the uranium content of a given sorber sample within an experimentally determined uncertainty (one sigma) between 4.9 and 28.1% (see Appendix A.3). The minimum level of detection was of the order of a 0.1 microgram (see Appendix B), with a combined geometric and intrinsic efficiency for the detectors of up to 24%. There are, however, some procedures which could be modified to improve the accuracy and the minimum level of detection for this system.

The uranium contamination in the polyethylene rabbits and vials was determined to be on the order of 71 ppb by weight. During the execution of the counting procedure, time constraints were such that samples would be inserted for irradiation before the previous sample had been completely counted, separated from its rabbit and stored under a hood. Because of the overlap between counting cycles for different samples, there was insufficient time to

remove the sample from the rabbit prior to counting. If this were done, it would essentially eliminate the background contribution from the polyethylene, since most of the polyethylene is found in the rabbit. Counting the sample in the vials alone would reduce the background count anywhere from 150 to 300 counts per minute for an individual sample. This reduction would result in a 16 to 37% reduction in the minimum level of detection for a background count rate of 500 counts per minute. If increased sensitivity is desirable, then counting samples after they have been removed from their rabbits would be advisable. A smaller central rabbit tube has been fabricated to fit into the existing tube in the detector assembly to hold the smaller diameter vials in a reproducible central position. It should be noted that this additional handling of the irradiated sample prior to counting will increase the neutron and gamma-ray exposure dose to the experimenter, since the removal of the rabbit from the sample vial cannot be done remotely at this time.

Remote sample handling between the receive station of the IPH1 transfer tube and the detector assembly and then to the hood for temporary storage, if it could be implemented, would also permit the measurement of the neutron count rate in samples which emit many low energy gamma rays. Currently, these samples would pose too significant a radiation dose risk to make such runs worthwhile. There

are two observations which support the detectors' ability to discriminate against low energy gamma activity. First, the  $^3\text{He}$  tube lower threshold level was set at 1.3 MeV with  $^{60}\text{Co}$  gamma rays. And second, counted samples which showed gamma activity when surveyed with a Geiger-Mueller detector did not raise the background count rate above that measured for the empty  $^3\text{He}$  tube assembly as samples were accumulated in the storage hood during an irradiation run.

The extent to which variations in the irradiation geometry of the sample affects its measured count rate could be more accurately assessed if the neutron flux in the LPH1 pneumatic tube were more precisely characterized with respect to position. This is less of a concern when the uranium content in a sample is determined by comparison with a background blank of nearly the same shape and non-uranium content, but when comparing the count rate of a sample of unusual geometry for which a standard blank cannot be made or measured, knowledge of the flux variation with position would facilitate the estimation of analytic correction factors. Similarly, it would be desirable to include flux monitors (gold or cobalt foils) in each sample to provide an independent measurement of the ambient neutron exposure if further work indicates that run-to-run flux/position variations constitute the largest source of uncertainty in the entire DFN method (as employed in the present work).

The preparation of sorber background "blank" samples would be improved if sorbers were exposed to seawater which had had all of its uranium removed, leaving the trace element composition virtually the same as in undepleted seawater. This seawater depletion might be accomplished by repeatedly exposing unloaded samples of the sorbers to a fixed volume of seawater, until the sorbers showed two consecutively exposed batches to have the same count rate per unit mass when measured by delayed fission neutron counting. If these samples exhibited a higher count rate per unit mass than fresh sorber samples, which had not been contacted with any seawater, then the increased count rate could be attributed to seawater exposure -- the sorption of elements which, when exposed to a neutron flux, emitted neutrons or high energy gamma rays. In this case, elemental activation analysis could determine the identity of those elements.

Finally with respect to the counting electronics, it was noted in Section 2.3.2.1, Detector Plateau Curves, that the location of the plateau on the plot of count rate versus voltage supplied to the  $^3\text{He}$  tubes had shifted from its original voltage range when remeasured after all of the counting experiments had been completed. The cause of this shift should be identified and rectified to ensure the stability of the measured count rate.

### 5.3 Column Loading Experiment

It was found that the equilibrium screening experiments performed at the Rohm and Haas (R&H) Company did not yield results consistent with similar experiments conducted as part of the work performed at M.I.T. This may be due to the use of spiked uranium concentrations for the ion-exchange resin loading experiments at R&H whereas natural seawater was used at M.I.T., and to their measurement of uranium remaining in solution as an indicator of sorber uptake, versus the direct measurement of uranium in the sorbers in this study. Although the R&H experiments did find that the Acrylic Amidoxime (SGM251) showed the highest capacity of the four resins sent to M.I.T., M.I.T. equilibrium experiments showed no uranium uptake for SGM251; its superior performance was not evident until the ion-exchange column loadings were performed at the Woods Hole Oceanographic Institute. (Sorber performance in M.I.T. and R&H experiments will be compared further in section 5.4). Hence, it appears that sorber performance can only be accurately assessed under operating conditions similar to those which would be encountered in a practical extraction process, that is, long-term exposure to natural seawater.

Many of the practical problems peculiar to a natural seawater ion-exchange test system were solved in the design of the test columns used in this study (see section 3.4, Column Experiments). The final system performed reliably and achieved the design objectives of contacting a measured

quantity of clean, undepleted natural seawater with sorbers. There are, however, several suggestions for improvements which could be made to facilitate the operation of the system.

The fitting corrosion problem which was encountered might be reduced by using a more corrosion-resistant metal, such as bronze, whenever metal components show a tendency to oxidize over long times. These include the stainless steel hose clamps which were used to clamp the rubber tubing to the polyethylene and polyvinylchloride (PVC) fittings, and the interface between the stainless steel sorber support screens and the stainless steel screws which held them to the plexiglass column frame. Where fouling of the components is not a concern, oil-based corrosion-preventive treatment should be applied. These include all metal-metal interfaces which are external to the seawater flow path.

Biological growth was evident on the inside surface of some of the clear rubber tubing, although none was evident inside any of the opaque, PVC, elements of the system. This implies that the absence of visible light inhibits the growth of biological materials. Thus, application of paint, tape, or a removable cowl to the outside of the clear tubing might reduce the growth of this material and thereby reduce the clogging by biological growth. It would also reduce the load on the

prefilters by reducing the likelihood of growth sluffing-off into the seawater as it rushed by at high velocity.

In addition to reducing the load on the seawater prefilters by reducing biological growth, the frequency of filter cartridge replacement might be further reduced by increasing the filtering capacity of the prefilter system. At present, the cartridges for the double-cartridge filter housings must be replaced every three to four days to prevent complete loss of flow. This is clearly inconvenient for the longer loading runs. Construction of a sand-bed filter or use of a commercial (swimming-pool) filter should be investigated.

#### 5.4 Sorber Performance and Development

Acrylic Amidoxime showed the greatest uranium capacity (324 ppm at 30 days) in the column loading experiments of all of the ion-exchange resins tested, and even outperformed Hydrous Titanium Oxide (HTO) when considered on an equal seawater volume basis. The Amidoxime functional group showed uranium loading capacity superior to the Iminodiacetate group when supported by either Acrylic- or Styrene-divinylbenzene polymer backbones, as evidenced by the order of magnitude superior loadings of Acrylic Amidoxime (SGM251) and Styrene Amidoxime (SGM245) over both Styrene Iminodiacetate (XE318) and Acrylic Iminodiacetate (AID), respectively. The Acrylic polymer backbone did not confer superior

mass transfer capabilities to the resins when compared to the Styrene backbone, as was suggested by the Rohm and Haas (R&H) findings (M3). Evidence for these conclusions is summarized in Table 5.1 for equilibrium and column experiments performed at M.I.T. and at the R&H Company.

The differences in performance evidenced in Table 5.1 transcend discrepancies explainable by the facts that different seawater uranium concentrations were involved and different analytical procedures were used. For example, in the equilibrium experiments the R&H loadings are considerably below the M.I.T. values for XE318 and HTO (despite the higher uranium content of the seawater), but the SGM251 appeared to be inert in the M.I.T. test. Rohm and Haas maximum capacity values show roughly the same trend as M.I.T.'s WHOI runs, but again are an order of magnitude lower; here again, however, the M.I.T. data includes one "inert" performer -- this time AID.

One can only conclude that the three basic classes of experiments (M.I.T. equilibrium, R&H equilibrium, M.I.T.-WHOI Column), while showing consistent qualitative trends in some respects, differ substantially on a quantitative basis, and are mutually inconsistent in several specific instances. Superficial explanations for these differences can be advanced, but they do not survive detailed scrutiny. For example, roughly one M.I.T. DFN measurement in fifteen yielded an unexpected zero net activity result (perhaps



due to a failure of the rabbit to undergo irradiation properly, or a momentary interruption of the counting circuitry). This would lead to a projection of inertness on the part of the sorber. However, in all cases, sufficient repeat measurements were made on each sample to spot and reject such anomolous runs.

Thus unexplained discrepancies remain which deserve further examination. For the present, it must be concluded that no single laboratory screening process can be accepted as a completely reliable indication of sorber performance. It also appears to be preferable to assign a greater confidence to the column loading experiments over those performed in the laboratory, on the grounds that they involve the least artificial circumstances, and to the DFN uranium assay method, since it measures sorber uptake directly, and was able to confirm an HTO capacity similar to those quoted in the literature (391 ppm U compared with 212 ppm (B6) and 660 ppm (K3) reported for UEB 1.5 mm HTO pellets at 20 days loading and Japanese powdered HTO at 77°F respectively).

With the foregoing caveats in mind, other general observations can also be made. In particular, the anticipated superior kinetics reported by R&H of the ion-exchange resins relative to HTO did not result in greater loading capacity per unit volume or per unit time in ion-exchange

column experiments having exposure times between 1 and 30 days. In the column experiments, the velocity of the seawater should have been high enough to minimize the fluid-side resistance to mass transfer relative to the solid-side resistance. However, all of the sorbers tended to load comparably for exposure time less than one day and only the SGM251 loaded to a capacity comparable to that of HTO.

Superior mechanical strength was exhibited by all of the ion-exchange resins relative to HTO. This is very important for minimizing sorber attrition, and the attendant costs (sorber and product loss, and bed plugging), in a practical extraction process design.

In future sorber development work, it is recommended that the loading performance of the Amidoxime functional group on Acrylic and Styrene polymer backbones be optimized by varying the crosslinking, particle size, surface area, or other parameters which affect uranium uptake in natural seawater. Elution experiments should also be performed to measure the removal rate and efficiency characteristics of candidate sorbers under realistic process conditions. Whereas uranium loading can be more accurately determined by measurement of the uranium content in the sorber phase, elution efficiency can be satisfactorily determined by measurement of the uranium concentration of the eluate.

Table 5.1  
 Comparison of M.I.T. and Rohm and Haas Company  
 Data on Sorber Performance

Sorber	MIT Equilibrium Experiments (0.5 gm sorber/l seawater)	Rohm & Haas Equilibrium Experiments (0.5 gm sorber/l seawater)
	Sorber Loading (ppm)*	Sorber Loading (ppm)**
XE318	29.0	3.6
HTO	25.7	2.9
SGM245	23.9	-
AID	1.5	-
SGM251	0.0	8.7

MIT Column Experiments at WHOI Rohm & Haas Maximum Capacity  
 (30 day exposure)

Sorber	Sorber Loading (ppm)*	Sorber Loading (ppm)***
HTO	391.0	> 34.9
SGM251	324.4	> 44.1
SGM245	30.1	15.0
XE318	23.3	11.2
AID	1.3	30.4

\* 2.9 ppb seawater

\*\* 5.1 to 5.9 ppb seawater

\*\*\* 2.54 ppb seawater

XE318=Styrene Iminodiacetate

HTO=Hydrous Titanium Oxide

SGM245=Styrene Amidoxime

AID=Acrylic Iminodiacetate

SGM251=Acrylic Amidoxime

## 5.5 Conclusion

The results of the present work indicate that the delayed fission neutron assay provides an accurate, reliable and convenient method for measurement of trace fissionable isotopes at the sub-microgram level. Sorber loading experiments showed that laboratory batch experiments did not yield results representative of tests in the field under conditions which were as close as possible to those which would be encountered in large-scale industrial works. These latter results demonstrated that first-generation, developmental ion-exchange resins can already match the performance of Hydrous Titanium Oxide with respect to kinetics and capacity, and far surpass it in physical durability. Hence, optimization of the Amidoxime functional group on Acrylic or Styrene polymer bases holds promise for the development of superior sorbers for an uranium-from-seawater extraction process.

REFERENCES

- A1 Abdullah M.S. Almasoumi, "Characterization of MITR-II Facility for Neutron Activation Analysis," S.M. Thesis, MIT, August 1978, pp. 69-83.
- A2 S. Amiel, "Analytical Applications of Delayed Neutron Emission in Fissionable Elements," Analytical Chemistry, 34, 13, December 1962, pp. 1683-92.
- B1 S.E. Binney and R.I. Sherpelz, "A Review of the Delayed Neutron Technique," Nuclear Instruments and Methods 154 (415), 1978.
- B2 F.R. Best and M.J. Driscoll, "Prospects for the Recovery of Uranium from Seawater," M.I.T., January 1980, Energy Lab. Report No. MIT-EL80-001, p. 189.
- B3 Ibid., p. 191.
- B4 Op. cit., Binney, p. 413.
- B5 Op. cit., Best, p.25.
- B6 J. Bitte, M.I. Fremery and H.G. Bals, "On the UEB Concept of Uranium Extraction from Seawater," in the Proceedings of the Topical Meeting on the Recovery of Uranium from Seawater, Cambridge, Mass. 02139, Dec. 1 and 2, 1980, F.R. Best and M.J. Driscoll (Eds.), Energy Laboratory Report No. MIT-EL80-031, p. 172U.
- D1 H. DeBaar (personal correspondence), Clark Laboratory, Woods Hole Oceanographic Institute, Woods Hole, Mass.
- K1 G.F. Knoll, Radiation Detection and Measurement, John Wiley & Sons, New York, 1979, p. 533.
- K2 Teh-Lung Ku, K.G. Knauss and G.G. Mathieu, "Uranium in Open Ocean: Concentration and Isotopic Concentration," Deep Sea Research 24 (1005-1070), 1977.
- K3 M. Kanno, "Adsorption and Elution of Uranium in Seawater," in the Proceedings of the Topical Meeting on the Recovery of Uranium from Seawater, Cambridge, Mass. 02139, Dec. 1 and 2, 1980, F.R. Best and M.J. Driscoll (Eds.), Energy Laboratory Report No. MIT-EL80-031, p. 48U.
- M1 Y. Miyake, K. Saruhashi and Y. Sugimura, Records of Oceanographic Works in Japan 12 (23-24), 1973.

- M2 T. Murata, Y. Ozawa, H. Yamashita and F. Nakajima, "Uranium Extraction from Seawater with Composite Adsorbents, (II), Uranium Adsorption on Composite Hydrous Titanium (IV) -- Iron (II) Oxide," Journal of Nuclear Science and Technology 16 (671-678), September 1979.
- M3 S.G. Maroldo, "Extraction of Uranium from Seawater with Synthetic Ion Exchange Resins," Rohm and Haas Company Report, #7388-7/C1, OCR 81-2-101, included as Appendix D.
- O1 N. Ogata, "Extraction of Uranium from Seawater (I), Coprecipitation of Uranium in Sea Water with Metal Hydroxides," Nihon Genshiryoku Gakkai Shi 10 (12), 1968, pp. 672-678.
- R1 For a detailed description of the distinction between RECEIVE mode and SEND/RECEIVE mode, see MITR Reactor Operations document entitled "IPH1: Information for Operation, 8/1/79."
- S1 Y. Shigetomi, T. Kojima and M. Shinagawa, "Basic Study on Uranium Extraction from Sea Water, (II), Extraction of U(VI) by Polyacrylamide Gel Containing Various Metal Hydroxides," Journal of Nuclear Science and Technology 14 (11), November 1977, pp. 811-815.
- V1 R. Van Konynenburg, "Detection Limits and Accuracy of Elemental Determinations by Instrumental Neutron Activation Analysis (INAA)," internal LLNL memorandum, April 30, 1979.
- Y1 H. Yamashita, Y. Ozawa, F. Nakajima and T. Murata, "The Collection of Uranium from Sea Water with Hydrous Metal Oxide. IV. Physical Properties and Uranium Adsorption of Hydrous Titanium (IV) Oxide," Bulletin of the Chemical Society of Japan 53 (11), November 1980, pp. 3050-3053.
- Y2 H. Yamashita, Y. Ozawa, F. Nakajima and T. Murata, "The Collection of Uranium from Sea Water with Hydrous Metal Oxide. II. The Mechanism of Uranium Adsorption on Hydrous Titanium (IV) Oxide," Bulletin of the Chemical Society of Japan 53 (1), January 1980, pp. 1-5.

APPENDIX A

The tables which follow (designated as sub-Appendices A.1.1 through A.3.5) document the experimental data acquired during the course of the subject project, together with pertinent comments on data treatment and intermediate computations.

## APPENDIX A.1.1

## Polyethylene Uranium Contamination

<u>Polyethylene Weight (grams)</u>	<u>Normalized Net Counts Per Min</u>	<u>+ Error</u>
2.522	110	7
2.525	1558	81
4.602	47	3
4.677	32	2
6.084	29	2
6.246	50	4
25.44	256	16
25.62	310	19
27.37	264	17
27.40	1106	59
28.36	179	12
28.50	227	14



## APPENDIX A.1.2

## Neutron Absorption in Sorbers:

## Unloaded Sorber Counting

<u>Sorber</u>	<u>Sorber Weight</u>	<u>Normalized Net Cts/Min</u>
Acrylic Iminodiacetate (AID)	0.101705	-14
	0.101705	-135
	0.111911	-22
	0.111911	-243
	0.517758	+2
	0.968953	+58
Styrene Iminodiacetate (XE318)	0.096916	+70
	0.096916	-171
	0.104772	-25
	0.104772	-339
	0.496892	-87
	0.755563	-37
Styrene Amidoxime (SGM245)	0.107806	-153
	0.538047	-106
	0.928706	-111
Acrylic Amidoxime (SGM251)	0.089797	+132
	0.542100	+193
	0.709341	-63
Hydrous Titanium Oxide (HTO)	0.115052	+123
	0.504381	-14
	0.993383	+179

## APPENDIX A.1.3

Neutron Absorption in Sorbers:  
 Effect of Varying Sorber Weight  
 with Constant Uranium Content

<u>Sorber</u>	<u>Sorber* Weight(gram)</u>	<u>Normalized Net Counts/Min</u>	<u>± Absolute Error</u>
Acrylic	0.1027	329704	32,317
Amidoxine	0.1030	325204	31,876
(SGM251)	0.4927	329133	32,314
	1.0281	323279	31,687
	1.0341	294571	28,874
Hyrdous	0.1060	319542	31,321
Titanium	0.1173	331942	32,536
Oxide	0.5009	323324	31,692
(HTO)	0.5028	328327	32,182
	1.0171	321382	31,501
	1.0029	287664	28,197

\*Uranium content =  $7.10559 \times 10^{-4}$

## APPENDIX A.2.1

Average Neutron Flux Normalization Factors,  $\phi_i$ 

Irradiation Date; Run Std. Index	NET COUNTS/MINUTE				
	7/24/81 i = 1	8/6/81 i = 2	8/28/81 i = 3	10/1/81 i = 4	10/23/81 i = 5
6 UO <sub>2</sub>	42,340	-	46,411	-	44,848
7 UO <sub>2</sub>	64,906	-	71,732	-	70,315
5 UO <sub>2</sub>	-	-	-	60,106	66,405
18 UN	-	495	1,129	578	800
16 UN	-	10,108	10,289	9,212	9,424

RATIOS OF  $\frac{\text{COUNTS } 10/23/81}{\text{COUNTS}(i)} = \phi_i$

1.059235	1.616162	0.9663226	1.104798	$\phi_5 = 1.0$
1.083336	0.9323308	0.9802459	1.384083	by
<u>Ave.=1.071285</u>	<u>Ave.=1.274246</u>	0.7085917	1.023013	definition
$\pm 0.871\%$	$\pm 10.1\%$	0.9159296	<u>Ave.=1.170632</u>	
		<u>Ave=0.8927725</u>	$\pm 9.8\%$	
		$\pm 4.71\%$		

The above averages were used to multiply all net counts from irradiation dates other than 10/23/81. Normalized data were then converted to uranium contents by division with the net counts/min./gmU conversion factor determined by measurement of the NBS uranium standard on 10/23/81.

The uncertainties in the averages were propagated from the uncertainties calculated for each ratio, which were in turn calculated from the uncertainties determined for each measurement of net counts per minute as in Appendices A.2.3 and A.2.4.

UN = Uranyl Nitrate

APPENDIX A.2.2

Uranium Dioxide and Uranyl Nitrate Data

(normalized to 10/23/81 NBS uranium standard)

Irrad. Date	Fractional Error	Sample #	Abs. Error	$U^{nat}$ (grams)	Net Cts/min/gm	Normalized Net Cts/min/gm
7/24/81 $UO_2$	0.7990	1	$1.3662 \times 10^9$	$6.2587 \times 10^{-5}$	$1.5962 \times 10^9$	$1.7100 \times 10^9$
	0.7990	2	$1.2825 \times 10^9$	$5.9061 \times 10^{-5}$	$1.6163 \times 10^9$	$1.7315 \times 10^9$
	0.4467	3	$5.6602 \times 10^8$	$1.1195 \times 10^{-4}$	$1.1827 \times 10^9$	$1.2670 \times 10^9$
	0.3886	4	$3.5278 \times 10^8$	$1.2870 \times 10^{-4}$	$8.4732 \times 10^8$	$9.0772 \times 10^8$
	0.2545	5	$2.7239 \times 10^8$	$1.9657 \times 10^{-4}$	$9.9892 \times 10^8$	$1.0701 \times 10^9$
	0.2271	6	$1.6174 \times 10^8$	$2.2038 \times 10^{-4}$	$6.6478 \times 10^8$	$7.1217 \times 10^8$
	0.1815	7	$1.5824 \times 10^8$	$2.7591 \times 10^{-4}$	$8.1397 \times 10^8$	$8.7199 \times 10^8$
	0.1605	8	$1.0080 \times 10^8$	$3.1205 \times 10^{-4}$	$5.8611 \times 10^8$	$6.2789 \times 10^8$
	0.1261	9	$8.3912 \times 10^7$	$3.9756 \times 10^{-4}$	$6.2104 \times 10^8$	$6.6531 \times 10^8$
	0.1224	10	$6.9747 \times 10^7$	$4.0990 \times 10^{-4}$	$5.3209 \times 10^8$	$5.7002 \times 10^8$
8/6/81 UN	0.6472	42	$3.9041 \times 10^8$	$1.3942 \times 10^{-7}$	$4.7337 \times 10^8$	$6.0319 \times 10^8$
	0.1504	49	$2.0605 \times 10^8$	$2.8188 \times 10^{-7}$	$1.0749 \times 10^9$	$1.2697 \times 10^9$
	0.1056	47	$2.1381 \times 10^7$	$2.8188 \times 10^{-6}$	$1.5893 \times 10^8$	$2.0252 \times 10^8$
	0.0967	48	$2.1637 \times 10^7$	$2.8188 \times 10^{-6}$	$1.7561 \times 10^8$	$2.2377 \times 10^8$
	0.1622	31	$8.1127 \times 10^6$	$7.1065 \times 10^{-6}$	$3.9260 \times 10^7$	$5.0027 \times 10^7$
	0.2291	32	$7.9297 \times 10^6$	$7.1065 \times 10^{-6}$	$2.7158 \times 10^7$	$3.4606 \times 10^7$
	0.1963	37	$9.3544 \times 10^6$	$1.3942 \times 10^{-5}$	$3.7397 \times 10^8$	$4.7653 \times 10^8$
	0.1917	38	$9.6797 \times 10^6$	$1.3942 \times 10^{-5}$	$3.9627 \times 10^8$	$5.0495 \times 10^8$
0.1574	45	$7.0510 \times 10^6$	$2.8188 \times 10^{-5}$	$3.5164 \times 10^8$	$4.4808 \times 10^8$	

Irrad. Date	Fractional Error	Sample #	Abs. Error	$U^{nat}$ (grams)	Net Cts/min/gm	Normalized Net Cts/min/gm
	0.1565	46	$7.1522 \times 10^6$	$2.8188 \times 10^{-5}$	$3.5859 \times 10^8$	$4.5693 \times 10^8$
	0.0152	29	$2.3220 \times 10^6$	$7.1065 \times 10^{-5}$	$1.2999 \times 10^8$	$1.6564 \times 10^8$
	0.0151	30	$2.5545 \times 10^6$	$7.1065 \times 10^{-5}$	$1.3246 \times 10^8$	$1.6879 \times 10^8$
	0.0109	35	$6.3152 \times 10^6$	$1.3942 \times 10^{-4}$	$4.5408 \times 10^8$	$5.7861 \times 10^8$
	0.0109	36	$6.3054 \times 10^6$	$1.3942 \times 10^{-4}$	$4.5332 \times 10^8$	$5.7764 \times 10^8$
	0.0105	43	$6.1599 \times 10^6$	$2.8188 \times 10^{-4}$	$4.5946 \times 10^8$	$5.8547 \times 10^8$
	0.0105	44	$6.1652 \times 10^6$	$2.8188 \times 10^{-4}$	$4.5987 \times 10^8$	$5.8599 \times 10^8$
8/28/81		542		$1.3942 \times 10^{-7}$	$-6.7420 \times 10^8$	$-6.0191 \times 10^8$
UN		541		$1.3942 \times 10^{-7}$	$-6.0248 \times 10^8$	$-5.3788 \times 10^8$
		550		$2.8188 \times 10^{-7}$	$-6.3856 \times 10^8$	$-5.7009 \times 10^8$
		549		$2.8188 \times 10^{-7}$	$-8.8689 \times 10^7$	$-7.9179 \times 10^7$
		534		$7.1065 \times 10^{-7}$	$-8.4430 \times 10^7$	$-7.5377 \times 10^7$
		533		$7.1065 \times 10^{-7}$	$-1.4072 \times 10^7$	$-1.2563 \times 10^7$
	0.1302	540	$2.8436 \times 10^7$	$1.3942 \times 10^{-6}$	$2.4458 \times 10^8$	$+2.1835 \times 10^8$
	0.1262	539	$2.8698 \times 10^7$	$1.3942 \times 10^{-6}$	$2.5462 \times 10^8$	$2.2732 \times 10^8$
	0.0652	548	$2.3320 \times 10^7$	$2.8188 \times 10^{-6}$	$4.0052 \times 10^8$	$3.5757 \times 10^8$
	0.0860	547	$1.7004 \times 10^7$	$2.8188 \times 10^{-6}$	$2.2137 \times 10^8$	$1.9763 \times 10^8$
	0.1319	532	$5.5331 \times 10^6$	$7.1065 \times 10^{-6}$	$4.7140 \times 10^7$	$4.2085 \times 10^7$
	0.1130	531	$5.8370 \times 10^6$	$7.1065 \times 10^{-6}$	$5.7835 \times 10^7$	$5.1634 \times 10^7$
	0.0500	537	$1.7524 \times 10^7$	$1.3942 \times 10^{-5}$	$3.9261 \times 10^8$	$3.5051 \times 10^8$
	0.0488	546	$1.5903 \times 10^7$	$2.8188 \times 10^{-5}$	$3.6501 \times 10^8$	$3.2587 \times 10^8$

Irrad. Date	Fractional Error	Sample #	Abs. Error	U <sup>nat</sup> (grams)	Net Cts/min/gm	Normalized Net Cts/min/gm
	0.0475	529	5.7354x10 <sup>6</sup>	7.1065x10 <sup>-5</sup>	1.3519x10 <sup>8</sup>	1.2069x10 <sup>8</sup>
	0.0476	535	1.9635x10 <sup>7</sup>	1.3942x10 <sup>-4</sup>	4.6249x10 <sup>8</sup>	4.1290x10 <sup>8</sup>
UO <sub>2</sub>	0.8479	557	4.3338x10 <sup>8</sup>	5.9061x10 <sup>-5</sup>	5.7250x10 <sup>8</sup>	5.1111x10 <sup>8</sup>
	0.8003	556	4.1133x10 <sup>8</sup>	6.2587x10 <sup>-5</sup>	5.7570x10 <sup>8</sup>	5.1397x10 <sup>8</sup>
	0.4491	558	1.6526x10 <sup>8</sup>	1.1195x10 <sup>-4</sup>	4.1216x10 <sup>8</sup>	3.6797x10 <sup>8</sup>
	0.3914	559	9.1067x10 <sup>7</sup>	1.2870x10 <sup>-4</sup>	2.6063x10 <sup>8</sup>	2.3268x10 <sup>8</sup>
	0.2587	560	7.2697x10 <sup>7</sup>	1.9657x10 <sup>-4</sup>	3.1474x10 <sup>8</sup>	2.8099x10 <sup>8</sup>
	0.2318	561	4.3577x10 <sup>7</sup>	2.2038x10 <sup>-4</sup>	2.1060x10 <sup>8</sup>	1.8802x10 <sup>8</sup>
	0.1873	562	4.3472x10 <sup>7</sup>	2.7591x10 <sup>-4</sup>	2.5998x10 <sup>8</sup>	2.3210x10 <sup>8</sup>
	0.13436	563	1.7744x10 <sup>7</sup>	3.9756x10 <sup>-4</sup>	1.4792x10 <sup>8</sup>	1.3206x10 <sup>8</sup>
	0.1308	564	2.3563x10 <sup>7</sup>	4.0990x10 <sup>-4</sup>	2.0178x10 <sup>8</sup>	1.8014x10 <sup>8</sup>
	0.1248	565	1.8859x10 <sup>7</sup>	4.3282x10 <sup>-4</sup>	1.6925x10 <sup>8</sup>	1.5110x10 <sup>8</sup>
10/1/81	0.1764	608	4.3262x10 <sup>7</sup>	1.3942x10 <sup>-6</sup>	2.0944x10 <sup>8</sup>	2.4518x10 <sup>8</sup>
UN	0.2597	609	3.7508x10 <sup>7</sup>	1.3942x10 <sup>-6</sup>	1.2337x10 <sup>8</sup>	1.4442x10 <sup>8</sup>
	0.1265	610	3.0365x10 <sup>7</sup>	2.8188x10 <sup>-6</sup>	2.0505x10 <sup>8</sup>	2.4004x10 <sup>8</sup>
	0.1416	611	2.5647x10 <sup>7</sup>	2.8188x10 <sup>-6</sup>	1.5468x10 <sup>8</sup>	1.8107x10 <sup>8</sup>
	0.2007	612	7.9665x10 <sup>6</sup>	7.1065x10 <sup>-6</sup>	3.3913x10 <sup>7</sup>	3.9699x10 <sup>7</sup>
	0.1779	613	8.4413x10 <sup>6</sup>	7.1065x10 <sup>-6</sup>	4.0526x10 <sup>7</sup>	4.7441x10 <sup>7</sup>
	0.0997	614	4.0067x10 <sup>7</sup>	1.3942x10 <sup>-5</sup>	3.4342x10 <sup>8</sup>	4.0202x10 <sup>8</sup>
	0.0989	615	3.7841x10 <sup>7</sup>	2.8188x10 <sup>-5</sup>	3.2681x10 <sup>8</sup>	3.8257x10 <sup>8</sup>
	0.0988	616	1.4000x10 <sup>7</sup>	7.1065x10 <sup>-5</sup>	1.2100x10 <sup>8</sup>	1.4165x10 <sup>8</sup>
	0.0982	617	4.6819x10 <sup>7</sup>	1.3942x10 <sup>-4</sup>	4.0716x10 <sup>8</sup>	4.7663x10 <sup>8</sup>

Irrad. Date	Fractional Error	Sample #	Abs. Error	$U^{nat}$ (grams)	Net Cts/min/gm	Normalized Net Cts/min/gm
	0.0982	618	$4.6866 \times 10^7$	$2.8188 \times 10^{-4}$	$4.0776 \times 10^8$	$4.7734 \times 10^8$
NBS	0.0982	679	$1.3578 \times 10^7$	$3.5398 \times 10^{-4}$	$1.1817 \times 10^8$	$1.3833 \times 10^8$
	1.0000	653	$1.7459 \times 10^8$	$3.4377 \times 10^{-5}$	$1.4914 \times 10^8$	$1.7459 \times 10^8$
	0.7937	652	$1.6548 \times 10^8$	$5.5531 \times 10^{-5}$	$1.7812 \times 10^8$	$2.0851 \times 10^8$
	0.6748	654	$1.2617 \times 10^8$	$6.6109 \times 10^{-5}$	$1.5974 \times 10^7$	$1.8699 \times 10^8$
	0.1584	651	$3.1454 \times 10^7$	$3.5434 \times 10^{-4}$	$1.6963 \times 10^8$	$1.9957 \times 10^8$
10/23/81	0.0054	679		$3.4014 \times 10^{-4}$	$1.3051 \times 10^8 \pm 7.02721 \times 10^5$	-
NBS	0.0054	679		$3.4014 \times 10^{-4}$	$1.3037 \times 10^8 \pm 7.0228 \times 10^5$	-
UO <sub>2</sub>	0.2001	626	$4.0716 \times 10^7$	$2.2036 \times 10^{-4}$	$2.0352 \times 10^8$	-
	0.1598	627	$4.0724 \times 10^7$	$2.7589 \times 10^{-4}$	$2.5486 \times 10^8$	-
	0.1244	651	$2.3320 \times 10^7$	$3.5434 \times 10^{-4}$	$1.8740 \times 10^8$	-
UN	0.0552	610	$1.5680 \times 10^7$	$2.8188 \times 10^{-6}$	$2.8381 \times 10^8$	-
	0.0131	615	$4.3792 \times 10^6$	$2.8188 \times 10^{-5}$	$3.3436 \times 10^8$	-

## APPENDIX A.2.3

## Uranium Dioxide Error Calculation

A brief derivation of the prescription used to estimate the value of  $\sigma$  for the  $\text{UO}_2$  calculation experiment follows.

Let  $N = \text{Net Counts/Minute}$

$$= G - B$$

$\sigma N = \text{Absolute Error in Net Counts/Minute}$

$$= \sqrt{\sigma G^2 + \sigma B^2}$$

$$= \sqrt{G + \sigma B^2}$$

$$= \sqrt{N + B + \sigma B^2}$$

and  $N/W_U = \text{Net Cts/gm U}$ .

$$\begin{aligned} \text{Then } \sigma N/W_U &= \sqrt{\left(\frac{\sigma N}{N}\right)^2 + \left(\frac{\sigma W}{W_{\text{UO}_2}}\right)^2} \times \frac{N}{W_U} \\ &= \sqrt{\frac{(N + B + \sigma B^2)}{N^2} + \left(\frac{\sigma W}{W_{\text{UO}_2}}\right)^2} \times \frac{N}{W_U} \end{aligned}$$

Then  $N/W_U$  must be normalized to the equivalent value for the 10/23/81 irradiation according to  $NN/W_U = \phi \cdot N/W_U$ .

$$\begin{aligned} \text{Therefore, } \frac{\sigma NN/W_U}{(NN/W_U)} &= \text{Fractional Error in Normalized Net Counts/} \\ &\quad \text{Min/gm U} \\ &= \sqrt{\left(\frac{\sigma N/W_U}{(N/W_U)}\right)^2 + \left(\frac{\sigma \phi}{\phi}\right)^2} \end{aligned}$$

Where  $G = \text{gross counts per minute (min}^{-1}\text{)}$   
 $B = \text{total background counts per minute (min}^{-1}\text{)}$   
 $W_U = \text{uranium weight (gm)}$   
 $W_{\text{UO}_2} = \text{uranium dioxide weight (gm)}$   
 $\sigma \phi / \phi = \text{fractional error due to neutron flux}$   
                   normalization correction (see Appendix A.2.1)  
 $NN = \text{normalized net counts per minute (min}^{-1}\text{)}$

The above equations were used to compute the results quoted in Appendix A.2.2 for  $\text{UO}_2$  measurements. As can be seen there, the one sigma values are not negligible. Thus, a more reliable uranium standard for calibration was sought.



## APPENDIX A.2.4

## Uranyl Nitrate Error Calculation

The error in the net counts is computed as for the normalized net counts in Appendix A.2.3. The overall error in the sample uranium content depends upon the errors in the concentration and volume measurements.

$$\begin{aligned} \text{So, } \frac{\sigma N/W_U}{(N/W_U)} &= \sqrt{\left(\frac{\sigma N}{N}\right)^2 + \left(\frac{\sigma W_{UN}}{W_{UN}}\right)^2 + \left(\frac{\sigma \phi}{\phi}\right)^2} \\ &= \sqrt{\frac{(N + B + \sigma B^2)}{N^2} + \left(\frac{\sigma W_{UN}}{W_{UN}}\right)^2 + \left(\frac{\sigma \phi}{\phi}\right)^2} \end{aligned}$$

$$\text{and } \frac{\sigma W_{UN}}{W_{UN}} = \sqrt{\left(\frac{\sigma C_i}{C_i}\right)^2 + \left(\frac{\sigma V}{V}\right)^2},$$

$$\text{since } W_{UN} = C \cdot V,$$

where  $N$  = net counts/minute ( $\text{min}^{-1}$ )

$W_U$  = uranium weight in the sample (gm)

$W_{UN}$  = uranyl nitrate weight (gm)

$\phi$  = neutron flux normalization factor  
(see Appendix A.2.1)

$B$  = total background counts/minute ( $\text{min}^{-1}$ )

$C_i$  = uranyl nitrate concentration (gmUN/ml)  
for solution set  $i$

$i$  = identification label

$v$  = volume of solution in a sample (ml)

$\sigma_x$  = absolute error in quantity  $x$ .

The error in the solution concentration,  $C_i$ , depends upon the magnitude of the concentration. Since all of the solutions were sequentially diluted from the same set of stock uranyl nitrate solutions, the uncertainty in concentration increases with decreasing concentration. The solutions were labeled A through E, from lowest to highest concentration corresponds to the addition of  $M$  grams of uranyl nitrate powder to 100 ml of deionized water.

$$\begin{aligned} \text{Thus, } \sigma_E &= C_E \sqrt{\left(\frac{\sigma_M}{M}\right)^2 + \left(\frac{\sigma_V}{V}\right)^2} \\ &= \frac{M}{100} \sqrt{\left(\frac{5 \times 10^{-5}}{M}\right)^2 + \left(\frac{0.1}{100}\right)^2} \end{aligned}$$

where  $C_E$  = stock solution concentration

$$= \frac{M \pm 5 \times 10^{-5} \text{ gm}}{100 \pm 0.1 \text{ ml}}$$

$M$  = mass of uranyl nitrate added to 100 ml deionized water (gm).

Each stock solution provided one ml which was diluted to a tenth of its concentration by addition of water.

$$\text{Thus, } C_D = \frac{C_E \cdot V_O}{V_D}$$

$$\text{and } \sigma_D = C_D \sqrt{\left(\frac{\sigma_E}{C_E}\right)^2 + \left(\frac{\sigma_{V_D}}{V_D}\right)^2 + \left(\frac{\sigma_{V_O}}{V_O}\right)^2}$$

$C_D$  = concentration of diluted solution (gm UN/ml)

$V_O$  = volume of stock solution (1.000 ± 0.005 ml)

$V_D$  = final volume of diluted solution (10.00 ± 0.01 ml)

and so on for subsequent dilutions. The fractional errors in uranyl nitrate weight for one ml samples of all solutions are given in the following table. As can be seen in Appendix A.2.2., for uranyl nitrate, the one sigma uncertainties due to solution concentration are a negligible contribution to the total calculated uncertainty in the normalized net counts/min./gmU.

	$M_1 = 2.9415$		$M_2 = 5.9470$		$M_3 = 1.4993$	
Solution Label	Concentration (gm UN/ml) $\times M_1$	Percent Error in Concentration	Concentration (gm UN/ml) $\times M_2$	Percent Error in Concentration	Concentration (gm UN/ml) $\times M_3$	Percent Error in Concentration
E	1.0	0.10143	1.0	0.10035	1.0	0.10541
D	0.1	0.51989	0.1	0.51968	0.1	0.52068
C	0.01	0.72821	0.01	0.72806	0.01	0.72877
B	0.001	0.88898	0.001	0.88886	0.001	0.88944
A	0.0001	1.02480	0.0001	1.02470	--	--

## APPENDIX A.3.1

Sample Normalization and Uranium Content Calculation  
and Discussion of the Propagation of Uncertainties

Given  $G$  = gross counts per minute ( $\text{min}^{-1}$ )

$B$  = total background counts per minute ( $\text{min}^{-1}$ )

Then  $N$  = net counts per minute ( $\text{min}^{-1}$ )

$$= G - B$$

Let  $NN$  = normalized net counts per minute ( $\text{min}^{-1}$ )

$$= N \cdot \phi_i$$

where  $\phi$  = neutron flux normalization factor

for irradiation date  $i$ , (see Appendix A.2.1).

Then  $C$  = uranium loading of the sorber sample ( $\text{gmU/gm}$ )

$$= \frac{NN}{W \cdot X}$$

where  $W$  = measured weight of sorber sample ( $\pm 5 \times 10^{-5} \text{ gm}$ )

$X$  = NBS standard conversion factor measured

on 10/23/81 ( $1.3044 \times 10^8 \pm 7 \times 10^4$  cts/min/gmU).

And the fractional error associated with  $C$  is given by:

$$\frac{\sigma_C}{C} = \sqrt{\left(\frac{\sigma_{NN}}{NN}\right)^2 + \left(\frac{\sigma_W}{W}\right)^2 + \left(\frac{\sigma_X}{X}\right)^2}$$

where  $\sigma_j$  = absolute error in quantity  $j$ ,

$$\frac{\sigma_{NN}}{NN} = \sqrt{\left(\frac{\sigma_N}{N}\right)^2 + \left(\frac{\sigma_{\phi_i}}{\phi_i}\right)^2}$$

and

$$\frac{\sigma_N}{N} = \sqrt{\frac{(N + B + \sigma_B^2)}{N^2}}$$

This prescription was used to calculate the error columns in Appendices A.3.2 and A.3.3.

In the present work the term "error" has been employed in the following ways:

- (1) the numeral one-sigma uncertainty ( $\sigma$ ) in Poisson counting statistics: the square root of the number of counts
- (2) estimated standard-deviation-from-the-mean (SDM) values inferred from multiple measurements on quantities such as weights and volumes
- (3) an estimated overall error,  $\sigma$ , in the end results of a series of calculations, determined by appropriate analytic combination of type (1) and (2) uncertainties.
- (4) SDM values for duplicate independent measurements of the same quantity (not however including Students' t-factor allowance for the small number of samples generally involved.)

While the fourth approach would be preferred in principle if time and money had permitted a larger number of samples to be run for each item tested, the third conceptualization of "error" was generally emphasized. Although this "error" estimate could in theory give values larger or smaller than the experimental  $\pm \sigma$  value (item 4 above), in all cases for which both values were determined in the present work, the analytically compounded value proved to be a conservative overestimate.

Hence quoted errors in the present work should be interpreted as qualitative estimates. In any event, the errors,

however determined, are well within the bounds required of a performance screening program of the type carried out here.

## APPENDIX A.3.2

Equilibrium Experiment Loading Data  
(for 16 hour exposures in 2.9 ppb seawater)

Sorber	Gm/liter	Sample #'s	Avg. Loading (GmU <sup>nat</sup> /gm sorber)	Absolute Error	Fractional Error
Acrylic Iminodiacetate (AID)	0.5	53	$1.4969 \times 10^{-6}$	$1.569 \times 10^{-7}$	.105
	1.0	54	$2.0045 \times 10^{-6}$	$2.095 \times 10^{-7}$	.105
	1.5	11	$1.6415 \times 10^{-5}$	$1.714 \times 10^{-6}$	.104
Hydrous Titanium Oxide (HTO)	0.1	21	$3.5059 \times 10^{-4}$	$3.5936 \times 10^{-5}$	.103
	0.5	23,24	$2.5690 \times 10^{-5}$	$4.437 \times 10^{-6}$	.173
	1.0	25,26	$8.7439 \times 10^{-6}$	$1.569 \times 10^{-6}$	.179
Styrene Iminodiacetate (XE318)	0.1	13	$2.9468 \times 10^{-4}$	$3.021 \times 10^{-5}$	.103
	0.5	15,16	$2.9043 \times 10^{-5}$	$4.554 \times 10^{-6}$	.157
	1.0	17,18,59	$5.8704 \times 10^{-5}$	$1.650 \times 10^{-5}$	.281
	1.5	19,20,60	$2.9049 \times 10^{-5}$	$6.684 \times 10^{-6}$	.230
Styrene Amidoxime (SGM245)	0.1	666	$2.3898 \times 10^{-6}$	$2.424 \times 10^{-7}$	.101
	1.0	668	$2.4847 \times 10^{-6}$	$2.511 \times 10^{-7}$	.101
	1.5	669,670	$5.1527 \times 10^{-7}$	$9.400 \times 10^{-8}$	.182

Note: all sorbers (except the AID) were exposed to natural seawater of concentration 2.9 ppb U<sup>nat</sup>; the AID seawater concentration is not known, but is comparable.

## APPENDIX A.3.3

## Column Experiment Loading Data

<u>Sorber</u>	<u>Exposure Time/Volume (ft<sup>3</sup>)</u>	<u>Average Seawater Temperature (°F)</u>	<u>Average Loading (gmU/gm sorber)</u>	<u>Fractional Error</u>
Acrylic Amidoxime (SGM251)	1 day/267.5	70.4	$2.3744 \times 10^{-5}$	0.100
	3 days/661.0	73.5	$6.7208 \times 10^{-5}$	0.0982
	7 days/2,035.5	71.3	$1.4383 \times 10^{-4}$	0.0970
	30 days/4,897.4	68.4	$3.2439 \times 10^{-4}$	0.171
Hydrous Titanium Oxide (HTO)	1 day/320.0	73.8	$3.8743 \times 10^{-5}$	0.124
	3 days/976.0	71.0	$1.0579 \times 10^{-4}$	0.178
	7 days/2,782.0	71.8	$2.4410 \times 10^{-4}$	0.177
	30 days/10,654.0	72.7	$3.9101 \times 10^{-4}$	0.118
Styrene Amidoxime (SGM245)	1 day/187.0	70.4	$5.5062 \times 10^{-6}$	0.106
	3 days/1,109.0	73.5	$1.5630 \times 10^{-6}$	0.103
	7 days/1,124.0	71.3	$2.1860 \times 10^{-6}$	0.103
	30 days/7,507.8	68.4	$3.0137 \times 10^{-5}$	0.172
Styrene Iminodiacetate (XE318)	1/2 day/10.3	60.0	$8.9728 \times 10^{-6}$	0.0616
	1 day/449.0	66.0	$2.3011 \times 10^{-5}$	0.0473
	3 days/791.5	65.8	$2.7331 \times 10^{-6}$	0.250
	7 days/1,179.0	66.9	$7.0211 \times 10^{-7}$	0.0869
	30 days/5,171.5	72.7	$2.3317 \times 10^{-5}$	0.0498
Acrylic Iminodiacetate (AID)	1 day/293.0	70.3	$8.9546 \times 10^{-7}$	0.0782
	30 days/11,810.3	70.6	$1.2770 \times 10^{-6}$	0.150



## APPENDIX A.3.4

Properties of Sorbers after 16 hours in Seawater  
From Experiments Performed by  
the Rohm and Haas Company (M3)

<u>Sorber</u>	<u>Functionality</u>	<u>Capacity at 2.54 ppb U*</u> ( gm U/gm sorber, dry)	<u>Density</u> (gm/cm <sup>3</sup> )	<u>Particle Size</u> (mm)
HTO	TiO <sub>2</sub>	>34.99**	1.45	1.0 - 2.0
SGM251	Acrylic Amidoxime	>44.1	1.13	0.63
AID	Acrylic Iminodiacetate	30.4	1.13	0.86
XE318	Styrene Iminodiacetate	22.1	1.14	0.75
SGM245	Styrene Amidoxime	15.0	1.21	--

\* Measured after 16 hours and checked for significant difference after 6 days

\*\* Measured after 27 days

## APPENDIX A.3.5

Equilibrium Experiment: Rohm and Haas Company  
Laser-Induced Fluorescence Measurements

<u>Sorber</u>	<u>gm/liter</u>	<u>Loading</u> <u>(gm U/gm sorber)</u>	<u>Seawater Concentration</u> <u>(ppb U)</u>
Hydrous Titanium Oxide (HTO)	0.1	$1.12 \times 10^{-5}$	5.7 ↓
	0.5	$2.94 \times 10^{-6}$	
	1.0	$1.30 \times 10^{-6}$	
	1.5	$1.82 \times 10^{-6}$	
Styrene Iminodi- acetate (XE318)	0.1	0.0	5.9 ↓
	0.5	$3.64 \times 10^{-6}$	
	1.0	--	
	1.5	$2.02 \times 10^{-6}$	
Acrylic Amidoxime (SGM251)	0.1	$2.08 \times 10^{-5}$	5.1 ↓
	0.5	$8.66 \times 10^{-6}$	
	1.0	$5.11 \times 10^{-6}$	
	1.5	$3.35 \times 10^{-6}$	
Acrylic Iminodi- acetate (AID)	0.1	--	21.1 ↓
	0.5	$3.46 \times 10^{-5}$	
	1.0	$2.13 \times 10^{-5}$	
	1.5	$1.44 \times 10^{-5}$	
Styrene Amidoxime (SGM245)	0.1	--	21.2 ↓
	0.5	$1.56 \times 10^{-5}$	
	1.0	$1.40 \times 10^{-5}$	
	1.5	$1.31 \times 10^{-5}$	
HTO	0.1	0.0	25.4 ↓
	0.5	$3.21 \times 10^{-5}$	
	1.0	$9.53 \times 10^{-6}$	
	1.5	$9.81 \times 10^{-6}$	
XE318	0.1	--	25.4 ↓
	0.5	$7.62 \times 10^{-6}$	
	1.0	$1.44 \times 10^{-5}$	
	1.5	$1.37 \times 10^{-5}$	
SGM251	0.1	$4.68 \times 10^{-5}$	21.2 ↓
	0.5	$4.33 \times 10^{-5}$	
	1.0	$2.17 \times 10^{-5}$	
	1.5	$6.92 \times 10^{-6}$	

## APPENDIX B

## Minimum Level of Detection

The minimum level of detection (MLD) of a system, is defined here and in reference (B1) as the fissionable mass required to give a net count that is equal to three times the standard deviation in the background count. This relationship is given by

$$MLD = \frac{3\sqrt{B} A}{\epsilon \nu N_A \sigma_f \phi \left[ \sum_{i=1}^6 (\beta_i / \lambda_i) (1 - e^{-\lambda_i t_0}) (e^{-\lambda_i t_1}) (1 - e^{-\lambda_i \Delta t}) \right]} \quad (B.1)$$

where B = total background count (during  $\Delta t$ )  
 A = atomic mass number of the fissionable nucleus  
 E = detector intrinsic plus geometric efficiency  
 $\nu$  = average number of neutrons emitted per fission  
 $N_A$  = Avogadro's number  
 $\sigma_f$  = microscopic fission cross section of fissionable nuclide ( $\text{cm}^2$ )  
 $\phi$  = neutron flux to which sample was exposed ( $\text{cm}^{-2} \text{sec}^{-1}$ )  
 $\beta_i$  = fraction of delayed neutrons emitted in group i  
 $\lambda_i$  = decay constant of delayed neutron group i  
 $t_0$  = irradiation time (sec)  
 $t_i$  = decay time (sec)  
 $\Delta t$  = counting time (sec)

All of the parameter values are known, except for the efficiency,  $\epsilon$ , and the neutron flux,  $\phi$ . A sample calculation for the 10/23/81 irradiation date will be done.  $\phi$  is taken to be  $8.0 \times 10^{12} (\text{cm}^{-2} \text{sec}^{-1})$  in the present work, the value cited by the MITR Operations Group for the IPhI facility.

The NBS uranium standard used in the present work has a  $U^{235}$  content of  $8.30519 \times 10^{-7} \text{gm}$ ; the irradiation and counting experiment conducted on 10/23/81 gave net counts/minute values of 44,392 and 44,344.

A computer algorithm was used to compute the intrinsic plus geometric efficiency,  $\epsilon$ , of the DFN detector array from this data. The program is listed in Table B.1. The average computed fractional efficiency was 0.2449 for the 10/23/81 NBS uranium standard data given above.

For the total background count equal to 374 for a one minute counting interval, the MLD, computed using Eq. (B.1) and parameter values cited here and in Chapter 1, section 1.2.2, is  $1.09 \times 10^{-9} \text{gm } ^{235}\text{U}$ , or  $1.53 \times 10^{-7} \text{gm}$  natural uranium (0.153 micrograms). Since we are interested in measuring sorber loadings ranging from 1 to 1000 ppm in approximately one gram samples, corresponding to 1 to 1000  $\mu\text{gm U}$ , the

apparatus as built and used in the present work proved quite suitable. Measurements on natural seawater ( $\sim 3$  ppb U) are beyond the systems' current capability unless concentration prior to measurement is employed, most likely accompanied by separation of the uranium from sea-salts which would contribute an unacceptable gamma background and exposure dose.

Table B.1 Computer Program for Calculating Detection Efficiency

```

10 REM calculation of intrinsic plus geometric efficiency of
20 REM the delayed neutron counting system
30 REM
40 REM list of variables
50 REM     e= intrinsic plus geometric efficiency
60 REM     n= average number of neutrons emitted per fission
70 REM     M= mass of fissionable nuclide,(gm)
80 REM     v= avogadro's number
90 REM     s= microscopic fission cross section of fissionable
100 REM     nuclide,(cm2)
110 REM     p= neutron flux, (neutrons/cm2/sec)
120 REM     a= atomic mass number of fissionable nuclide
130 REM     b(i)= fraction of delayed neutrons emitted in group i
140 REM     l(i)= decay constant of delayed neutron group i
150 REM     t1= irradiation time,(sec)
160 REM     t2= decay time,(sec)
170 REM     t3= counting time,(sec)
172 REM     s2= summation in denominator of mid equation
174 REM     p2= prefactor without mass and counts
180 REM     c= net counts minus background minus blank rabbit counts
182 REM
190 REM initialize constants
191 DIM B(6),L(6),E(1000),C1(1000),M1(1000)
192 B(1)=2.15E-4
193 B(2)=0.001424
194 B(3)=0.001274
195 B(4)=0.002568
196 B(5)=7.48E-4
197 B(6)=2.73E-4
200 N=2.418
201 L(1)=0.01244
202 L(2)=0.0305
203 L(3)=0.11141
204 L(4)=0.3013

```

```

205 L(5)=1.13607
206 L(6)=3.01304
210 U=6.02E+23
220 S=5.822E-22
225 A=235
230 P=8.0E+12
232 P2=A/N/U/S/P
235 PRINT "p2=",P2
260 T1=60
270 T2=60
280 T3=60
285 S2=0
287 E2=0
290 REM #####
300 FOR I=1 TO 6
310 S2=S2+B(I)*(1-EXP(-L(I)*T1))*EXP(-L(I)*T2)*(1-EXP(-L(I)*T3))/L(I)
320 NEXT I
330 K=0
340 PRINT "input net counts"
350 INPUT C
360 IF C<0 THEN 900
370 PRINT "input mass of fissionable nuclide"
380 INPUT M
390 K=K+1
400 E(K)=C*P2/M/S2
405 E2=E2+E(K)
410 GO TO 340
900 PRINT "K", "      ", "efficiency(K)"
905 FOR J=1 TO K
910 PRINT J, "      ", E(J)
915 NEXT J
916 E3=E2/K
918 PRINT "average efficiency=",E3
920 REM calculation of fissionable mass using average det. efficiency
930 K2=0

```

```

940 PRINT "input net counts for resin"
950 INPUT C
960 IF C<0 THEN 1005
970 K2=K2+1
980 C1(K2)=C
990 M1(K2)=C1(K2)*P2/E3/S2
1000 GO TO 940
1005 PRINT "n","net counts","fissionable mass"
1010 FOR N1=1 TO K2
1020 PRINT N1,C1(N1),M1(N1)
1030 NEXT N1
1040 END

```

```

RUN
p2= 3.466194161E-14
input net counts
44392
input mass of fissionable nuclide
8.30519E-7
input net counts
44344
input mass of fissionable nuclide
8.30519E-7
input net counts
-1
K
1 efficiency(K) 0.245070291754
2 0.244805303152
average efficiency= 0.244937797453

```

## APPENDIX C

User's Guide to the Delayed Fission Neutron (DFN)  
Counting Facility

The following describes procedures which should be followed when using the DFN counting system assembled for the present work.

## I. Authorization for Use of the DFN Counting System

1. Authorization from its custodian (Prof. Driscoll) the Reactor Radiation Protection Office (RPO) or the MIT Radiation Protection Office must be obtained.
2. Radiation dosimeters and film badges must be worn by all personnel involved in the experiment.
3. Reactor irradiation time in the 1PH1 pneumatic tube/irradiation facility must be reserved through MITR-II Reactor Operations.
4. If the send/receive station in the Nuclear Chemistry Laboratory (NCL) is to be used, then authorization to operate the 1PH1 pneumatic tube must be obtained from both the Radiation Protection Office and the Director of the Nuclear Chemistry Laboratory.

## II. Preparation of Detector Electronics and Irradiation Samples

1. The high voltage,  $\pm 15$  volts and  $+5$  volts power supplies should be provided with 60 Hz, 110 volt line power. BNC cables should be connected between the following components:



- the 1.0 to 5.0 kV outlet of the power supply and the +1200 volt input of the DFN detector assembly.
- the output of the DFN assembly and the positive input of the counter/timer.

The high voltage power supply and the counter/timer should be supplied with line voltage from the NIM-BIN rack. In the present work, the high voltage power supply is an ORTEC model 459, and the counter/timer is a Tennelec model TC545A. The  $\pm 15$  volt and +5 volt power supplies were built by the Electronics section of the Nuclear Reactor Laboratory.

2. Plateau curves should be taken to determine the stable operating high voltage range supplied to the  $^3\text{He}$  tubes as described in section 2.3.2.1 of reference N1. This procedure can be done with the  $^{252}\text{Cf}$  neutron source available from the Radiation Protection Office. Work to date indicates that the plateau should occur between roughly 1200 and 1300 volts. At no time should the high voltage exceed 1400 volts.
3. Discriminator levels internal to the DFN detector circuit should be calibrated with a  $^{252}\text{Cf}$  neutron source and a  $^{60}\text{Co}$  gamma-ray source (both available from RPO) as described in section 2.3.2.3 of reference N1, with the high voltage set at the level determined in the previous step, (approximately 1260 volts).

4. The lower level discriminator of the counter/scaler should be set to recognize the logic output pulses of a certain magnitude determined by the calibration procedure described in the previous step. The counter threshold setting is described in section 2.3.2 of reference N1. This setting should allow the counter to recognize logic pulses of approximately 3 volts in magnitude.
5. Irradiation, decay and counting times should be chosen according to the theoretical and practical limitations described in section 1.2.2 of reference N1, all 60 seconds for  $^{235}\text{U}$  in the present work.
6. Irradiation samples should be prepared according to current MITR Reactor Operation specifications and procedures, similar to those described in sections 2.4.4.3 and 3.4.4 of reference N1 for liquid and solid samples, respectively. Background samples should be made as nearly similar to the geometry and non-fissionable isotopic content of the unknown sample as possible. Rabbits and vials can be obtained from Reactor Operations and the styrofoam packing and other tools from the NCL.

### III. Pre-counting Preparation

1. The DFN counting electronics should be provided with 60 Hz, 110 V line voltage at least 12 hours prior to any counting procedure to allow the circuitry to

reach a stable equilibrium. Any interruption in the line voltage may result in a counting rate which subsequently increases with time.

2. In order to ensure the counting system stability, the neutron source, ( $^{252}\text{Cf}$ ) should be used to determine a stable and reproducible count rate before any samples have been irradiated. (This procedure should be repeated immediately after all counting has been completed). Before the first irradiated sample is counted, the neutron source must be taken outside the range of the detector system, preferably out of the room. In the present work, a  $^{252}\text{Cf}$  neutron source of approximate activity 5  $\mu\text{Ci}$  was obtained from RPO. (Note that  $^{252}\text{Cf}$  sources decay with a half-life of 2.64 years).
3. An average reproducible count rate should be established for the laboratory background level when the central rabbit-holding tube of the detector is empty. This "air count" should be repeated periodically during the irradiation run and after all counting has been completed so that the background level can be monitored. This procedure monitors the possible accumulation of interference from irradiated samples. Typically, these count rates ranged from 140 to 200 counts per minute.

4. If the send/receive station in the NCL will be used, then the 1PH1 blower should be turned on at least 30 minutes before the first sample is inserted, to prevent the condensation of water inside the tube which would contribute increased gamma activity to the samples being sent to the irradiation site.

#### IV. DFN Counting

1. The geometry of the sample (the axial and radial location in the rabbit) should always be carefully controlled during irradiation and counting to ensure consistent results from sample to sample.
2. The general behavior of the reactors' neutron flux should be monitored by noting the channel 7 fission chamber reading periodically. The NBS uranium standard could also be irradiated and counted periodically during an irradiation run to ensure uniform neutron flux conditions, or permit a systematic correction to be made.
3. Insertion of samples into the irradiation site can be done from the reactor send station or the NCL send station, (see section 2.2.1 of reference N1). The latter is preferable since handling costs are not incurred.
4. The irradiation time is displayed in two locations: at the reactor send/receive station and at the NCL send/receive station.

5. The decay time is automatically counted starting from the moment of sample ejection from the irradiation site within the reactor. It is displayed in the Nuclear Chemistry Laboratory. Occasionally, an irradiated sample has been ejected from the reactor, but the decay timer switch has not been activated so that the decay time is not counted unless it has been timed manually. Stopwatches are available from the NCL for this purpose.
6. The irradiated samples arrive at the NCL receive station after 18 seconds for a Reactor Operation activity monitor setting of 15 seconds. The monitor measures the activity of every irradiated sample that leaves the reactor containment to ensure an exposure dose level less than 10 mr/hr at one meter. The monitoring time can be varied from 0 to 60 seconds.
7. After the sample is manually transferred from the receive station into the DFN detector sample tube, the counting must be started manually by pushing the start button or start switch on the counter/timer front panel after the predetermined decay time has elapsed. The counting stops automatically after the present counting time has elapsed.
8. The previously counted sample should be removed from the detector before the next sample is counted by manually inverting the central sample tube; it should then be stored in a shielded area reasonably removed from the DFN counting site (~10 feet).

## V. Post-counting Procedures

1. The same neutron source used in step III.2 should be used to determine an average reproducible count rate so that it can be compared to that taken prior to the irradiation/counting runs. The average count rate should not vary significantly. The "air count" rate measurement in the absence of the neutron source should also be repeated (as in step III.3) at this time.
2. The IPH1 blower should be turned off.
3. The area immediately around the detector assembly should be monitored for contamination with an area monitor available in the Nuclear Chemistry Laboratory.
4. Activated samples should be stored under the Pb-brick shielded hood in the NCL until their activity decays enough to be moved to a pre-arranged storage location.
5. All power supplies should be turned-off and line voltage should be disengaged.

### Reference:

- N1 Nitta, C., "Delayed Fission Neutron Assay to Test Sorbers for Uranium-from-Seawater Applications," S.M. thesis, M.I.T., January 1982.

APPENDIX D

Rohm and Haas Company Report:  
Extraction of Uranium from Seawater with  
Synthetic Ion Exchange Resins

To: G. H. Beasley

From: S. G. Maroldo

Subject: Extraction of Uranium from Seawater with Synthetic  
Ion Exchange Resins



## I. Introduction

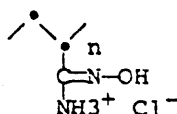
The worlds oceans contain about 4000 million tons of uranium <sup>1</sup> in the form of a 3.3 ppb uranyl tricarbonate solution.<sup>2</sup> Currently, the most promising method of extraction of uranium from sea water sorption of the uranium on hydrous titanium oxide (HTO).<sup>3</sup> This sorbent suffers from slow kinetics of sorption and appreciable losses through attrition. These disadvantages may be minimized through the synthesis and modification of advanced ion exchange materials which permit variation of performance by changing the structure and composition of the sorbent.

The Department of Nuclear Engineering of the Massachusetts Institute of Technology contracted Rohm and Haas Company to synthesize and screen three experimental ion exchange resins capable of extracting uranium from sea water. These resins were characterized for the usual ion exchange properties and based on a crosslinked polystyrene or a crosslinked polyacrylic backbone. The samples furnished were functionalized with iminodiacetate or amidoxime chelating groups and were screened for their capability to sorb uranium from both natural and spiked (25 or 30 ppb) sea water. A total of seven sorbers were screened resulting in four samples submitted to MIT for further testing at Woods Hole Oceanographic Institute.

## II. Experimental

### A. Preparation of Sorbers

1. Acrylic Amidoxime Resin SGM223 was prepared from a macroporous copolymer by reaction with hydroxylamine.



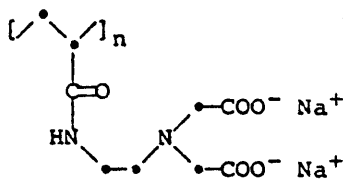
Two batches, SGM223 and SGM247 were combined to give SGM251 which was sent to MIT.

Elemental Analysis: Found C:48.00; H:5.57; N:16.93; Cl:11.46; O:15.11 Calculated C:48.05; H:6.56; N:16.00; Cl:20.25; O:9.14

2. Styrenic Sulfonamide Diamidoxime: SGM209 (II) was prepared from macroporous styrene copolymer.

2. Styrenic Amidoxime: SGM209 is in a class of resins with a styrene - DVB backbone that were developed prior to this contract. Rohm and Haas is currently applying for patent coverage for these resins and the details of this resin will follow after a patent application is made.

3. Acrylamide Iminodiacetate: SGM227 (III) was prepared from a porous crosslinked methylacrylate copolymer.



(III)

Elemental Analysis: Found C:56.51; H:7.03; N:19.41; O:19.43;  
Calculated C:56.57; H:7.45; N:22.78; O:13.01

#### B. Characterization of the Sorbers

All sorbers prepared and sampled to MIT were characterized by elemental analysis, capacity, density, mode particle size, and percent solids using standard techniques. These are summarized in Table I.

### C. Uranium Analysis

There are numerous methods for the analysis of uranium with varying levels of sensitivity. The standard<sup>7</sup> uranium analysis used is a colorimetric method using Arsenazo III.<sup>8</sup> The sensitivity of this analytical technique is low, being on the order of 0.5 ppm  $U_3O_8$ . Application of this method of analysis to the extraction of uranium from seawater therefore requires either concentration of the sample or using  $U_3O_8$  spiked samples and extrapolating the results to a thousandfold more dilute solution. Concentration is usually achieved by solvent extraction followed by evaporation, ion exchange sorption, adsorbing colloid flotation, or coprecipitation. Each procedure assumes that 100% of the uranium in the sample is being concentrated which is suspect at the ppb level. Also, extrapolation of sorption results to more dilute solutions is risky due to the possibility of competing processes (i.e. the sorption of other ions from seawater) altering the kinetics and the capacity of sorption of the resin.

More sensitive techniques are delayed neutron counting (<0.1 ppb  $U_3O_8$ )<sup>9</sup>, neutron activation analysis (0.1 ppb  $U_3O_8$ ),<sup>10</sup> and the most sensitive method available, nuclear (fission) track analysis (<0.01 ppb  $U_3O_8$ ).<sup>11</sup> However, each of these methods requires a neutron source which limits their availability. In addition, neutron activation requires and assumes quantitative sorption of the uranium on a solid support such as an ion exchange resin.

Presently, the most popular method is optical fluorimetric analysis<sup>12,13</sup> which has a sensitivity of 0.1 ppb  $U_3O_8$ . This technique uses a high carbonate flux fused salt which requires moderately high temperatures to prepare.

The method of analysis we chose was that of laser induced fluorescence,<sup>14</sup> a technique which is commercially available (Scintrex, Inc.), provides high sensitivity (0.05 ppb  $U_3O_8$ ) and relatively simple sample preparation. The instrument for the technique was developed for analysis of uranium in ground water and is primarily used by geologists for searching for uranium ore bodies. The primary advantage of this technique is its high sensitivity.

#### D. Screening of Sorbers

In order to compare the performance of new sorbers, a screening test was devised which consisted of placing 0.1, 0.5, 1.0 and 1.5 g of sorber in 1L of natural or spiked (25 or 30 ppb  $U_3O_8$ ) sea water of known  $U_3O_8$  concentration. The final  $U_3O_8$  concentration was then measured after 16 hours agitation. Some samples were measured again after six days of standing to assure that no additional significant sorption of uranium had occurred. Once the equilibrium or final concentration of  $U_3O_8$  was known, the capacity of the resin could be determined at that  $U_3O_8$  concentration. A plot of capacity of the resin versus final concentration of the  $U_3O_8$  allowed determination of the capacity of the resin at the uranium concentration of natural seawater.

#### III. Results

In the course of this study, seven sorbers were screened in spiked seawater (25 or 30 ppb  $U_3O_8$ ) according to the procedure described above. These data are given in Table II. Several of those sorbers were also screened in natural seawater. These data are given in Table III. The data in Tables II and III are plotted in Figures 1-6.

Table I - Summary of Sorbents Used to Extract Uranium from Seawater

<u>Sorbent</u>	<u>Functionality</u>	<u>Sorption Capacity in Seawater* at 3.3 ppb U<sub>3</sub>O<sub>8</sub> mg/g dry</u>	<u>Resin*** Capacity meq/g dry</u>	<u>Resin Density g/ml</u>	<u>Resin Mode Particle Size mm</u>
HTO	-	>41.1(27 days)**	-	1.45	1.0-2.0
SGM223	Acrylic Amidoxime	>52	6.25	1.13	0.63
SGM209	Styrenic Amidoxime	17.7	3.36	1.21	-
XE318	Styrenic Iminodiacetate	13.2	5.12	1.14	0.75
XE318G	Styrenic Iminodiacetate	26.1	5.12	1.14	
SGM227	Acrylamide Iminodiacetate	35.9	7.89	1.13	0.86

\* Measured after 16 hours and checked for significant difference after 6 days.

\*\* Measured after 27 days.

\*\*\* For amidoxime resins the capacity is a measure of the basic sites in the resin; for iminodiacetate it is the number of carboxyl acid groups per gram of resin. In the latter resins the number of iminodiacetate groups is one half the quantity of carboxylic acid groups.

TABLE II

Final Concentration of  $U_3O_8$  in Spiked Seawater after Contact

with Sorber-16 Hours and 6 Days

Sorber/ [ $U_3O_8$ ] (ppb)	Amount of Sorber Added (g Sorber/L Seawater)									
	0	0.1		0.5		1.0		1.5		
		16 Hours	6 Days	16 Hours	6 Days	16 Hours	6 Days	16 Hours	6 Days	
SGM227	25	-	-	5.0	-	0.4	-	0	-	
SGM209	25	25.6	-	16	-	8.9	-	2.3	-	
XE-318	30	-	22.4	25.6	14.2	13.4	5.8	6.3	5.1	
XE-318 (Ground)	25	-	21.7	-	5.3	-	2.2	-	0.95	
SGM223	25	19.6	-	0	-	0	-	1.2	-	
HTO*	30	30	20.5	11.5	5.1	19.0	10.4	13.0	6.2	

\*Uranezbergban - GmbH

7388-7/C15  
OCR-81-2-101

Table III

Final Concentration of  $U_3O_8$  in Natural Seawater after Contact with Sorber

Sorbent/ [ $U_3O_8$ ] (ppb)	Amount of Sorber Added (g Sorber/L Seawater)								
	0	0.1		0.5		1.0		1.5	
		16 Hours	6 Days	16 Hours	6 Days	16 Hours	6 Days	16 Hours	6 Days
SGM223	6	3.6	-	1.0	-	0.1	-	0.2	-
XE-318	7	7.0	6.4	4.9	4.9	-	3.2	3.5	3.0
HTO	6.7	5.4	6.0	5.0	-	5.2	5.2	4.6	3.9

7388-7/C16  
OCR 81-2-101

Figure 1: Uranium Concentration of Spiked and Natural Seawater after 16 hrs. of Contact with Various Amounts of Acrylic Amidoxime Sorber (SGM223)

46 1331

U.S. GOVERNMENT PRINTING OFFICE: 1964 O 3331

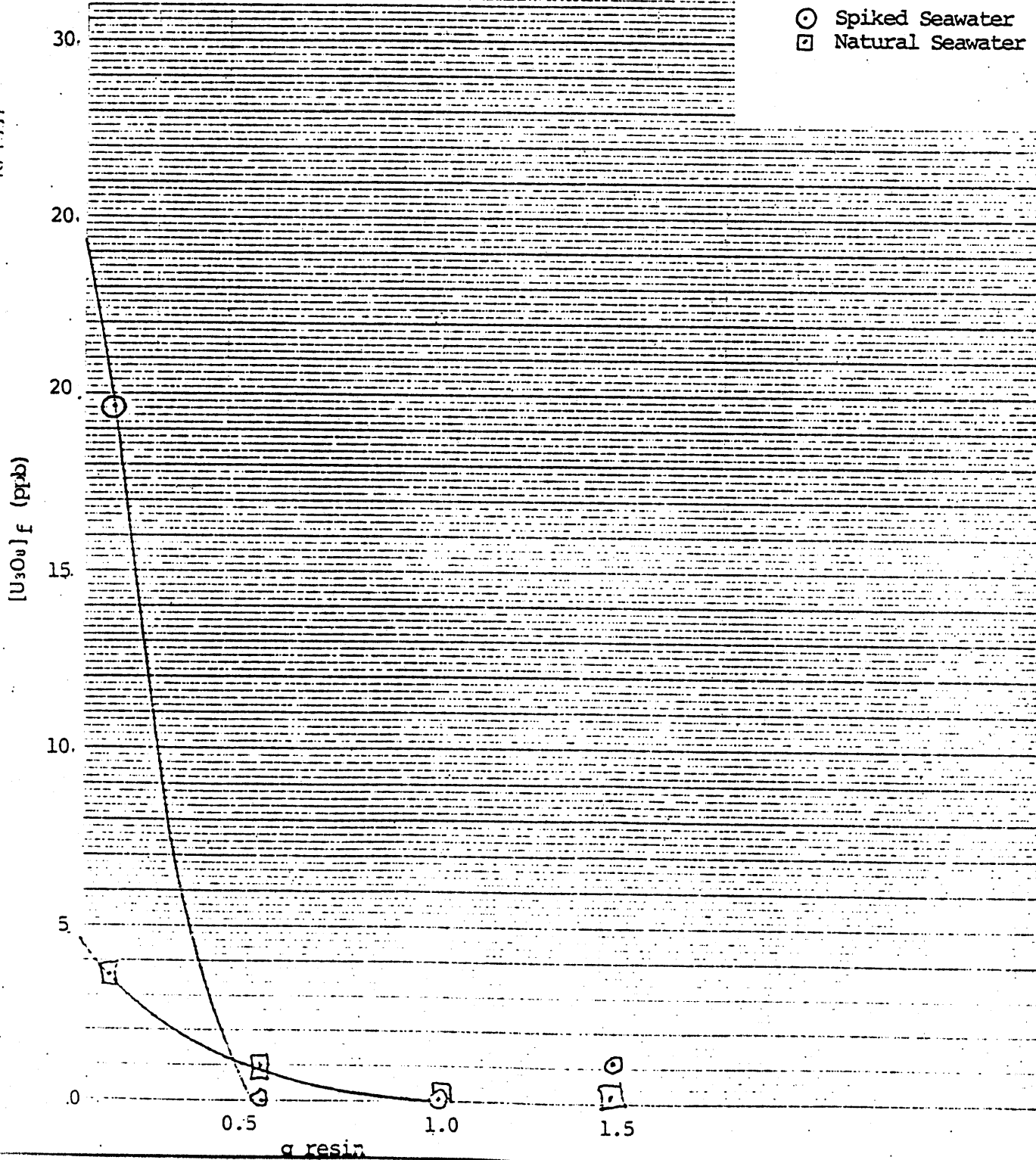




Figure 2: Uranium Concentration of Spiked Seawater at 16 hrs. of Contact with Various Amounts of Acrylic Iminodiacetate

410 1.531  
12.5 10.5 10.0 9.5 9.0 8.5 8.0 7.5 7.0 6.5 6.0 5.5 5.0 4.5 4.0 3.5 3.0 2.5 2.0 1.5 1.0 0.5 0

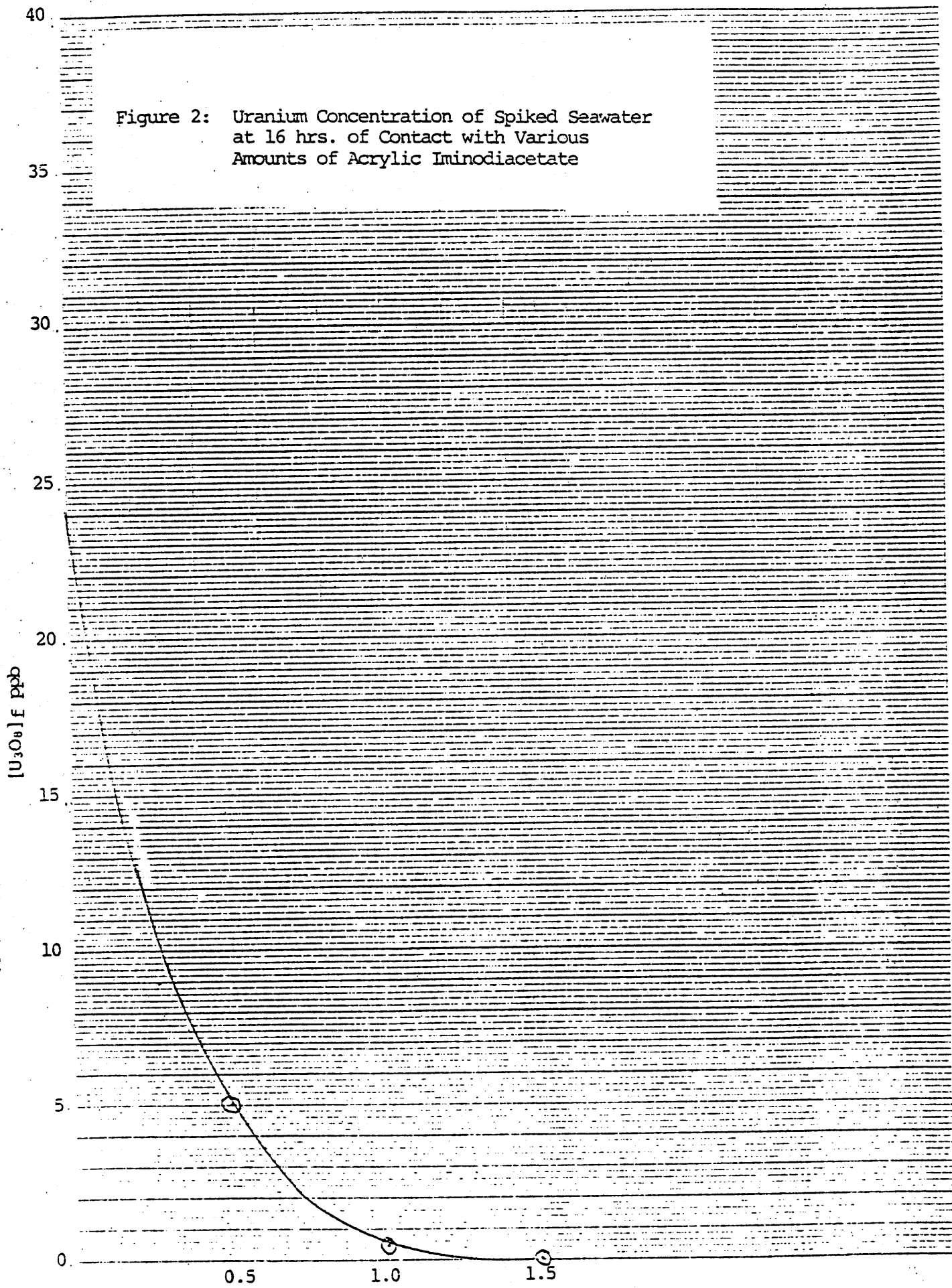


Figure 3: Uranium Concentration of Spiked Seawater  
at 16 hrs. of Contact with Various  
Amounts of Styrenic Amidoxime  
Sorber (SQM209)

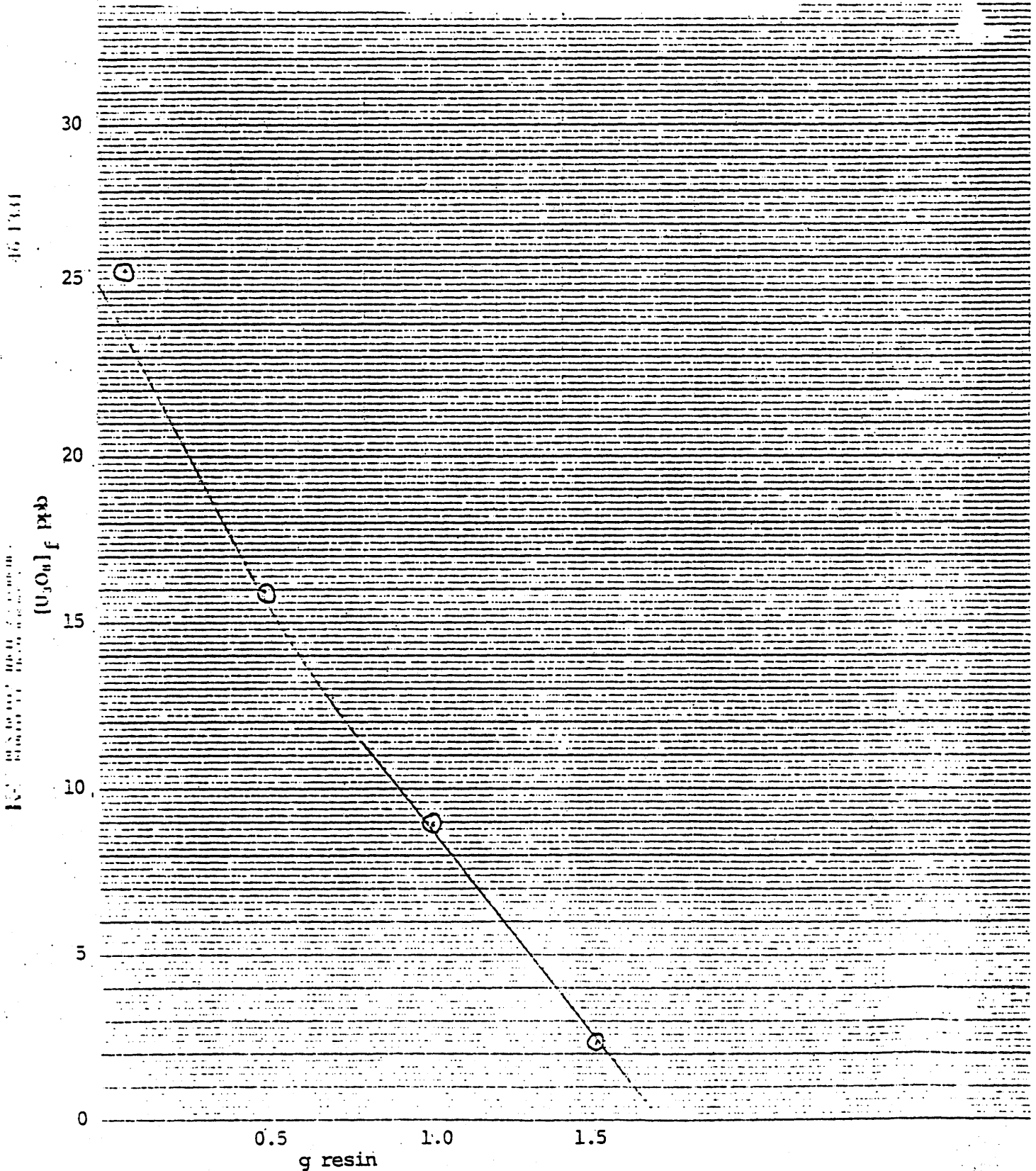


Figure 4 Uranium Concentration at 16 hrs. and 6 Days of Contact with Various Amounts of XE318

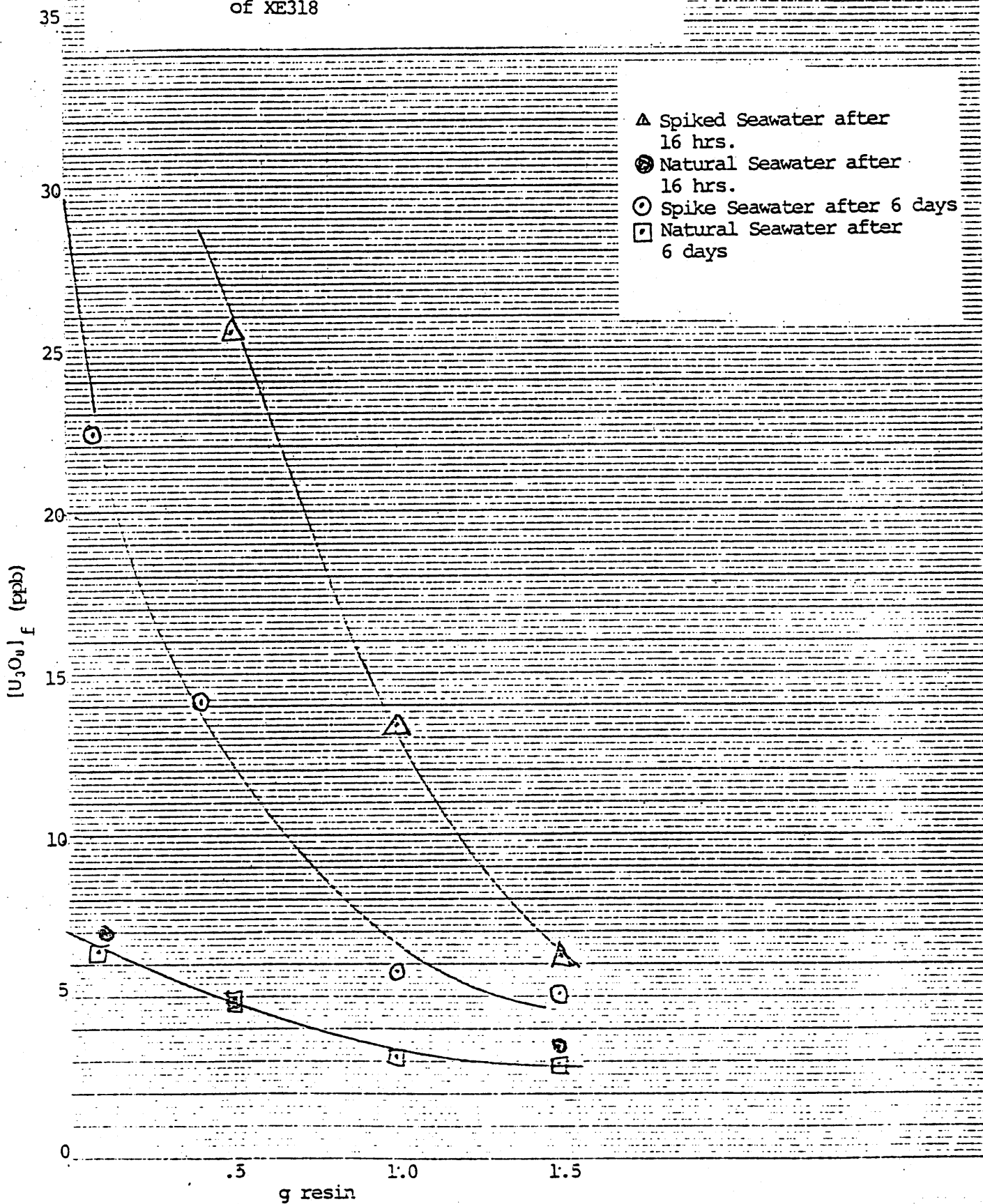


Figure 5 Uranium Concentration after 6 Days of Exposure to XE-318 and Ground XE-318

- Ground XE-318 6 days
- 318 6 days
- Spiked { ● Ground 318 6 days
- Seawater { ■ 318 6 days

46 1331

$[U_3O_8]_f$  (ppb)

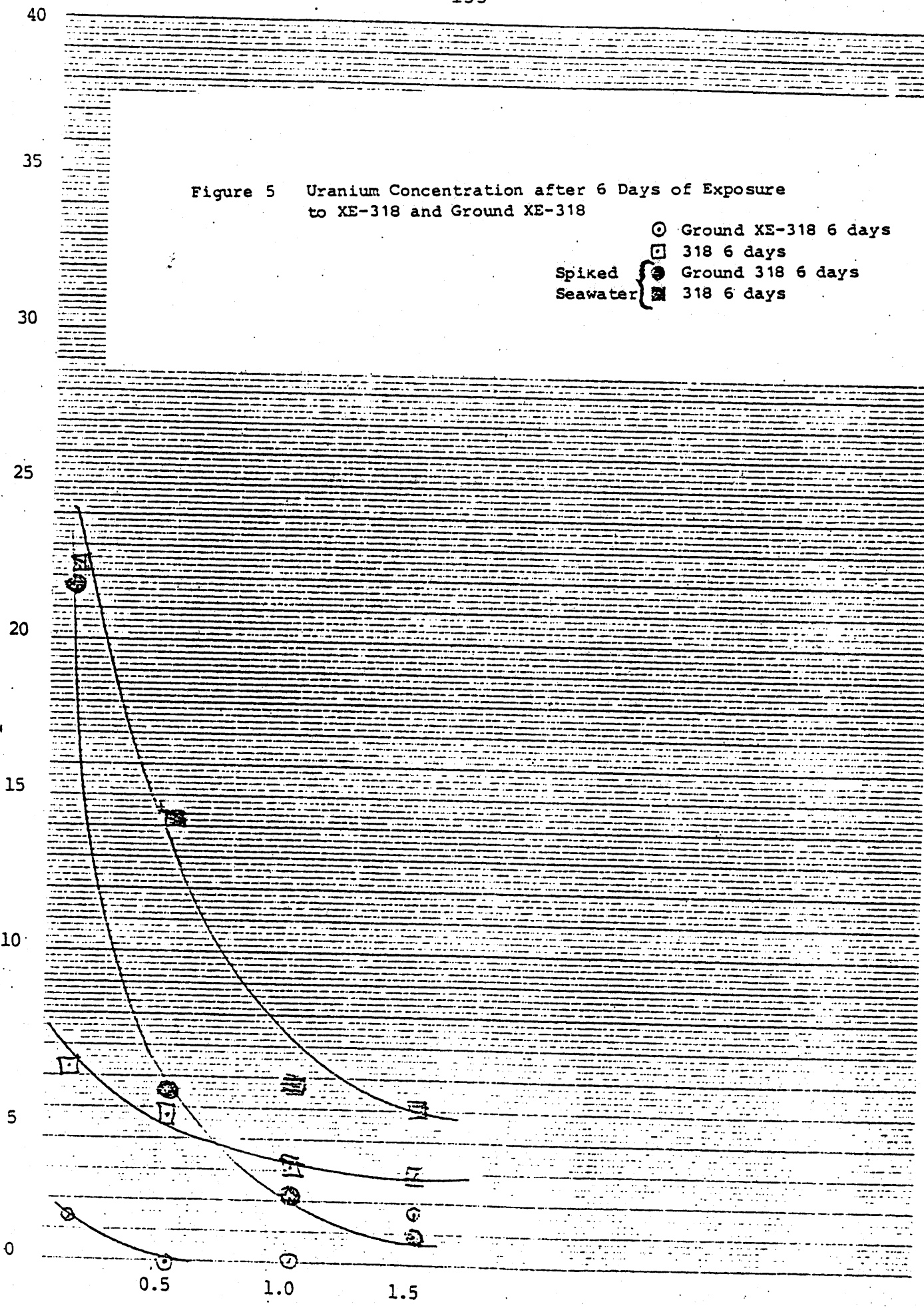
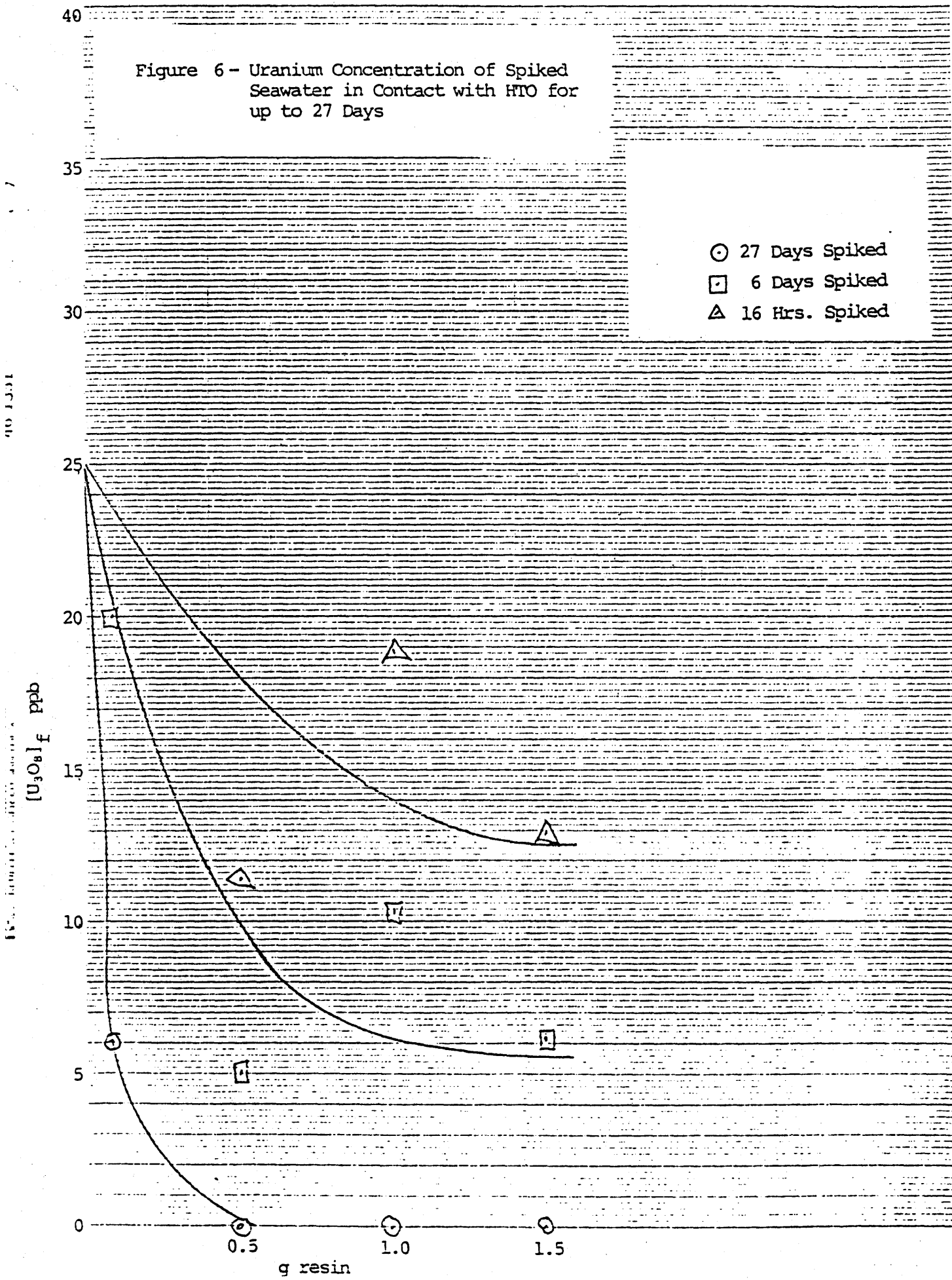


Figure 6 - Uranium Concentration of Spiked Seawater in Contact with HTO for up to 27 Days



All of the sorbers show reasonable ability to remove uranium from sea water. In addition, they all show much superior kinetics of sorption to that observed for HTO (Uranerzbergbau (GmbH) under the identical sorption conditions. In natural sea water, there is no difference in resin performance measured after 16 hrs. or 6 days. However, in spiked seawater, there are substantial differences in the 16 hrs. and 6 day points when 0.1, 0.5, or 1.0 g of resin per liter is used but not when 1.5 g of resin per liter is used. This may indicate that sorption is occurring primarily at chelating functionality located on the surface of the resin and not in the interior of the bead. The penetration of uranyl ion to the interior of the bead may be prevented by backbone crosslinking or by crosslinking by sorbed uranyl ion between chelating functionality on different chains. On the basis of our data, we can not differentiate between these two possibilities. However, a comparison of the results obtained using resins with a styrene/DVB polymer backbone and those obtained using an acrylic/DVB polymer backbone, the acrylic backbone gives better performance (Table IV). This indicates the importance of the polymer used in optimizing sorber performance for extraction of uranium from seawater.

The batch sorption studies described allowed the determination of the capacity of each of the resins at each final concentration. For one liter of solution, the difference between the initial and final concentrations is the amount of uranium sorbed on the resin. Since the amount of sorber added is known, the capacity in g  $U_3O_8$ /g resin dry is also known. A plot of capacity versus final concentration gives the capacity of the sorber at seawater concentration. These values are contained in Table IV.

The acrylic amidoxime is the only resin that shows a capacity that is comparable to that of HTO. However, since the final uranium concentration was below our detection limits, these are the minimal capacities. All of these capacities reflect very low sorption efficiencies with much less than 1% of the sites on the resin beads utilized.

It is interesting to note that XE318 shows half of the capacity of the same resin that has been ground up. This is surprising because XE318 is a high porosity macroreticular resin with high percentage of surface functionality. As such, this resin should not be very sensitive to grinding or particle size. Scanning electron micrographs<sup>15</sup> show that the ground up sample consists of irregular shaped particles that are composed of microspheres. It appears that only the macrospheres were broken on grinding and that the microspheres remained intact. Currently surface area measurements are being done for a further comparison.

The acrylic amidoxime resin is similar to a Japanese resin that has appeared in the literature<sup>16</sup> However, our resin appears to have 2-7 times the capacity of the Japanese resin when exposed to 0.01 M  $UO_2(NO_3)_2$  for 96 hrs. at room temperature<sup>17</sup> The differences in the two resins are not clear at this time.

Table IV

The Capacities of the Resins for Sorbing  
Uranium from Seawater after 16 hours

Sorbent	Functionality	Capacity at 3 ppb $U_3O_8$ g $U_3O_8$ /g resin dry
HTO	$TiO_2$	>41.1 *
SGM223	Acrylic Amidoxime	>52 **
SGM227	Acrylamide Iminodiacetate	35.9
XE-318G	Styrenic Iminodiacetate	26.1 **
SGM209	Styrenic Amidoxime	17.7
XE-318	Styrenic Iminodiacetate	13.2

\* 27 Days

\*\* Six Days

\*\* ( $U_3O_8$ ) final is zero. Therefore, this is a minimum value

#### IV. Conclusions

The work described in this report resulted in the sampling of four experimental resins to MIT.

These resins were styrene-DVB iminodiacetate, acrylic iminodiacetate, acrylic amidoxime, and styrene-DVB sulfonamide amidoxime. The acrylic amidoxime resin was the only resin with a capacity competitive with HTO but all samples show much faster kinetics than HTO.

Data obtained with SGM227 and XE-318 indicate that the nature of the polymeric matrix can significantly affect uranium capacity; p with an acrylic matrix providing almost three times the capacity. This difference in uranium capacity cannot be explained by differences in particle size (Table I) or by the 24 percent higher iminodiacetate content of SGM227.

This work was primarily concerned with functionalizing existing copolymers and determining their affinity for uranyl tricarbonate complex in sea water. None of the resins were optimized for performance. Further work would investigate the uranium capacities of other functionalities such as anthranilic acid, citrate, and aminoacids when placed on a polymeric backbone. Resin performance can be changed by modifications of the form of the sorber (i.e. flocks, fibers, or hollow fibers), physical characteristics of the ion exchange beads (i.e. porosity and surface area), and changes of the polymeric backbone structure that would increase hydrophilicity. Interesting changes in the backbone structure which may increase the hydrophilicity of the sorber include hydrophilic crosslinkers or hydrophilic monomer in styrene-DVB copolymers. Finally, elution studies should be carried out on each sample to determine the best eluent and how much the resin actually concentrates uranium from sea-water.



## Bibliography

1. Keen, N. J. Chem and Ind. 16 July 1977, p 579-82.
2. Wilson, J. D. et al. Anal. Chem. Acta, 1960, 23, 505.
- 3a. Rodman, M. R., Campbell, M. H., Binney, S. E., "Extraction of Uranium from Seawater; Evaluation of Uranium Resources and Plant Siting," Vol. I and II, Exxon Nuclear Company, Inc., 1979.
- 3b. Campbell, M. H.; et al. "Extraction of Uranium from Seawater: Chemical Process and Plant Design Feasibility Study," Vol. I and II, Exxon Nuclear Company, Inc., 1979.
4. Copolymer was obtained from Paul Ellis.
5. Beasley, G. H., Rohm and Haas Research Report B-10,685, March 27, 1980.
6. J. O. Naples, JO-339A, Notebook Number 034396.
7. Research Committee on Extraction of Uranium from Seawater, The Atomic Energy Society of Japan, Energy Developments in Japan, 1980, 3, 67-69.
8. Fritz, J. S., Johnson, Richard M., Anal. Chim. Acta, 1959, 20, 164-71.
9. Best, F., private communication.
10. Fleischer, R. L., Delany, A. C. Anal. Chem., 1976, 48, 642-45.
11. Waterbury, G. K., "Fluorimetric Analysis for Uranium in Natural Waters. HSSR Symposium, 1977, Grand Junction, Colorado.
12. Croatto, U.; Degetto, S.; Baracco, L., Ann. Chim. (Rome) 1978, 68 (7-8), 659-69.
13. Robbins, J. C., "Direct Analysis of Uranium in Natural Waters," Scintrex, Toronto, Canada, 1979.
14. McGreevy, L. M. Analytical Research Group 57, Technical Report Number 81-176.
- 15a. Egawa, H., Harada, H., Nippon Kagaku Kaishi, 1979, 7, 958-9.
- 15b. Egawa, H., Harada, H., Nonaka, T., Nippon Kagaku Kaishi, 1980, 8, 1767-1771.

- 15c. Egawa, H., Harada, H., Shuto, T., Nippon Kagaku Kaishi, 1980,  
8, 1773-1776.
16. Memorandum from S. G. Maroldo to G. H. Beasley, June 4, 1981.